Investigations of electrostatic ion waves in a collisionless plasma

Michelsen, Poul

Publication date:
1980

Document Version
Publisher's PDF, also known as Version of record

Risø-R-417

RISØ

Risø-R-417

Investigations of Electrostatic Ion Waves in a Collisionless Plasma

Poul Michelsen

Risø National Laboratory, DK-4000 Roskilde, Denmark
June 1980

INVESTIGATIONS OF ELECTROSTATIC ION WAVES IN A COLLISIONLESS PLASMA

BY

POUL MICHELSEN

RISØ-R-417

INVESTIGATIONS OF ELECTROSTATIC ION WAVES IN A COLLISIONLESS PLASMA

Poul Michelsen

Abstract. This report reviews a series of publications concerning theoretical and experimental investigations of electrostatic ion waves in a collionsless plasma. The experimental work was performed in the Risø Q-machine under various operational conditions. Besides a description of this machine and the diagnostic techniques used for the measurements, two kinds of electrostatic waves are treated, namely, ion-acoustic waves and ion-cyclotron waves. Due to the relative simplicity of the ion-acoustic waves, these were treated in detail in order to get a more general understanding of the behaviour of the propagation properties of electrostatic waves. The problem concerning the difficulties in describing waves excited at a certain position and propagating in space by a proper mathematical model was especially considered in depth. Furthermore, ion-acoustic waves were investigated which propagated in a plasma with a density gradient, and afterwards in a plasma with an ion beam. Finally, a study of the electrostatic ion-cyclotron waves was undertaken, and it was shown that these waves were unstable in a plasma traversed by an ion beam.

UDC 533.951.3

June 1980
Risø National Laboratory, DK 4000 Roskilde, Denmark

Denne afhandling er af det naturvidenskabelige fakultet ved Aarhus Universitet antaget til offentligt at forsvares for den naturvidenskabelige doktorgrad.

Aarhus Universitet, den 16. september 1981.

Karl Pedersen
dekan

Forsvaret finder sted
fredag d. 30. oktober 1981 kl. 14 prc. i
Fysisk Auditorium, Det fysiske Institut,
Aarhus Universitet, Ny Munkegade.

ISBN 87-550-0678-7
ISSN 0106-2840

Risø repro 1980

CONTENTS

Page

APPENDICES

PREFACE

The present report reviews a series of investigations on electrostatic ion waves in a collisionless plasma. Most of the work was published from 1971 to 1979, and these publications are listed below. In the text they are referenced by Roman numerals and can be found in Appendices I to X.

I Andersen, S.A., Jensen, V.O., Michelsen, P., and Nielsen, P. (1971). Determination and shaping of the ion-velocity distribution function in a single-ended Q machine. Phys. Fluids 14, 728-736.

II Michelsen, P. and Pécseli, H.L. (1973). Propagation of density perturbations in a collisionless Q-machine plasma. Phys. Fluids 16, 221-225.

III Christoffersen, G.B., Jensen, V.O., and Michelsen, P. (1974). Investigation of ion acoustic waves in collisionless plasma. Phys. Fluids 17, 390-399.

IVa D'Angelo, N., Michelsen, P. and Pécseli, H.L. (1975). Damping-growth transition for ion-acoustic waves in a density gradient. Phys. Rev. Lett. 34, 1214-1216.

IVb D'Angelo, N., Michelsen, P. and Pécseli, H.L. (1976). Ion acoustic waves in a density gradient. Z. Naturforsch. 31a, 578-582.

V Jensen, V.O., Michelsen, P. and Hsuan, H.C.S. (1974). Absolute and convective ion beam instability studied through Green's function. Phys. Fluids 17, 2208-2214.

VI Michelsen, P., Rasmussen, J.Juul and Sato, N. (1976) Propagation properties of density pulses in an ion-beam plasma system. Phys. Fluids 19, 1021-1025.

VII Jensen, T.D., Michelsen, P. and Rasmussen, J.Juul (1979). Wave propagation in an ion beam-plasma system. Plasma Phys. 21, 173-182.

VIII Michelsen, P. (1976). Stability limits of the ion beam excited electrostatic ion cyclotron instability. Phys. Fluids 19, 337-339.

IX Michelsen, P., Pécseli, H.L., Rasmussen, J.Juul, and Sato, N. (1976). Unstable electrostatic ion cyclotron waves excited by an ion beam. Phys. Fluids 19, 453-456.

X Michelsen, P., Pécseli, H.L. and Rasmussen, J.Juul (1977). Ion-beam-excited electrostatic ion cyclotron instability. Phys. Fluids. 20, 866-867.

1. INTRODUCTION

To get more insight into the nature of plasmas and be able to utilize their many possible application, it is necessary to understand the basic phenomena of plasma physics. To describe the behaviour of most plasmas of interest classical theory is sufficient, i.e. the equations describing the plasma are those of Boltzmann and Maxwell, and from these the dynamics of a plasma can be calculated in principle. In practice, however, these equations can be solved only analytically in special cases and only after introducing assumptions of various kinds in the equations. In some cases it is possible from a theoretical point of view to state for which values of the variables the assumptions are valid, but in many cases only experiments can indicate this. In this connection as well, numerical simulations of plasma phenomena can sometimes be considered to be "experiments". In the late fifties there were nearly no possibilities of comparing theories with experimental results in plasma physics. This was due to both an inadequate knowledge of plasmas and lack of experimental plasmas which could be utilized in basic investigations. At that time plasmas were produced by applying large currents and fields to some neutral gases yielding noisy plasmas of short lifetimes which were not useful in enabling careful measurements to be made.

The introduction of the Q-machine (Q for quiescent) at the beginning of the sixties caused a breakthrough in experimental plasma physics. In a few years several new types of plasma waves and instabilities were observed, diffusion across the magnetic field was measured, and damping of ion-acoustic waves due to a collisionless mechanism was observed. The main reasons for the success of the Q-machine were as follows: 1) the plasma could be produced without any of the large internal electric fields necessary to generate other kinds of plasmas, 2) the plasma was in a steady state, and 3) the plasma parameters covered a new and important range of plasma studies.

The Risø Q-machine was constructed in 1966-67 and since then a large number of plasma phenomena have been studied utilizing it. Some of these experiments together with theoretical considerations and calculations are reported in detail in the papers in Appendixes I-X, while a short review of this work with some comments is given and discussed in the following chapters.

Chapter 2 gives a description of the Q-machine, the parameters of the plasma, and the diagnostic methods which have been used to measure these parameters. It also contains the main conclusions from paper I concerning measurements of the ion velocity distribution. Chapter 3 describes the main conclusions from papers II-III and also contains a discussion of the correctness of using a first pole approximation in order to describe propagation of linear ion-acoustic waves. Chapter 4 discusses the work in paper IV concerning ion-acoustic waves in an inhomogenous plasma. The topic of Chapter 5 is the propagation of stable and unstable ion-acoustic waves and pulses in an ion-beam plasma, a work which is described in detail in papers V-VII. Finally in Chapter 6 the work from papers VIII-X about the electrostatic ion-cyclotron waves is discussed.

2. THE Q-MACHINE

The principle of the Q-machine, its history and a review of the most important work concerning Q-machine research up to about 1972, can be found in the book "Q-Machines" by R.W. Motley (1975). Here we shall just briefly describe the principle of the machine, (see Motley's book for details) as well as the special features used in the Risø Q-machine, a sketch of which is shown in Fig. 1. After this the diagnostic tools (the Langmuir probe and the ion energy analyzer) will be discussed. These two important tools are also described in the Q-machine book with special attention to the problems which arise when they are used in the Q-machine plasma.

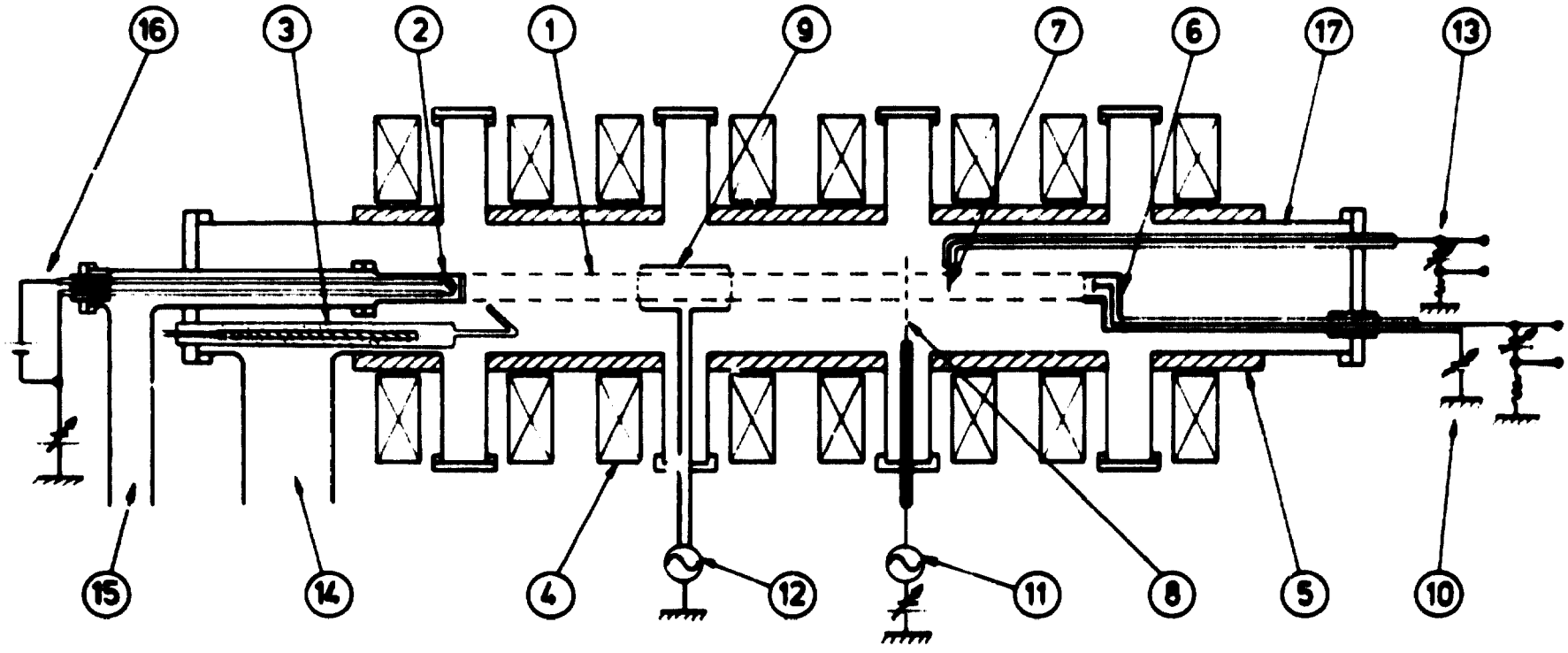

Fig. 1. The Q-machine. 1) Plasma column, 2) Hot plate, 3) Cesium oven, 4) Magnetic field coils, 5) Cooling system for vacuum vessel, 6) Energy analyser, 7) Langmuir probe, 8) Grid for wave excitation, 9) Microwave cavity for electron heating, 10) Circuit for energy analyser, 11) Wave oscillator, 12) Microwave oscillator, 13) Circuit for probe, 14) and 15) Pumping tubes, 16) Power supply for heating of the hot plate.

Plasma production in the Q-machine is based on thermal contact ionization. When vapour of a metal with a low ionization potential hits another metal with a work function higher than or comparable to the ionization potential of the first metal, a considerable number of the impinging atoms will be ionized. This phenomenon was discovered by Langmuir and Kingdon in 1925, but not until much later was it used for plasma physical purposes, by Rynn and D'Angelo in 1960. Since electrons are also necessary for plasma production the ionizing plate must be heated to at least 2000 K to emit electrons by Richardson emission. The only metals which satisfy the two conditions of low work function and high melting point are tungsten, tantalum, rhenium and molybdenum. For the materials to be ionized the alkali metals are mostly used as well as some divalent metals as strontium and barium, and it has been reported that even uranium could be utilized (Hashmi 1971). Since cesium has the lowest ionization potential of any metal, it is most efficiently ionized. To choose the metal for the ionization surface a compromise is necessary as the work function should be as low as possible to yield a high emission of electrons; on the other hand it must lie above the ionization potential of the metal to be ionized. In the Risø Q-machine tantalum plates are used, while several of the alkali metals (Cs, Rb, K and Na) have been applied. The hot plate (or plates) confines the plasma in the axial direction. In the radial direction the plasma is confined by a strong magnetic field. To reduce the gyro radius of cesium ions to a value much smaller than the radius of the plasma column (1.5 cm) the strength of the magnetic field has to be higher than $\simeq 0.2$ T. To investigate phenomena that depend on the B-field, it is of course necessary that this field can be varied in a specified range. In the Risø Q-machine the maximum field is around 1.8 T, while the normal field strength is $\simeq 0.3 - 0.4$ T.

One of the main advantages of the Q-machine is that the plasma is effectively collisionless, at least for low plasma densities, i.e. collisions are unimportant for the phenomena investigated and only collective effects can be expected to play any role.

To avoid neutral collisions the background pressure is normally $\simeq 2 \cdot 10^{-6}$mm Hg, which gives a mean free path for ion-neutral collisions on the order of 10^2-10^3 m. The largest ion-neutral collision cross section is the charge exchange cross section, which for cesium at low energies is about $6 \cdot 10^{-14} cm^2$. This was measured by a special technique in the Q-machine by Andersen et al. (1972). To keep the neutral cesium pressure low, the walls of the vacuum vessel are cooled down to -16°C, at which temperature the vapour pressure of neutral cesium is 10^{-8}mm Hg, giving a mean free path for charge exchange on the order of 500 m.

The cesium is produced in an oven where a mixture of CsCl and Ca is heated to a few hundred degrees centigrade. At this temperature cesium vapour is produced and brought to strike the hot plate by a tube. If a plasma of very low density ($n \lesssim 10^{13}$ m^{-3}) is desired, the machine can be run in a vapour pressure mode without using the ovens. Then the background Cs-pressure will be sufficient to supply the hot plates with cesium atoms. Besides this, it is possible to operate the machine in a double-ended mode with two hot plates or in a single-ended mode where only one hot plate is used to produce the plasma. In the latter case the plasma column is terminated on a cold plate. The advantages of double-ended operation are that it is possible to obtain a high density (about 10^{18} m^{-3} with Cs-plasma) and the plasma drift velocity can be decreased to a negligible value by adjusting the temperature of the hot plates. If these two things are unnecessary for enabling an experiment to take place, the single-ended operation is more convenient. In the single-ended operation the terminating plate is normally biased negatively thereby reflecting electrons and absorbing ions. The opposite case with positive end plate makes the plasma noisy due to the current-driven ion-acoustic instability (Michelsen et al. 1979) or the current-driven ion-cyclotron instability (Motley and D'Angelo 1963). For a negatively biased terminating plate the absorption of ions gives rise to a drifting of the ions from the hot plate towards the cold plate. The velocity of this drift is normally larger than the ion thermal velocity, as a plasma sheath, due to a surplus of electrons, will create a negative plasma potential. In this case the ions will, therefore,

be accelerated when passing the negative sheath in front of the hot plate. This is called electron-rich conditions and is the normal state of operation. Ion-rich conditions arise when either the temperature of the hot plate is low or the plasma density is very high, i.e. in cases with a deficit of electrons, which implies that the plasma potential be positive. This state normally also introduces instabilities in the plasma which make it noisy (Butchelnikova et al. 1966). The main advantage of the single-ended mode operation is the possibility of using the cold end plate either as an energy analyzer, as ion collector to measure density, or as a wave exciter. The existence of an ion drift velocity may also be an advantage in many cases, both when measuring the ion energy distribution function, and also when treating some wave experiments as initial value problems instead of the more difficult boundary value problems wher the plasma drift velocity is larger than the phase velocity of the wave.

For the Q-machine experiments up to about 1970, knowledge about the ion velocity distribution, the spatial variation of the plasma potential along the column axis, and the ion temperature were based on theoretical considerations. It was normally assumed that both electron and ion velocity distribution functions were Maxwellian, in some cases with small drift velocities and with temperatures very close to that of the hot plate. For wave studies, knowledge of the distribution functions is a crucial point at least when the phase velocity of the wave is comparable to the thermal velocity of the ions or electrons.

The first thorough investigation of the parallel (i.e. $\neq \underline{B}$) ion energy distribution function was carried out in the Risø Q-machine and the results are presented in Appendix I, which contains all the experimental details. The main finding of this investigation was that the ion velocity distribution function, $f_o(v)$, was strongly dependent on both plasma density and plate temperature, i.e. electron emission. At high densities ($n > 10^{16}$ m^{-3}) charge exchange processes in front of the hot plate were of importance and gave rise to ion temperatures, T_i, considerably above the hot plate temperature, T_{HP}, and in some cases even caused double-humped ion velocity distributions. For

low densities ($n < 10^{15}$ m^{-3}) it was found that the ions were adiabatically cooled when passing the electron-rich sheath in front of the hot plate to temperatures well below T_{HP}. The variation with plate temperature of the plasma potential, ϕ_p, and the drift velocity of the ions V_o, was found in agreement with theory. In most cases the ion drift velocity was shown to be large compared with the ion thermal velocity, in agreement with the large negative potential drop in front of the hot plate. These results were obtained for a plasma in a single-ended operation, since the energy analyzer terminates the plasma column. Some results for a double-ended machine obtained with a small energy analyzer were later presented by the author (Michelsen (1971). The main conclusion of that work was that in double-ended operation the ion distribution function is double humped at low plasma densities. But even with a small analyzer (diameter = 2 mm) shadow effects are unavoidable, at least for electrons, since the electron cyclotron radius, ρ_e, is on the order of $5 \cdot 10^{-5}$ m in the Q-machine plasma. Another restriction on the use of the energy analyzer is that it has to be biased negatively to reflect electrons. In a plasma which is terminated on a positive end plate, some instabilities arise and determination of the distribution function is difficult. Several calculations of the velocity distribution function and the potential versus distance were given by Michelsen et al. (1979), while a thorough theoretical analysis of the problem was recently presented by Kuhn (1979).

All measurements mentioned in this report were performed by means of either the energy analyzer or Langmuir probes. From an experimental point of view the Langmuir probe is a simple diagnostic tool. Analytical calculation of the current voltage characteristics is possible in only a few special cases, however, namely when the probe is either very small or very large compared to the Debye-length and, furthermore, only for non-magnetized, isotropic plasmas. Probe theories for stationary and flowing plasmas can be found in the book by Chung et al. (1975), for instance. Detailed investigations of probes in Q-machine plasma have been performed by Chen et al. (1968), who found that the numerical calculations of Lam (1965) and Laframboise (1966)

gave rsults in reasonable agreement with probe measurements. Since detailed investigations of Langmuir probes can be found in the literature, and the use of such probes in the investigations described in I-X is directly mentioned in every case, it shall not be discussed further here.

3. ION-ACOUSTIC WAVES

Many kinds of waves are known to exist in plasmas. Among these the electrostatic waves, propagating in a homogeneous plasma parallel to the magnetic field, are probably the simplest to investigate seen both from a theoretical and an experimental point of view. The electrostatic waves can be divided into two kinds or branches. The low frequency branch ($\omega \lesssim \omega_{pi}$), where both ions and electrons take part in the wave motion, includes, for instance, ion-acoustic and ion-cyclotron waves. The high frequency branch, where predominantly the electrons oscillate, is represented by Langmuir waves or, if the geometry in the direction perpendicular to the propagation is finite, the Trivelpiece-Gould mode. From an experimental point of view the ion-acoustic waves are easier to investigate partly due to the low frequencies and partly to the easier diagnostics. On the other hand, because of the strong damping of ion-acoustic waves (at least for $T_e \approx T_i$) wave propagation in a dispersive plasma, which involves a lot of interesting nonlinear phenomena, can be studied more effectively using the high-frequency branch (see, e.g. Michelsen et al. 1978, Lynov et al. 1979 and Michelsen 1980). Therefore, one reason to study ion-acoustic waves is to gain some insight into one kind of plasma wave, which can then hopefully be used to understand the propagation properties of other more complicated plasma waves. Besides this, ion-acoustic waves are of direct importance for several reasons. One, because they provide a means of carrying energy into a plasma and, thereby, of heating it. Despite the supporting of the plasma by a magnetic field in many cases, this does not preclude the propa-

gation of ion-acoustic waves. This follows because, e.g., in the region of fusion interest, the ion plasma frequency exceeds the ion cyclotron frequency, and the waves propagate freely across the magnetic field as well as along it. As a result, we take note of the phenomenon of ion heating by turbulence, in which ion-acoustic waves are identified as being directly responsible, (Wharton et al. 1971, Hamberger et al. 1971). A second reason why these waves are important is that they can be used for diagnostic purposes, in order to determine the plasma flow velocity (Hsuan et al. 1975) or electron temperature, for instance (Appendix X and Schrittwieser 1978).

Propagation and damping of ion-acoustic waves were first studied by Hatta and Sato (1961) and by Little (1961). The former excited the waves by applying oscillating potentials to a grid immersed in a discharge plasma, while the latter used a coil for excitation. However, the first experimental observation of Landau damping as described theoretically by Landau in 1946 for electron waves and by Fried and Gould in 1961 for ion-acoustic waves was reported by Wong et al. (1962 and 1964). Since the concept of Landau damping is unique to plasma physics and as there has been some discussion of the interpretation of Wong et al.'s results, we shall devote ourselves to a review of this discussion in this chapter, and to a further analysis of a few of the problems which have arisen in this connection. The Landau damping has also been investigated in connection with electron plasma waves, but the discussion here will be restricted to ion-acoustic waves.

3.1. First pole approximation

The fundamental equations describing ion-acoustic waves, which were already introduced by Fried and Gould (1961), are the Vlasov equation for ions and electrons, and the Poisson equation, which gives the relation between particle densities and the electric field. The main assumptions are that collisions can be neglected and that the waves considered are electrostatic. Furthermore, in the following we will restrict the discussion to

wave propagation in one dimension since the plasma normally is confined by a strong magnetic field, i.e. ($\omega << \omega_{ci}$ and $\omega_{pe} << \omega_{ce}$). In a work by Jensen (1962) the equations were simplified further by assuming that the phase velocity, $\omega/k << c_e$ = electron thermal velocity. In this case it is realistic to consider the electrons as a fluid, and if their mass is neglected compared to that of the ions, the electrons will be Boltzmann distributed. In this case the system of equations after linearization can be written in the following way:

$$\frac{\partial f(x,v,t)}{\partial t} + v \frac{\partial f(x,v,t)}{\partial x} - \frac{e}{M} \frac{\partial \phi}{\partial x} \frac{df_o(v)}{dV} = 0$$

$$\frac{\partial^2 \phi}{\partial x^2} = - \frac{e}{\varepsilon_o} (n_i - n_e); \qquad n_i = \int_{-\infty}^{\infty} f(x,v,t)\, dv; \qquad (3.1)$$

$$\frac{1}{n_o} \frac{\partial n_e}{\partial x} = \frac{e}{\kappa T_e} \frac{\partial \phi}{\partial x}; \qquad n_o = \int_{-\infty}^{\infty} f_o(v)\, dv .$$

Here $f_o(v)$ and $f(v)$ are the zero and first-order ion velocity distribution functions, respectively, n_o is the zero-order density, while n_e and n_i are the first-order electron and ion density, respectively. The electric potential is ϕ and the other symbols have their normal meaning. When only long wavelengths, λ, are considered, i.e. $\lambda >> \lambda_D$ (λ_D = Debye length), we may assume quasi-neutrality; this means we neglect the $\frac{\partial^2 \phi}{\partial x^2}$ term in the Poisson equation and by eliminating the potential we can then get a simpler equation which will be considered in this chapter:

$$\frac{\partial f(x,v,t)}{\partial t} + v \frac{\partial f(x,v,t)}{\partial x} - \frac{c_s^2}{n_o} \frac{\partial n(x,t)}{\partial x} \frac{df_o(v)}{dv} = 0, \qquad (3.2)$$

where $c_s = (\kappa T_e/M)^{\frac{1}{2}}$ is called the sound speed. This equation was, in fact, the one discussed by Wong et al. (1962 and 1964). They calculated the phase velocity, $v_{ph} = \omega/k_r$, and the relative

damping constant, $\delta/\lambda = k_r/(2\pi k_i)$ based on Eq. 3.2 and found good agreement with their measurements when they assumed that the ion velocity distribution was a Maxwellian; it had a small drift velocity, which they found by fitting the theoretical results to the experimentally obtained values. The results of this work were later criticized, especially by Gould (1964) as well as by Hirshfield and Jacob (1968). We shall discuss these criticisms together with the solution, which Wong et al. used for comparison of their experimental results. Eq. 3.1 was solved by using a Fourier transform in time and a Laplace transform in space. The dispersion relation was obtained:

$$(k\lambda_D)^2 - \frac{1}{2}\frac{T_e}{T_i} Z'\left[\frac{1}{c_i}\left(\frac{\omega}{k} - V_o\right)\right] + 1 = 0,$$

where Z is the "plasma dispersion function" (Fried and Conte 1961), T_e and T_i are temperatures of electrons and ions, respectively, $c_i = (2\kappa T_i/M)^{\frac{1}{2}}$ is the ion thermal velocity, and V_o is the ion drift velocity. Then the $(k\lambda_D)^2$ term was neglected, which corresponds to using Eq. 3.2, and the solution to the equation:

$$Z'\left[\frac{1}{c_i}\left(\frac{\omega}{k} - V_o\right)\right] = 2\frac{T_i}{T_e}, \tag{3.3}$$

with the smallest negative imaginary part was chosen among the infinite number of solutions to the equation. For $T_e = T_i$ this solution is

$$\frac{\omega}{k} - V_o = c_i\ (1.447 - 0.602i). \tag{3.4}$$

According to the authors, the reason that the solution (Eq. 3.4) was chosen was that it was the least damped ion oscillation mode. As pointed out by Gould, this is correct only in the case where the equation is solved as an initial value problem. Then an asymptotic solution $\propto \exp[i(kx-\omega t)]$ for large t can be found following the same method as Landau used for electron waves. For a boundary value problem, on the contrary, the solution (Eq. 3.4) will give the spatially most damped mode when $V_o = 0$. When $V_o > 0$

there may be some other modes which are more damped, but there will always be an infinite number of modes with smaller damping than that of the solution (Eq. 3.4), which is the so-called "first pole approximation". This can easily be seen if the solution is written as:

$$\frac{1}{c_i}\left(\frac{\omega}{k} - V_o\right) = re^{i\phi},$$

since an asymptotic solution (Nielsen 1969) to Eq. 3.3 can be found to be:

$$r \sim [(2|p| - 5/4)\pi]^{\frac{1}{2}}$$

$$\phi \sim -\frac{\pi}{4} + \frac{1}{2r^2}\ln(2\sqrt{\pi}\theta r) \text{ for } p > 0 \qquad (3.5)$$

$$\phi \sim -\frac{5\pi}{4} + \frac{1}{2r^2}\ln(2\sqrt{\pi}\theta r) \text{ for } p < 0,$$

where

$$\theta = T_e/T_i,$$

and p, which we shall denote the "mode number", is an integer different from zero:

$$(|p| = 1, 2, \ldots).$$

The damping coefficient, δ, is then given by

$$\delta \equiv \frac{1}{k_i} = -\frac{c_i}{\omega}\,\frac{r^2 + 2r\cos\phi\; V_o/c_i + (V_o/c_i)^2}{r\sin\phi}$$

For $r \to \infty$, we get, for modes moving in the positive direction ($p > 0$), $\phi \to -\frac{\pi}{4}$, and therefore $\delta \to c_i r/\omega$. That is, the damping distance increases for increasing mode number. If one moves along with a spatially damped wave, we can also discuss temporal damping. The damping time will then be given by $\tau = \delta k_r/\omega$,

which, from the above given asymptotic approximation, can be seen to decrease with increasing mode number. Obviously, we can state that the reason why the spatial damping decreases for increasing mode number is that although the temporal damping increases, the phase velocity increases faster with mode number. The exact solution of Eq. 3.3 for the first 10 poles is given in Table 1 for $T_e = T_i$, together with the asymptotic solution (Eq. 3.5), which is seen to be a good approximation even for $p = 1$.

Table 1. The exact solutions of the equation $Z'(X_p+iY_p) = 2$ and the asymptotic solutions (Eq. 3.5): $X'_p+iY'_p$ for $p \leq 10$.

p	X_p	Y_p	X'_p	Y'_p
1	1.4467	-0.6020	1.3979	-0.6342
2	2.3583	-1.7906	2.3403	-1.7782
3	2.9711	-2.4909	2.9602	-2.4818
4	3.4711	-3.0418	3.4634	-3.0349
5	3.9050	-3.5106	3.8991	-3.5051
6	4.2939	-3.9256	4.2891	-3.9212
7	4.6496	-4.3019	4.6456	-4.2981
8	4.9793	-4.6486	4.9759	-4.6453
9	5.2882	-4.9716	5.2852	-4.9687
10	5.5797	-5.2753	5.5770	-5.2727

Many authors have described their experimental results either by using a first pole approximation, or by using a few of the lowest order modes. In the case of a drifting plasma, the mode with $p = -1$ may move in the same direction as the $p = 1$ mode. These two modes are then often called the slow and fast mode, respectively. For large temperature ratio ($T_e/T_i \to \infty$), wave propagation will be well described by the fluid equations, and only the slow and the fast mode will be solutions of the fluid dispersion relation.

In the paper by Gould (1964) a special case is considered where waves are assumed to be excited with a double grid which specifies the boundary condition. Nevertheless, it seems that most of his conclusions are quite general. Although the first pole gives the most damped mode, he found that this mode is excited so strongly that the other modes are smaller until about $x \approx 75 \frac{c_i}{\omega}$; this corresponds to about 7 wavelengths of the first mode. Along the same distance the wave is damped by about a factor of 10^{-3}. Furthermore, he shows that the decay of the ion wave is eventually limited by an electron contribution, already at $x \approx 30\ c_i/\omega$ for a cesium plasma. This electron contribution is not included in Eq. 3.2. Altogether he concludes that the first pole approximation is fairly good in a distance neither too close nor too far from the exciter. Since the level of excitation on the various modes depends on the excitation method alone, it can also be concluded that to compare the theory with experimental results it is important to study this excitation. Since the propagation itself depends on $f_o(v)$ and T_e/T_i, it is also of importance to know these two quantities.

3.2. Free-streaming model

Another weak point in the experiment by Wong et al. was discussed by Hirshfield and Jacob (1968). According to this work the experimental result could as well be explained by a "free streaming model", i.e. by the Vlasov equation without the collective term:

$$\frac{\partial f}{\partial t} + v \frac{\partial f}{\partial x} = 0. \qquad (3.6)$$

The solution of this equation solved as a boundary problem with the boundary condition: $f(x=0,v,t) \equiv g(v,t)$
is: $f(x,v,t) = g(v,t-x/v)$.
Since the collective term is proportional to T_e/T_i, the simple free-streaming equation (3.6) is exact for $T_e = 0$, and obviously a good approximation when T_e/T_i is sufficiently small. A formal solution to the Vlasov equation (3.2) including the collective term is (see III):

$$f(x,v,t) = g(v,t-x/v) + c_s^2 \frac{1}{n_o} f_o'(v) \frac{1}{v} \int_o^x \frac{\partial n(x',t')}{\partial x'} dx',$$

from which it can be seen that Eq. 3.6 also should be a good approximation for small values of x, except in cases where $\frac{\partial n}{\partial x} \to \infty$ for $x \to 0$ (see II). In the experiment by Wong et al. $T_e/T_i \simeq 1$. Then according to Hirshfield and Jacob the difference between the two solutions is too small to be observable in an experiment. In fact, it turns out (Jensen and Michelsen 1972) that the "waves" described by Eq. 3.6 undergo a stronger damping far from the exciter than waves described by the Vlasov equation (3.2), i.e. when a collective term is included in Eq. 3.6. When the collective forces get stronger, which happens when T_e/T_i increases, the damping gets smaller, and eventually vanishes for $T_e/T_i \to \infty$, in which case the fluid equations describe the wave propagation exactly. From this point of view the terms "Landau damping" or "collective damping" are somewhat misleading since the heavy damping is due to phase mixing of freely streaming particles, while the collective behaviour, in f ct, reduces this damping. The energy exchange between potential energy and ion kinetic energy in an ion-acoustic wave was recently considered (Jensen and Lynov 1979), and it was concluded that the kinetic absorption spectrum in velocity space is broad and rather complicated. The simple picture of Landau damping (e.g. Dawson 1961), as an interaction between the wave and particles of velocity close to the phase velocity is therefore rather useless for strongly damped waves as e.g. ion-acoustic waves when $T_i \lesssim T_e$.

3.3. Exact solutions and experiments

Finally, it was pointed out by Andersen et al. (1971) that a conclusive experiment of the effect of the collective term in the Vlasov equation could be performed only if the ion velocity distribution function of both the main plasma $f_o(v)$ and the initial perturbation, $g(v)$, as well as the electron temperature, T_e, were measured. This was done in the experiment by Andersen et al. (1971), for a case where the perturbation was a short pulse

(δ-function) and the results were compared with exact calculations utilizing the technique based on the use of Green's function. The main conclusion that collective effects were observed was, however, based on a direct measurement of the perturbation of the ion velocity distribution function, f(v). For velocities higher than the pulse velocity negative values of f(v) were observed. Since this showed up as a local minimum of the observed pulse, it was called an "undershoot", and it was shown that a similar result could not be obtained from the equation describing free-streaming particles (Eq. 3.6).

Further investigations of the propagation properties of linear ion-acoustic waves were performed by the author and co-workers and are reported in papers II and III.

In paper II the evolution of the ion velocity distribution function was calculated and measured for a case where the initial perturbation consisted of a steplike discontinuity of plasma density. In the experiment both a local minimum (undershoot) as also seen by Andersen et al. (1971), and a local maximum (overshoot) were observed; both of these could be explained theoretically in terms of the collective interaction. A detailed physical explanation of the undershoot was given by Jensen (1976). In the experiment it was estimated that the temperature ratio $T_e/T_i \simeq 1.5$, but still the perturbation due to the collective interaction was observed and calculated to be fairly small. If we consider the full Vlasov equation without linerization we see that the sole nonlinear term is the same as the one giving the collective effects. Since these are small, the nonlinear effect should be negligible. This was tested experimentally by increasing the perturbation level to about 100% ($\Delta n/n_o \simeq 1$), and no change of the curve shapes was observed.

In paper III a general investigation of wave propagation was performed with special attention given to sinusoidal waves. An exact solution of Eq. 3.2 was obtained with the boundary condition $f(x = 0, v > 0, t) = g(v)e^{i\omega t}$, by performing convolution integrals of the Green's functions. The calculations showed that the ion-acoustic waves in general were damped. For $T_e = 0$ the

damping is clearly caused solely by phase mixing of freely streaming ions and therefore the ratio δ/λ, i.e. damping length divided by wavelength, is given roughly by $v_{ph}/\Delta v$, where Δv is the width of the g(v) function. For $T_e > 0$, collective interaction, of course, plays a role in the wave damping. However, it can easily be seen that by assuming a proper g(v) function, one can get the same Green's function for the density for $T_e = 0$ as the one we obtain for $T_e > 0$. This also means that we can obtain the same amplitude curve versus distance for the case $T_e = 0$, as the one we obtain for $T_e > 0$. More generally it was shown for an initial value problem by Pécseli (1974), by using van Kampen (1955)-Case (1959) type solutions, that any amplitude function, n(k,t) which can be Fourier transformed can be obtained by choosing a proper g(v). For a boundary value problem it was shown by Hsuan and Jensen (1973) that a pure exponential damping for all x-values, i.e. a solution of the type $n(x) = \exp(ikx)$ with k complex, is not possible. This is in agreement with a more general statement, that for any amplitude function $n(\omega,x)$, from which the inverse Laplace transform can be found, a g(v) function can be obtained from this Laplace transform. This can easily be seen from a derivation similar to that of Pécseli (1975). It should be noted here that in the original paper by Landau (1946), where asymptotic solutions of the type $\exp(i\omega t)$ were obtained, it was assumed that g(v) and $df_o(v)/dv$ were holomorphic functions, an assumption which is not introduced in the van Kampen-Case solution method.

Further detailed numerical calculations based on the analytical result obtained in III and by Jensen and Michelsen (1972) showed, however, that when the perturbation function, g(v) and the zero-order distribution, $f_o(v)$, were both chosen to be drifting Maxwellians, and $T_e/T_i \gtrsim 1$, the resulting phase velocity and damping coefficient were in good agreement with a "first pole approximation" when measured a few wavelengths from the wave exciter position. On the other hand, when more complicated g(v) and $f_o(v)$ functions were chosen, the exact calculations gave results very different from the first pole approximation. It has been shown experimentally by Christoffersen (1971) that a variety of g(v) functions can be obtained depending on plasma parameters,

on dc-bias of the exciter grid,etc. Similar to the mentioned numerical calculations it has been observed in many experiments, Wong et al. (1962 and 1964), Andersen et al. (1968), Sato and Sasaki (1972), Buzzi (1974), Michelsen et al. (1978) and in III that the first pole approximation describes the results quite well in a distance not too close to the exciter. In all the experiments a strong damping is found and therefore only few wavelengths (~ 5 - 10) can be observed. The asymptotic behaviour is therefore of minor interest from an experimental point of view. From a theoretical point of view, however, one could claim that the "true" dispersion relation, if it exists, is obtained for large values of x, similar to the initial value problem as treated by Landau, where the first pole approximation gives the true asymptotic solution for large t. On the basis of the discussion above a general dispersion relation does not exist since it depends on g(v), i.e. the boundary conditions. However, if we assume that g(v) and $f_0(v)$ are drifting Maxwellians it can be shown analytically (see Appendix A) that asymptotically the density varies as $n(x,t) \sim \exp(-x^{2/3}-i\omega t)$ which means that the first pole approximation breaks down for large values of x. The same conclusion was obtained by Gould, but for another reason. He showed that the decay of the ion wave is eventually limited by a contribution associated with the electrons, which arises only if quasi-neutrality is not assumed. This electron contribution has also the asymptotic dependence $\exp(-x^{2/3})$.

3.4. Normal modes

It is of course of importance to know in which cases the first pole approximation can be used since this greatly simplifies calculations of problems where ion-acoustic waves are of importance. This is, e.g., the case in certain nonlinear calculations (Michelsen et al. 1978), or when ion-acoustic waves are used for diagnostics (Hsuan et al. 1975 and Schrittwieser 1978). We shall therefore discuss this problem in more detail.

As can be seer from III, the solution to Eq. 3.2 with the boundary conditions noted can be written as

$$n(x) = \frac{1}{2\pi i} \int_{-\infty-i\alpha}^{\infty-i\alpha} \frac{1}{k} M(\frac{\omega}{k}) e^{ikx} dk, \tag{3.7}$$

where

$$M(\frac{\omega}{k}) = \frac{\frac{\omega}{k} \oint_{-\infty}^{\infty} \frac{g(v)}{v-\omega/k} dv}{1-\frac{c_s^2}{n_o} \oint_{-\infty}^{\infty} \frac{f_o'(v)}{v-\omega/k} dv} + \eta, \tag{3.8}$$

and

$$\eta = \int_{-\infty}^{\infty} g(v) dv.$$

By closing the integration path in Eq. 3.7 in the upper half plane above all the poles (Gould 1964 and Nielsen 1969), we can in principle express n(x) as an infinite sum of all the residues, plus a contribution from the singularity in k = 0. Therefore, we can write

$$n(x) = \sum_{p=1}^{J} \frac{n_o}{c_s^2} \frac{\oint_{-\infty}^{\infty} \frac{g(v)}{v-\omega/k_p} dv}{\oint_{-\infty}^{\infty} \frac{f_o''(v)}{v-\omega/k_p} dv} e^{ik_p x} + \chi(x), \tag{3.9}$$

where k_p is the p'th solution of

$$1 - \frac{c_s^2}{n_o} \oint_{-\infty}^{\infty} \frac{f_o'(v)}{v-\omega/k_p} dv = 0;$$

$\oint$ means integration below the pole $v = \omega/k_p$, and $\chi(x)$ is the integral around the origin including all the poles from J+1 and

upwards. As discussed in III and also by others (Nielsen 1969 and Pécseli 1975) the solution (Eq. 3.7 and 3.8) is exact only when the boundary condition is specified with $g(v) = f_o(v) = 0$ for negative values of v. The velocity integrals in Eq. 3.8 can be expressed in terms of the plasma dispersion function (Fried and Conte 1961) if g(v) and $f_o(v)$ are Maxwellians or a sum of these. Since these functions are not identically equal to zero for negative velocities, the solution will be inexact, but a rather good approximation is obtained if $V_o > 2c_i$. In the experiment described in III, and in other ion-acoustic wave experiments performed in single-ended Q-machines, it is believed that under normal conditions the ion velocity distribution functions g(v) and $f_o(v)$ are truncated drifting Maxwellians. In the following we shall assume that g(v) and $f_o(v)$ both are drifting Maxwellian distributions with the same drift velocity, V_o. Therefore the v-integrals in Eq. 3.9 may be expressed in terms of the plasma dispersion function, Z, and we get:

$$n(\xi) = \sum_{p=1}^{L} \frac{2Z(u_p)}{\theta Z''(u_p)} \exp[i\xi/(u_p+u_o)] + \chi(\xi) \qquad (3.10)$$

where $u_o = V_o/c_i$ is the normalized drift velocity, $\xi = \omega x/c_i$ is the normalized distance from the exciter, and $u_p = \omega/c_i k_p$ is the normalized phase velocity determined from the dispersion relation:

$$1 - \frac{\theta}{2} Z'(u_p) = 0.$$

By using the relation (Fried and Conte 1961):

$$Z'(u_p) = -2[1 + u_p Z(u_p)],$$

we get from Eq. 3.10:

$$n(\xi) = \sum_{p=1}^{L} -\frac{1+\theta}{\theta(1+\theta-2u_p^2)}\exp[i\xi/(u_p+u_o)] + \chi(\xi).$$

From the asymptotic expansion for u_p (Eq. 3.5), it is easily seen that this sum diverges for $L\to\infty$ for all values of ξ. Therefore we can conclude that the solution for n(x) (Eq. 3.7) cannot be resolved into a sum of natural modes as is the case when the Vlasov equation 3.1 or 3.2 is solved as an initial value problem. The reason is that the contribution of the singularity in k=0 cannot easily be calculated. It is, however, interesting to consider the first few terms of Eq. 3.10, some of which are given in Table 2 for a case where $u_o = 3$. This velocity is higher

Table 2. The coefficients $2Z(u_p)/\theta Z''(u_p)$ and the exponents $i(u_p+u_o)^{-1}$ of the first few terms of Eq. 3.10 for $u_o = 3$ and $\theta = 1$. $p < 0$ indicate modes moving slower than u_o, but forward.

	$\frac{2Z(u_p)}{\theta Z''(u_p)}$		$\frac{i}{u_p + u_o}$	
p	real part	imag.part	real part	imag.part
1	0.2048	0.4883	-0.0299	0.2208
-1	0.2048	-0.4883	-0.2169	0.5597
2	0.0185	0.1154	-0.0561	0.1679
-2	0.0185	-0.1154	-0.4949	0.1774
3	0.0073	0.0668	-0.0595	0.1426
-3	0.0073	-0.0668	-0.4014	0.0047
4	0.0040	0.0470	-0.0595	0.1266
5	0.0025	0.0363	-0.0585	0.1151
6	0.0018	0.0296	-0.0572	0.1063
7	0.0013	0.0249	-0.0559	0.0993
8	0.0010	0.0216	-0.0545	0.0936
9	0.0008	0.0190	-0.0532	0.0887
10	0.0007	0.0170	-0.0520	0.0846

than the phase velocity of the three lowest backward-moving modes, and they will therefore move forward in this case. These

modes are indicated by negative p-values. In Fig. 2 the amplitude of n(x) is given. The full line is the exact solution found in III (Fig. 3c), while the dotted line is the first pole approximation, the dotted and dashed line includes also the first mode going backward with respect to u_o to the first pole approximation, and finally the dashed curve is the sum of the first 16 terms plus the three backward-moving waves. That is, by taking only the first few terms, a good agreement to the exact result is obtained for $\xi > 10$. If more terms are taken into account only a poor approximation is obtained. This resembles a normal asymptotic expansion, which often diverges if an infinite number of terms are taken into account but can be a good approximation if just the right number of terms are used.

3.5. Conclusion

In this chapter we have discussed linear ion-acoustic waves for cases when $T_e = T_i$. Most of the discussion was based on the assumption that both the zero-order and the perturbed ion velocity distribution function can be expressed in terms of Maxwell distributions where a drift velocity is included. Although it has been shown that a variety of distribution functions can be obtained in experiments, the drifting Maxwellians seem to be a fair approximation for most experiments. The exact solution to the Vlasov-Poisson equation with the above-mentioned approximations was found to describe the experimental results very well. It was also found that the commonly used first pole approximation gives results close to the exact solution, when the zero-order and the perturbed ion velocity distribution function both are drifting Maxwellian distributions. This explains why many experimental observations of ion-acoustic waves seem to be in agreement with the first pole approximation, in spite of the discovery that a resolution into normal modes is not possible even in the case in which smooth distribution functions as drifting Maxwellians are considered.

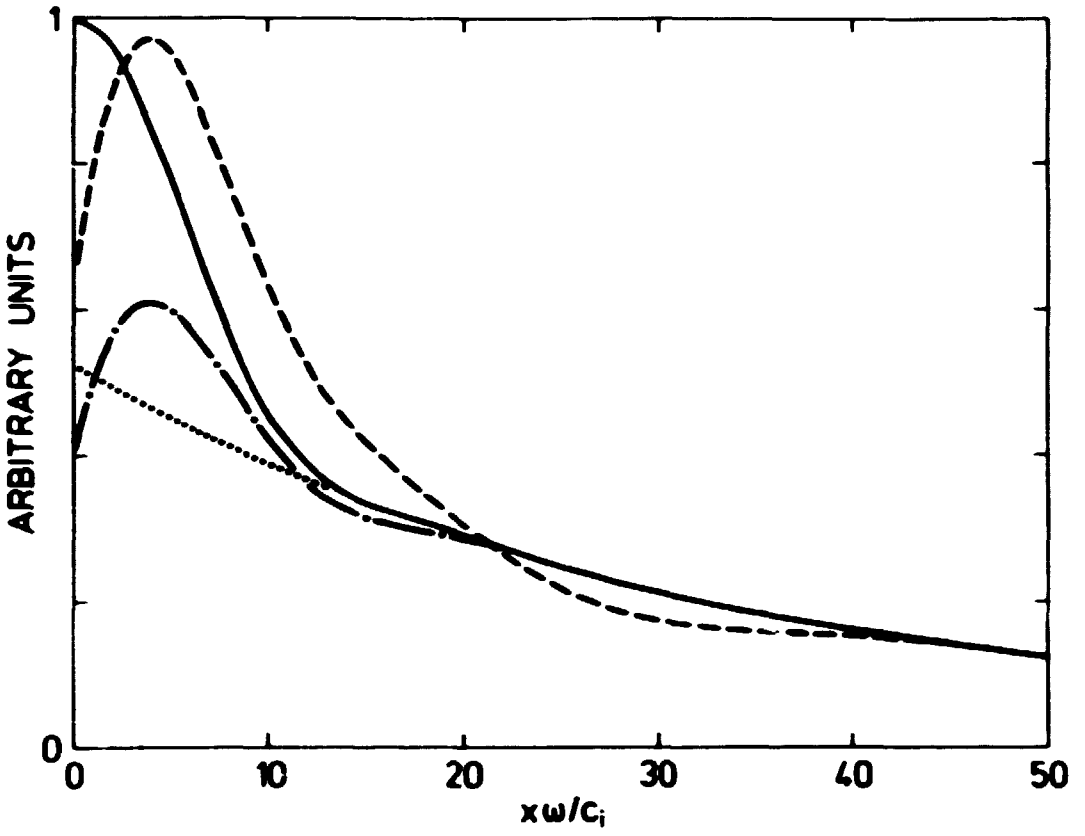

Fig. 2. Amplitude versus distance of an ion-acoustic wave. Drift velocity of $f_o(v)$ and $g(v)$, $V_o = 3c_i$. The solid line is the exact solution. The dotted line is the first pole approximation (fast mode). The dashed and dotted lines include both the fast and slow mode. The dashed line is the sum of the first 16 terms of the formal expression (Eq. 3.10) for a resolution into normal modes.

4. ION-ACOUSTIC WAVES IN A DENSITY GRADIENT

After the rather detailed discussion in the previous chapter on the propagation of ion-acoustic waves in a uniform plasma, we shall in this chapter discuss propagation in a non-uniform plasma, or more specifically in a plasma with a density gradient parallel to the direction of propagation. This problem has been studied by several authors in various contexts. Since it is difficult to find analytical solutions to the Vlasov-Poisson

equation even in the uniform plasma case, we would not expect it to be possible in a case where the zero-order quantities do have a spatial dependence. Nevertheless, Parkinson and Schindler (1969) solved these equations and found a dispersion relation for a case where the density gradient was produced in zero-order equilibrium due to a balance between gravitational and pressure forces. The reason for studying wave propagation in such a system arises from the idea suggested by D'Angelo (1968) that heating of the solar corona could be caused by absorption of ion acoustic waves excited near the solar surface. Parkinson and Schindler's calculations conclude that ion-acoustic waves propagating in a direction opposite to that of the density gradient are growing (i.e. unstable) when the wavelength is above a certain critical value, λ_c, which, for the case where $T_e \simeq T_i$, is $\lambda_c = 2\pi/k_c \simeq 6.22\ \ell_n$. Here ℓ_n is the e-folding length of the density gradient. This growth is known as hydrodynamic growth since it can also be found directly from the hydrodynamic equations. For wavelengths shorter t an the critical one the collisionless damping will exceed the hydrodynamic growth and the wave will be damped. This growth (or damping) is a growth of wave potential, and since (when the electrons are considered as a fluid) we have that $\frac{e\phi}{\kappa T} \simeq \frac{n_1}{n_o}$, it means a relative growth (or damping) with respect to the density perturbation.

Also in connection with other problems there is considerable interest in wave propagation in non-uniform plasmas. For instance, in connection with discharge tube walls and other boundaries it is known that in some cases ion-acoustic waves are absorbed at such boundaries and in other cases they are reflected. This problem was studied by Gary et al. (1976) and their paper contains other references concerning these problems. By using a fluid dynamic approach to the problem, Gary et al. found that ion-acoustic waves should not be reflected at a plasma sheath as long as the wavelength is short compared to the sheath thickness. In connection with problems of absorption and reflection of laser radiation in inhomogeneous plasmas, ion-acoustic waves are known to play an important role (see, for instance, Tsytovich et al. 1973).

4.1. Experiment

In order to investigate the propagation of ion-acoustic waves in a non-uniform plasma the experiment described in IV was performed. The experiment was conducted in the Q-machine in single-ended operation and a part of the plasma column was surrounded by a metal cylinder coaxial with the plasma column. When this cylinder was biased negatively a density gradient along the axis was observed. The loss mechanism was not investigated in detail, but strong low-frequency oscillations were observed at the plasma edge. This indicates a gravitational instability generated by the $\underline{E} \times \underline{B}$ rotation, thus giving rise to an enhanced radial diffusion of ions across the magnetic field. The bias of the surrounding cylinder decreased the plasma potential, which infers an acceleration of the ions and a deceleration and eventually a reflection of the electrons, and therefore also a decreasing density. The e-folding length = $\ell_n \sim n/(dn/dx)$ could be varied by varying the cylinder bias.

In this plasma ion-acoustic waves were excited by a grid precisely as in the case of wave excitation in a homogeneous plasma (see e.g. III), and the phase velocity and the growing or damping of the waves were measured as a function of frequency. For wavelengths $\lambda << \ell_n$ the propagation properties were found to be identical to the case where the plasma is uniform. Since the propagation of ion-acoustic waves should also be independent of density (at least for $\lambda >> \lambda_D$), one should indeed expect the propagation to be independent of the density gradient when $\ell_n >> \lambda >> \lambda_D$. In this range it was found that the relative damping distance δ/λ and the phase velocity $v_{ph} = \omega/k$ were independent of frequency as expected from theory. A detailed theoretical analysis for wave propagation in this frequency range could in principle be performed in the same way as discussed in Chapter 3, but using a WKB-approximation.

For wavelengths $\lambda \gtrsim \ell_n$ it turned out that a kinetic theory directly describing the experiment in question and similar to the theory by Parkinson and Schindler (1969) was not obtainable. The experimental results are therefore partly compared with the

theoretical results obtained by Parkinson and Schindler and partly to a dispersion relation derived from a simplified fluid theory. Although a fluid theory cannot substitute a correct microscopic analysis, it has been shown by Weitzner (1964) and Liboff (1962) that it is essentially correct in describing the zero-order state and the wave phenomena at long wavelengths. In the following we shall first discuss the zero-order state and then the long wavelength limit.

4.2. Zero-order solution

In paper IV the following zero-order fluid equations were assumed:

$$\frac{\partial}{\partial x}\,(n_o v_o) = -\gamma n_o$$

$$n_o v_o \frac{\partial v_o}{\partial x} + c_s^2 \frac{\partial n_o}{\partial x} = 0,$$

where n_o and v_o are the zero-order ion density and velocity, respecitively, γ is a constant which accounts for the radial losses and $c_s^2 = \frac{\kappa(T_e+T_i)}{M}$. The solution can be written as

$$(v_o^2 - c_s^2)\,\frac{dv_o}{dx} = c_s^2\gamma \qquad (4.1)$$

$$n_o(x) = \frac{N_o V_o}{v_o(x)}\,\exp[-\gamma \int_o^x \frac{dx'}{v_o(x')}], \qquad (4.2)$$

where N_o and V_o are the density and velocity, respectively, at $x = 0$. Equation 4.1 can be solved directly with respect to x, giving

$$x = \frac{1}{3\gamma c_s^2}\,[v_o^3 - V_o^3 - 3c_s^2(v_o - V_o)].$$

Substituting (4.1) into (4.2) and performing the integration yields:

$$n_o(x) = N_o \exp\left[-\frac{v_o^2(x) - V_o^2}{2c_s^2}\right].$$

From this expression or from the curves in Fig. 3, it is seen that $v_o(x)$ varies much more slowly with x than does $n_o(x)$. The same effect was seen in the experiment (IVb, Fig. 1).

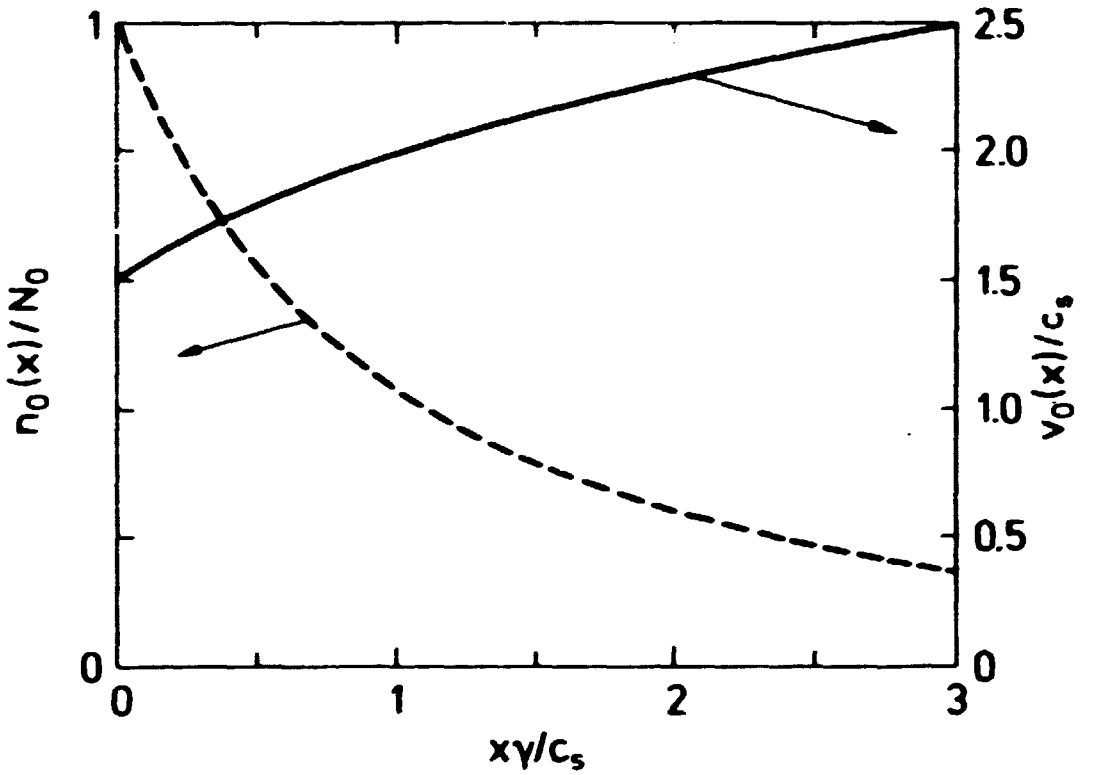

Fig. 3. The normalized density $n_o(x)$ and velocity $v_o(x)$ calculated from the zero-order fluid equations. $V_o/c_s = 1.5$.

A zero-order solution can also be found from a Vlasov model if, e.g., it is assumed that the zero-order E field is constant. Then we have the equation:

$$v\frac{\partial f_o}{\partial x} + \frac{eE}{M}\frac{\partial f_o}{\partial v} = -\gamma f_o,$$

where we have again introduced a loss term γ. This equation has the general solution:

$$f_o(x,v) = \exp[\psi(v^2 - 2\frac{eE}{M}x) - \frac{\gamma M}{eE} v],$$

where ψ is an arbitrary function. If the distribution function f_o is assumed to be a drifting Maxwellian at $x = 0$, i.e. $f(o,v) = \exp[-(v-V_o)^2]$ we get a solution:

$$f_o(x,v) = \exp[-(\sqrt{v^2-2ax} - V_o)^2 + \frac{\gamma}{a}\sqrt{v^2-2ax} - \frac{\gamma v}{a}],$$

where $a \equiv eE/M$.

4.3. First-order solution

In paper IVb the first-order equations were also solved, and a dispersion relation was calculated, under the assumption that the variation of the zero-order drift velocity was negligible compared to the density variation, as discussed above. The dispersion relation can be written as a quadratic equation in k (ω is real and k is complex):

$$(\omega-\alpha kc_s)[(\omega-\alpha kc_s) + i\frac{\gamma}{\alpha^2-1}] - kc_s^2[k + i\frac{\alpha\gamma}{(\alpha^2-1)c_s}] = 0,$$

where $\alpha = V_o/c_s$.

Equations 7 and 8 in IVb are derived from this dispersion relation under the assumption that the term $i\gamma/(\alpha^2-1)$ can be neglected. This turns out to be difficult to justify, but the exact solution is easily found to be:

$$c_s k = \alpha\beta \pm [(\alpha\beta)^2 - \omega\beta]^{\frac{1}{2}}, \qquad (4.3)$$

where

$$\beta = \frac{1}{\alpha^2-1}\left(\omega + i\frac{\gamma}{\alpha^2-1}\right).$$

Since the dispersion relation is appropriate only for long wavelengths, i.e. $\lambda \gtrsim \ell_n = (\alpha^2-1)c_s/(\gamma\alpha)$, we may assume $\omega << \gamma/(\alpha^2-1)$ and get:

$$c_s k = \begin{cases} \dfrac{\omega}{\alpha+1} - \dfrac{i\gamma}{2(\alpha+1)^2} & \text{(fast mode)} \\ \dfrac{\omega}{\alpha-1} + \dfrac{i\gamma}{2(\alpha-1)^2} & \text{(slow mode).} \end{cases}$$

That is, we get the two modes as in the case without density gradient with phase velocities: $v_{ph} = \omega/k = v_o \pm c_s$. The fast mode has a $k_i < 0$ and is therefore, a growing mode, while the slow mode is damped. In the experiment a growing mode was observed and the growth rate was seen to increase with increasing density gradient. Although a correct quantitiative agreement cannot be expected, it is seen from this result, and from the various details in paper IV, that the simple fluid equations give a qualitatively correct description of the wave growth phenomena.

In Chapter 3 it was pointed out that the wave propagation close to the exciter was described mainly by the free-streaming equation (3.6) and, therefore strongly dependent on the g(v)-function. Since the grid was positioned outside the density gradient region in the experiment, the value of this gradient should not affect the g(v)-function. This was also checked experimentally.

As mentioned earlier in this chapter, a fluid description should be essentially correct for very long wavelengths, according to Weitzner (1964) and Liboff (1962). This means that if the fluid equations are solved, e.g. as a boundary value problem, the sol-

ution will essentially be correct within a distance of the order of a wavelength. A solution to the first-order fluid equations as given in IV, when solved as a boundary value problem with the boundary conditions: $\zeta(x=0)$ and $v(x=0)$ and with a time variation $\exp(-i\omega t)$, can be found to be:

$$\zeta(x) = \frac{(Ak_1 + B)\exp(ik_1x) - (Ak_2 + B)\exp(ik_2x)}{c_s^2\ (\alpha^2 - 1)\ (k_1 - k_2)},$$

where $\zeta(x) = n(x)/n_o$ is the relative density perturbation, k_1 and k_2 are the two solutions to the dispersion relation (4.3), and the constant A and B are given by:

$$A = c_s^2\ (\alpha^2 - 1)\ \zeta(x=0)$$

$$B = -[\omega + \frac{i\gamma}{\alpha^2-1}\ (\alpha^2 + 1)]\ v(x=0) - [\omega + \frac{i2\gamma}{\alpha^2-1}]\ V_o\ \zeta(x=0).$$

For $\alpha \leq 1$ the k_2-mode can be neglected and the solution will be reduced to $\zeta(x) = \zeta(x=0)\exp(ik_1x)$ which is just the growing mode.

4.4. Conclusion

It was shown that it is possible to produce a variable axial density gradient in a Q-machine plasma by a negatively biased tube which surrounds the plasma column. The steady state of the plasma was found to be well described by a simple one-dimensional fluid model with a loss term included. Ion-acoustic waves of wavelengths much shorter than the e-folding length of the density gradient were seen to propagate as in the case without a density gradient. The hydrodynamic growth observed for long wavelengths was qualitatively described by a fluid model. An interesting observation from the experiment was that the growth-damping transition occurs at a critical wavelength $\lambda_c \simeq 2\pi\ell_n$ in agreement with the calculations of Parkinson and Schindler (1969), which may mean that these calculations have a broader validity than was originally assumed. The results from the ex-

periment have recently been used for describing some details in the solar wind spectra (D'Angelo 1976).

5. ION-BEAM PLASMA

The effect of ion or electron beams injected into a plasma has received much attention for several years, since such a beam-plasma system may give rise to plasma instabilities of the microscopic kind. Various kinds of instabilities may be excited depending on the type of beam particles (ions or electrons), the beam velocity, the densities and temperatures of beam and plasma, respectively, the beam direction with respect to the magnetic field, etc. In this chapter we shall consider cases where the wave vector is parallel to the beam direction and to the magnetic field. Furthermore, we shall consider only the low frequency modes which may be unstable due to the interaction between an ion beam and the plasma. Such ion-beam plasma systems were investigated theoretically by the author and co-workers in the papers V - VII. References to other work relevant to this subject can be found in these papers.

It is of course of general interest to study beam instabilities. Our interest in these problems was especially caused by the possibility of creating a plasma with a double-humped ion velocity distribution function, i.e. an ion-beam system in a Q-machine, which may be unstable under certain circumstances. Since it is possible to follow the development of such an instability in detail in this plasma, it is of interest to accurately calculate the development of perturbations in space and time. Experiments on this instability in Q-machines have been performed by Baker (1972 and 1973), and by Christoffersen and Prahm (1973), and also in DP-machines by several authors as mentioned in VI.

Preliminary results on calculations for an unstable plasma were presented by Michelsen and Prahm (1971). Very careful measurements in a stable Q-machine plasma with a double-humped ion distribution function were performed by Sato et al. (1975 and 1977).

5.1. Pulse propagation

In this chapter a short review of the essential conclusions of papers V - VII shall be given. In paper V we reported on a calculation of the development of a narrow perturbation in a plasma, which was unstable with respect to an ion-beam instability, i.e. the Green's function for the problem was found. The calculations were based on the linearized Vlasov-Poisson equations as discussed in Chapter 3, and they were performed as an initial value problem. The validity of the results was of course limited to the time period until the instability reached a nonlinear level. It was found that the excited narrow perturbation develops into two kinds of perturbations. A narrow perturbation consists of a broad band of frequencies from zero up to an upper limit determined by the original width of the perturbation. For the ion-beam instability only the lower frequencies will be unstable. The high frequency part of the pulse will therefore propagate as a damped pulse in a self-similar way, i.e. as $h(x/t)/t$ in agreement with the result found for propagation in a stable plasma (Andersen et al. 1971). The low frequency part of the pulse propagates as an oscillating growing perturbation. It was calculated in systems of references in which the instability was an absolute one (i.e. growing for all time), and in which it was convective (i.e. initially growing but eventually damping away). The results were found to be in qualitative agreement with the experimental results of Baker (1972, 1973).

In paper VI similar calculations were performed, but with special attention given to the importance of the initial conditions. Two kinds of initial conditions were especially considered, namely, one corresponding to density modulation and the other to velocity modulation. The main background for these investigations was some experimental results obtained by Sato et

al. (1975 and 1977). They reported an experiment on an ion-beam plasma system, performed in a double-plasma-operated Q-machine, where spatial growth of a perturbation was found even if the plasma was predicted to be stable according to standard stability theories. The growth was explained by linear beam bunching. This occurs in the case of velocity modulation, and growth is present for the ballistic contribution as well as for the collective modes. Since an experimental method of classifying a plasma as stable or unstable has been to observe the behaviour of an excited pulse, we found it of interest to perform exact calculations of such propagation. Our results supported the explanation of Sato et al. (1975 and 1977), that velocity-modulated pulses may grow for some time (or in some part of space) even in stable plasmas. In the case of velocity modulation a fast positve pulse and a slower negative one appear. Both grow initially, even under stable conditions, and reach a maximum amplitude. In the unstable situation, the slow pulse interacts with the plasma mode and forms the unstable mode, which continues to grow. The unstable mode consists of a negative pulse and a somewhat slower and smaller positive contribution. In the case of density modulation, growth appears only in the unstable situation. The unstable mode is similar to that obtained for velocity modulation but the polarity alters.

5.2. Sinusoidal wave propagation

In paper VII the calculations were extended to include propagation of sinusoidal waves in stable and unstable plasmas. Again the various kinds of modulation were investigated. The theory applied to this problem was similar to that in III and V but somewhat simpler and furthermore generalized to include unstable plasmas. In the experiment mentioned above performed by Sato et al. (1975 and 1977) both pulse propagation and sine wave propagation were investigated. Also for the sinusoidal wave propagation spatial growth was found in the case of a stable plasma. For this reason we especially concentrated the calculations on pure velocity modulation and for comparison also included pure density modulation. The excellent agreement

between the experimental results by Sato et al. (1975 and 1977) and our numerical results can be seen in Figs. 4 - 7 for various parameter cases. For a detailed discussion of the calculations and of the fine structures of the obtained result see paper VII and Jensen et al. (1978).

5.3. Conclusion

In this chapter various calculations on ion-acoustic wave and pulse propagation in an ion-beam plasma have been discussed. Special attention has been given to the importance of the boundary conditions, especially the cases characterized as density modulation and velocity modulation. For the latter case it was found that wave growth due to beam bunching could occur even in a stable plasma. The strength of the mathematical model was seen by comparing the results to the experimental measurements obtained by Sato et al. (1975 and 1977).

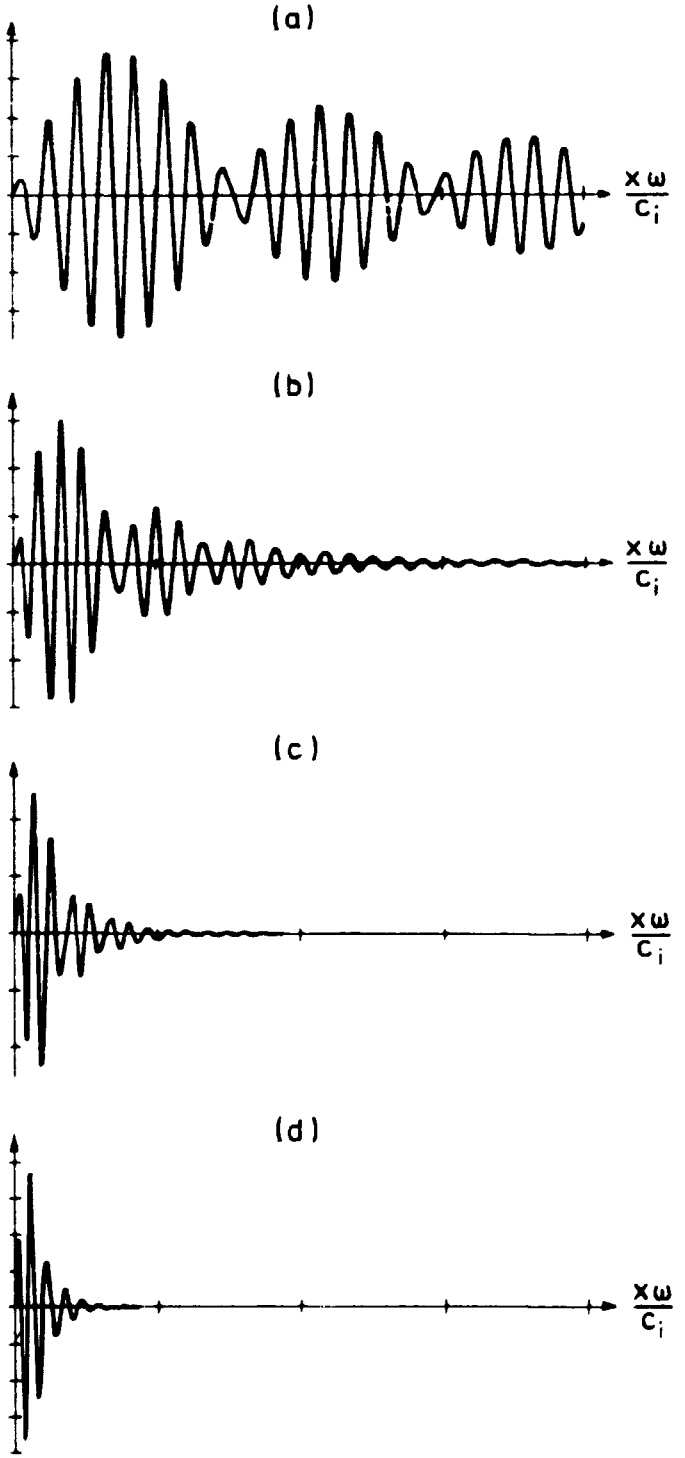

Fig. 4. The propagation of waves excited by velocity modulation for various beam velocities. The parameters of the distribution functions are chosen similar to those in the experiments of Sato et al. (1977) (*see Fig. 5;* for details see paper VII).

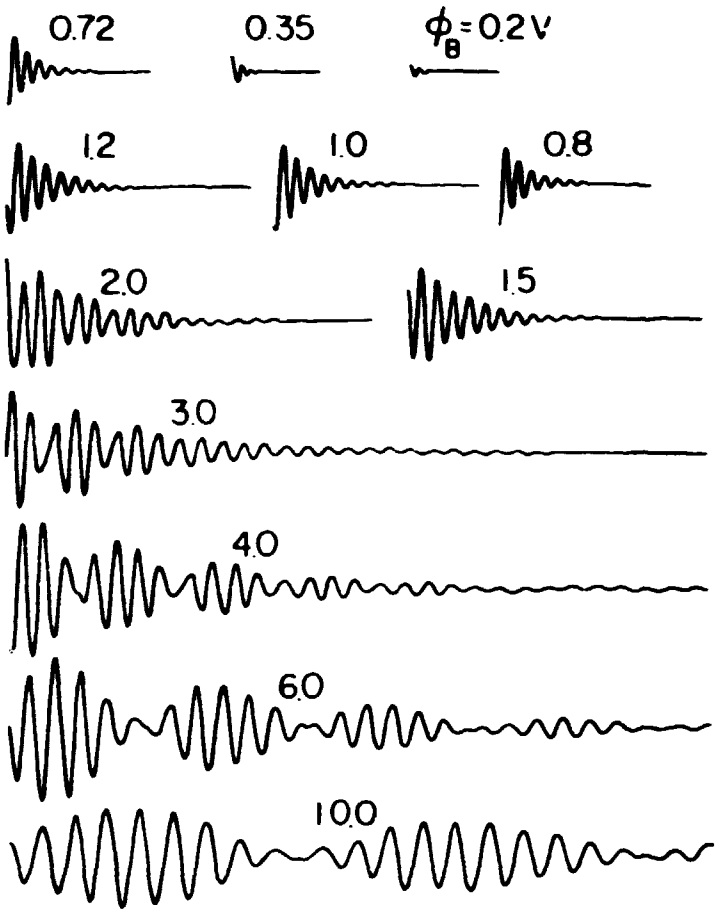

Fig. 5. Experimental results (Sato et al. 1977) of the spatial evolution of perturbations produced by a sinusoidal velocity modulation of $\omega/2\pi$ = 300 kHz for various beam energies, ϕ_B.

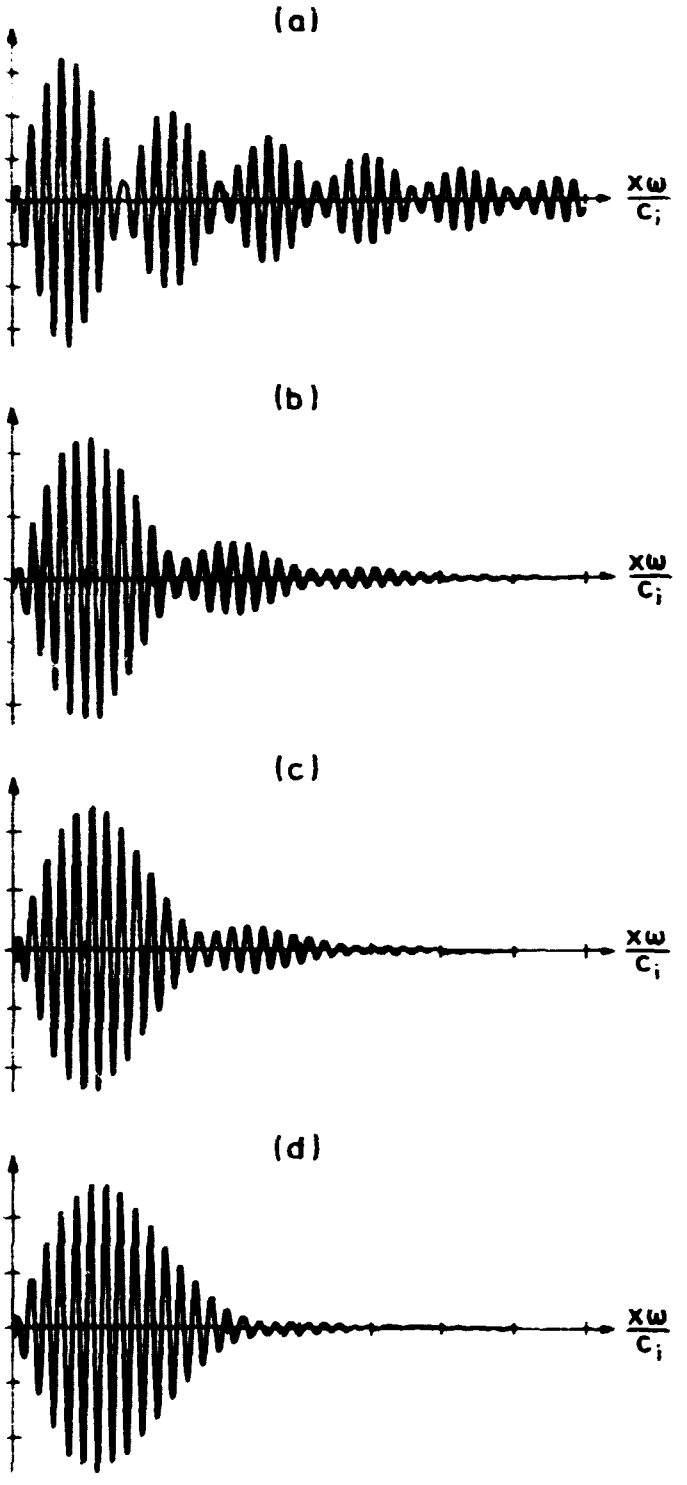

Fig. 6. The propagation of waves excited by velocity modulation for various relative beam densities, n_b/n_o. The parameters of the distribution functions are chosen similar to those in the experiments of Sato et al. (1977) (see Fig. 7, for details see paper VII).

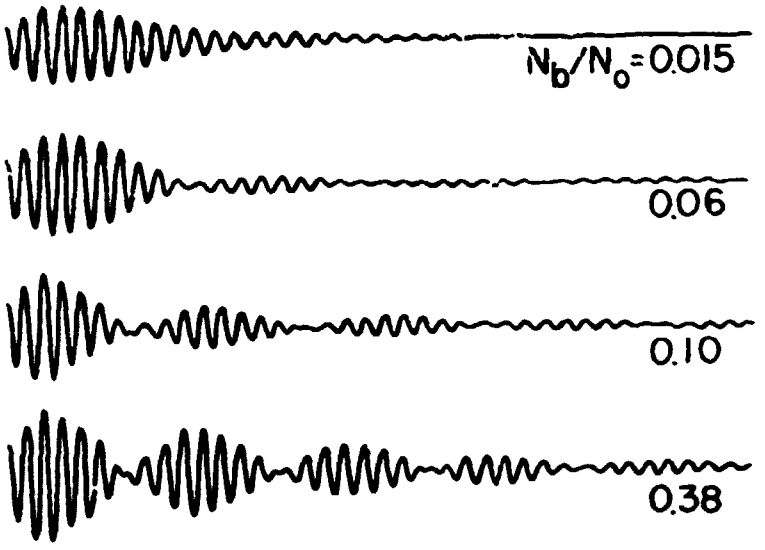

Fig. 7. Experimental results (Sato et al. 1977) of the spatial evolution of perturbations produced by a sinusoidal velocity modulation of $\omega/2\pi$ = 500 kHz for various relative beam densities, n_b/n_o.

6. ION-CYCLOTRON WAVES

In the previous chapter the ion-beam instability was discussed. However, if an ion beam traverses a plasma column various kinds of instabilities may arise. It has been shown by the author (paper VIII) that in a case where the beam density and temperature are equal to those of the background plasma, the electrostatic ion-cyclotron instability will have the lowest threshold for excitation when the beam velocity is just a little larger than the ion thermal velocity. This electrostatic ion-cyclotron instability is therefore often excited in an ion-beam plasma system, and this subject shall be treated in this chapter.

The electrostatic ion-cyclotron instability was first discovered by Motley and D'Angelo (1963) in a Q-machine experiment in which an electron current was drawn to a small target. A dispersion relation describing the measurements and derived from

the fluid equation was also given in this paper. An interpretation of the instability based on a kinetic approach was given by Drummond and Rosenbluth (1962). According to this theory the frequencies and the threshold beam velocity were in agreement with the experiment, but the theoretical growth rate was found to be much too low. Further experiments on the electron-beam-excited waves were e.g. performed by Levine and Kuckes (1966), Dakin et al. (1976) and Hatakeyama et al. (1980).

The ion-beam excitation may be of greater interest from a fusion plasma point of view. In a paper by Stix (1973) several instabilities were proposed which could arise under neutral beam injection, used for plasma heating and refuelling in fusion experiments. One of these was the electrostatic ion-cyclotron instability. These instabilites may be inconvenient to have since they may increase diffusion across the magnetic field. On the other hand they may also be an advantage in some cases since they can cause a faster and therefore desirable energy transport from the beam to the main plasma.

The ion-beam-excited ion-cyclotron instability was first observed by Ishizuka et al. (1974) in an experiment with very high beam energy (KeV range). In the interesting range where the beam energy is of the same order or somewhat higher than the plasma thermal energy the first experimental observations were performed by the author and co-workers (papers IX to X and Michelsen et al. (1976). Later on other groups have also investigated the ion-beam-excited instability (see e.g. Hendel et al. (1976) and Yamada et al. (1977).

6.1. Theory

In the previous chapters propagation only parallel to the magnetic field was considered, and it was assumed that the sole effect of the field was to make the problems one-dimensional. Electrostatic waves can of course also propagate obliquely with respect to the lines of force. Propagation of ion-acoustic waves at an angle to the magnetic field was investigated experi-

mentally by Hirose et al. (1970) in a discharge plasma with $T_e >> T_i$. In this plasma it was found that the frequency and wave number satisfied a simple dispersion relation:

$$1 = \frac{(k_{\parallel}c_s)^2}{\omega^2} + \frac{(k_{\perp}c_s)^2}{\omega^2-\omega_{ci}^2}, \qquad (6.1)$$

where $k_{\parallel}$ and $k_{\perp}$ denote the parallel and the perpendicular wave-numbers, respectively, and $c_s = (\kappa T_e/M)^{\frac{1}{2}}$ is the speed of sound.

This dispersion relation can easily be derived from the fluid equations under the same assumptions as introduced in Chapter 3, namely $(k\lambda_D)^2 << 1$ and $\frac{\omega}{k} << v_e$. In a plasma where $T_e \approx T_i$ it is necessary to use the dispersion relation based on the Vlasov-Poisson equations and this has been derived, for instance, by Stix (1962). However, the dispersion relation (6.1) can give some rough idea of the essential propagation characteristics. It is seen from (6.1) that a resonance (i.e. $k_{\parallel}\to\infty$) appears at $\omega = \omega_{ci}$, and that there is a stop band (i.e. no real solution for ω) for $\omega_{ci} < \omega < \sqrt{\omega_{ci}^2 + (k_{\perp}c_s)^2}$. In cylindrical geometry a Bessel function variation should be assumed in order to calculate the exact dispersion relation. However, if no azimuthal variation is assumed, we may use $k_{\perp} = p_{o,m}/r$ where $p_{o,m}$ is the m'th zero of the zero-order Bessel function and r is the radius of the plasma column. It can be shown that in this case we get exactly the same dispersion relation as (6.1).

By using the general dispersion relation derived from a kinetic theory (e.g. Stix 1962) more exact information about the wave propagation can be obtained. The main distinctions between it and the simple fluid description (Motley and D'Angelo (1963)) are the collisionless damping and the resonances at all the cyclotron harmonics ($\omega \approx n\omega_{ci}$). Concerning the collisionless damping, both Landau damping and cyclotron damping may occur for waves moving obliquely to the magnetic field.

In Fig. 8 the dispersion relation (6.1) is shown. The instability measured by Motley and D'Angelo (1963) satisfied the

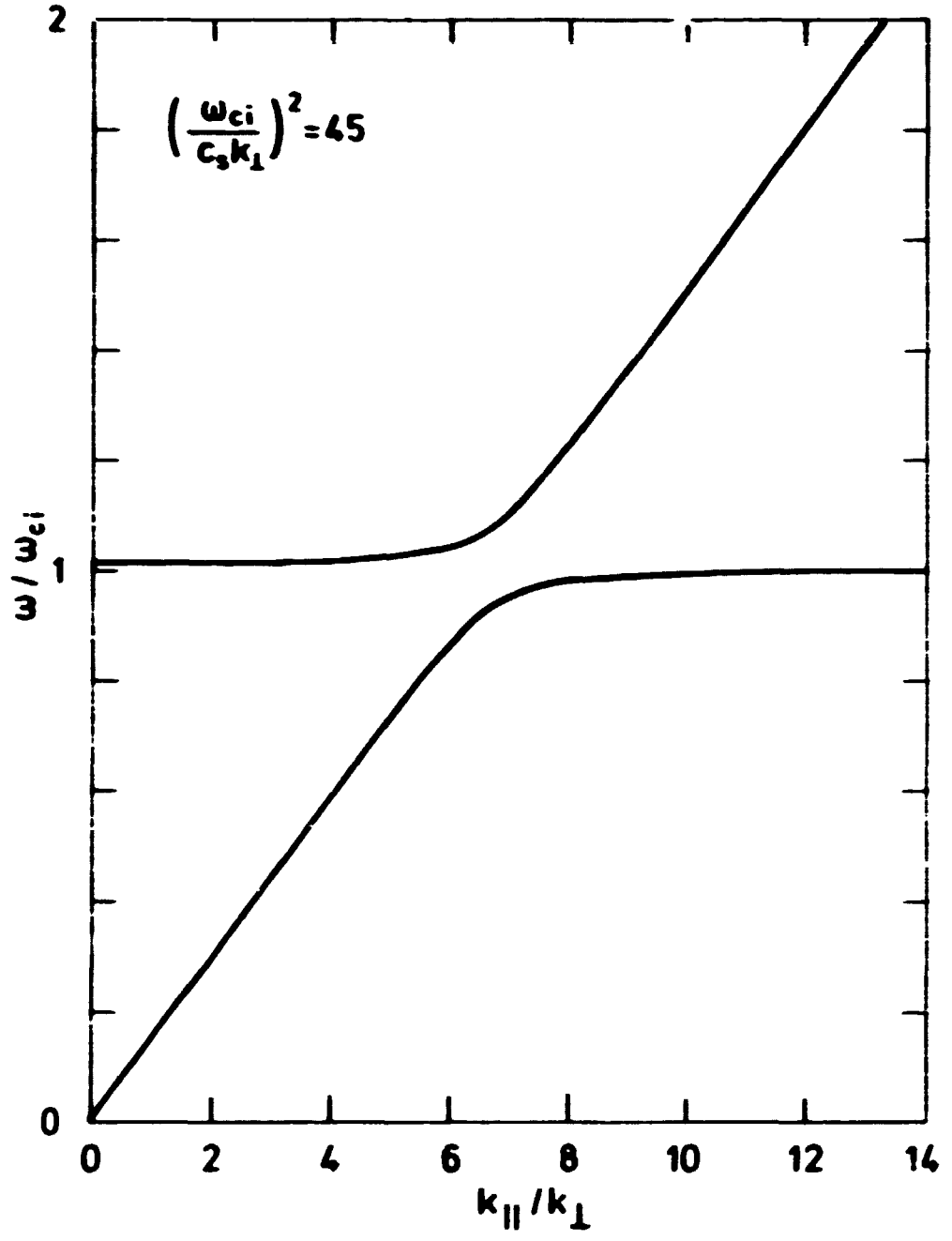

Fig. 8. Dispersion relation for ion-acoustic waves and for electrostatic ion-cyclotron waves derived from fluid equations.

point ($\omega = \sqrt{\omega_{ci}^2 + c^2 k_\perp^2}$, $k_\parallel \approx 0$), but no parallel variation could be measured.

The first theoretical discussion of the ion-beam-excited electrostatic ion-cyclotron waves was given by Weibel (1970). An analytical and numerical calculation of excitation thresholds and of the direction of propagation was later performed by the

author (paper VIII). The conclusions from these calculations were that many modes could be unstable in an ion-beam system, but only the two modes which have the lowest threshold were considered. For simplicity a system of two identical ion beams with opposite beam velocities was analyzed. For this case the instability with the lowest excitation threshold is found to be a purely growing mode with a phase velocity $\omega/k_{\parallel} = 0$. This mode has later been characterized as the cyclotron-cyclotron mode (Yamada et al. 1977). The other mode, which is an oscillating one with a higher threshold, is characterized as the resonant ion-cyclotron mode.

The physical explanation of the cyclotron-cyclotron instability is similar to that of the ion-beam instability discussed in Chapter 5, and to that of the well-known electron beam instability and is discussed by, for instance, Stix (1962). Initially, there is no energy either in the first-order particle motion or in the electric field. As the instability grows, particles pick up first-order energy at the expense of their zero-order streaming energy. The first-order particle motions lead to bunching, and the resultant space charge induces the electric field of the instability. These instabilities can also be explained in terms of negative and positive energy waves (see Rasmussen 1977).

The resonant ion-cyclotron mode is due to a somewhat different mechanism, and is the dominant one in cases where the beam density is small compared to the main plasma density. This mode is excited as a result of the coupling between the cyclotron mode of the main plasma, and the slow beam-acoustic mode, when the inverse Landau damping of the beam ions is larger than the cyclotron damping of the background plasma ions. The phase velocity for this instability is a little smaller than the beam velocity.

The dispersion relation for the electrostatic ion-cyclotron wave was, as mentioned, derived by Stix (1962) from the general dispersion relation

$$\underline{n} \times (\underline{n} \times \underline{E}) + \underline{\underline{K}} \cdot \underline{E} = 0, \qquad (6.2)$$

where $\underline{n} = \frac{\underline{k}c}{\omega}$ is the refractive index, $\underline{E}$ the electric field and $\underline{\underline{K}}$ the dielectric tensor. For electrostatic waves the electric field is parallel to the wave vector and Eq. (6.2) reduces to $\underline{n} \cdot \underline{\underline{K}} \cdot \underline{n} = 0$. If we choose the B-field to be in the z-direction, we may assume without loss of generality the wave vector to be in the x-direction, whereby $k_y = 0$. Now using $K_{zx} = K_{xz}$ we get

$$k_\perp^2 K_{xx} + 2k_\perp k_\parallel K_{xz} + k_\parallel^2 K_{zz} = 0.$$

The elements of the dielectric tensor were also calculated by Stix (1962). If we assume that the ion and electron velocity distribution functions can be written as sums of Maxwellians we get

$$k_\perp^2 + k_\parallel^2 + \sum_j \sum_{n=-\infty}^{\infty} \frac{\omega_{pj}^2 m_j e^{-\lambda_j} I_n(\lambda)}{\kappa T_\perp} A_{nj} = 0 \qquad (6.3)$$

$$A_{nj} = \frac{T_\perp}{T_\parallel} + \frac{(\omega - k_\parallel V_\parallel + n\omega_{cj}) T_\perp - n\omega_{cj} T_\parallel}{k T_\parallel} \left(\frac{m}{2\kappa T_\parallel}\right)^{\frac{1}{2}} Z(\alpha_{nj}),$$

where

$$\lambda_j = \frac{k_\perp^2 \kappa T_\perp}{\omega_{cj}^2 m_j}, \qquad \omega_{cj} = \left| \frac{Z_j e B_o}{m_j} \right|,$$

$$\omega_{pj} = \frac{n_j Z_j^2 e^2}{m_j \varepsilon_o}, \quad \alpha_{nj} \equiv \frac{\omega - k_\parallel V_\parallel + \omega_{cj}}{k_\parallel} \left(\frac{m_j}{2\kappa T_\parallel}\right)^{\frac{1}{2}},$$

$I_n(x)$ is the modified Bessel function, and $Z(\alpha_{nj})$ is the plasma dispersion function. The charge $Z_j e$, density n_j, drift velocity $V_\parallel$, and temperatures $T_\perp$ and $T_\parallel$ are to be evaluated for each type of particle. Various approximations have been used in order to simplify this dispersion relation (see, for example, paper VIII, IX, Perkins (1976), and Yamada et al. (1977)).

On the basis of the dispersion relation Eq. (6.3), it is possible to find the parameter range where the waves will be unstable

and therefore be excited spontaneously. Furthermore, from the real part of Eq. (6.3) some simplified dispersion relations for the real part of ω can be derived. However, this part can normally be derived easier from a fluid equation approach. For use in the next section, we just need the real part of the dispersion relation for the simple case where an ion beam with velocity V_b traverses a plasma with the much smaller velocity V_p and the density n_p. The total electron density is n_e and the perpendicular wavelength is called $k_\perp$. In this case we get

$$\omega^2 = (\omega_{ci}^2 + k_\perp^2 c_s^2 \frac{n_p}{n_e}) \ (1 + 2\frac{V_p}{V_b}). \qquad (6.4)$$

For a detailed derivation see Rasmussen (1977).

6.2. Experiments

Observation of the ion-beam-generated electrostatic ion-cyclotron instability in the case of a low energetic beam was first reported by Michelsen et al. (1976). This experiment was performed in the Q-machine running in double-ended operation as a double-plasma device. This means that the plasma column was separated into two parts by means of a negatively biased grid, which prevents the electrons from passing from one part to the other. Therefore, the plasma potential of one part of the column may be varied with respect to the other, and ions from the part of the column with the highest positive potential will be accelerated through the grid and penetrate the other part of the plasma column. The beam generated by this method excites the electrostatic ion-cyclotron wave. These events were observed using Langmuir probes connected to a spectrum analyzer, and the frequency of the observed instability was found to be in agreement with the simplified dispersion relation (Eq. 6.4).

In paper IX the instability was investigated in more detail using a different set-up. The ion beam was generated by means of an ion emitter (Sato et al. 1974), which is a platinum wire covered by a thin layer of sodium silicate. This ion emitter

emits sodium ions when heated to about 1100 K. The advantage of this method is that the plasma column may be terminated by the electrostatic ion energy analyzer (described in Chapter 2), and therefore the exact shape of the ion energy distribution function including the beam can be observed during the experiment. By measuring the ion distribution function it was found that the beam energy was given approximately by the ion emitter bias. This knowledge made it possible to test the instability criterion derived from the dispersion relation Eq. 6.3, and reasonably good agreement was found.

In the case of the electron-beam-excited electrostatic ion-cyclotron wave there have been some discussions concerning the theoretical explanation. Drummond and Rosenbluth (1962) found that the theoretical growth rate was too small to compete with various kinds of damping (neutral collisions, etc.). Levine and Kuckes (1968) found in an experiment that the electron beam velocity necessary for excitation of the instability, was increasing with increasing electron temperature in contradiction to the results derived from the theory of Drummond and Rosenbluth. Hatakeyama et al. (1977 and 1980) found experimentally that only the value of the magnetic field near the target of the electron current determined the frequency of the instability, while a variation of the B-field at a distance from the target made no difference.

These papers indicate that the excitation was due to some sheath instability mechanism. These problems have practically not been discussed in other papers on this instability, e.g. Dakin et al. (1976).

Similar problems do not seem to exist for the ion-beam-generated instability. An experimental study of the electron temperature dependence for the excitation threshold was published in paper X, and in some more detail by Michelsen et al. (1977). The electron temperature in these experiments was increased by microwave heating (Pécseli and Petersen 1973) and it was found that the beam energy necessary for excitation was decreasing with increasing electron temperature in agreement with the theory.

According to the dispersion relation (Eq. 6.4) the frequency of the instability should decrease with the beam energy. Experimental measurements together with the theoretical curve are shown in Fig. 9. For a constant beam energy we measured the instability frequency versus electron temperature, and some typical results are shown in Fig. 10, together with a theoretical curve derived from Eq. 6.4. It is seen that very good agreement between the measurements and the simple dispersion relation was obtained.

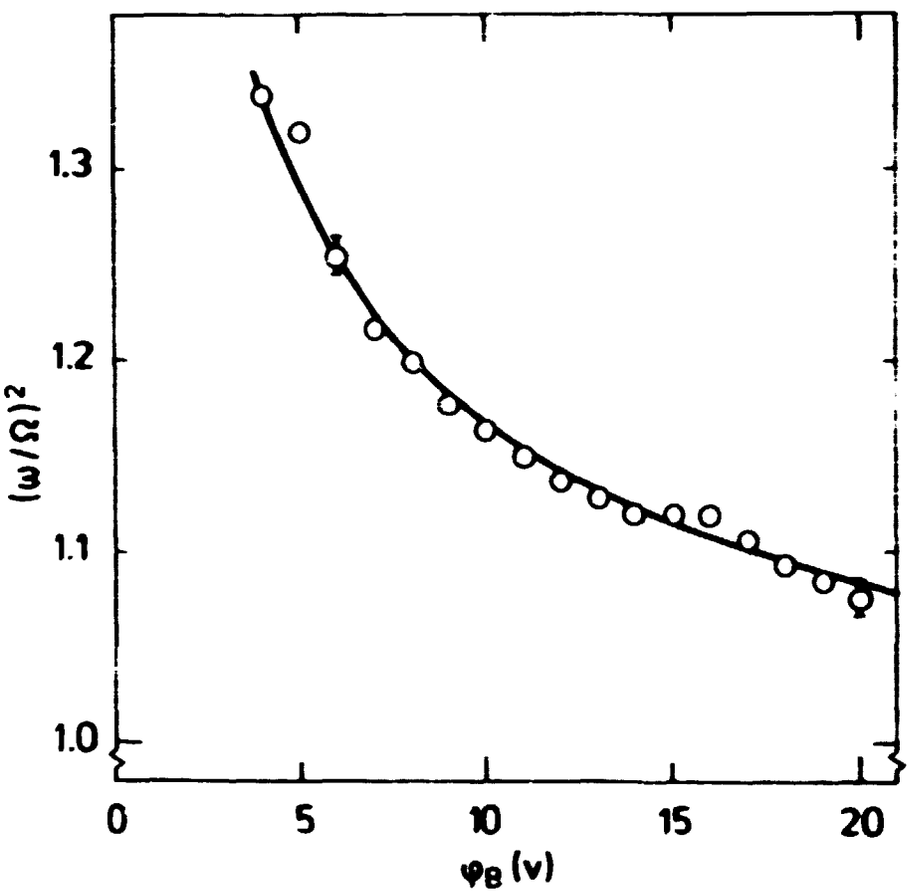

Fig. 9. Frequency dependence of the beam velocity.

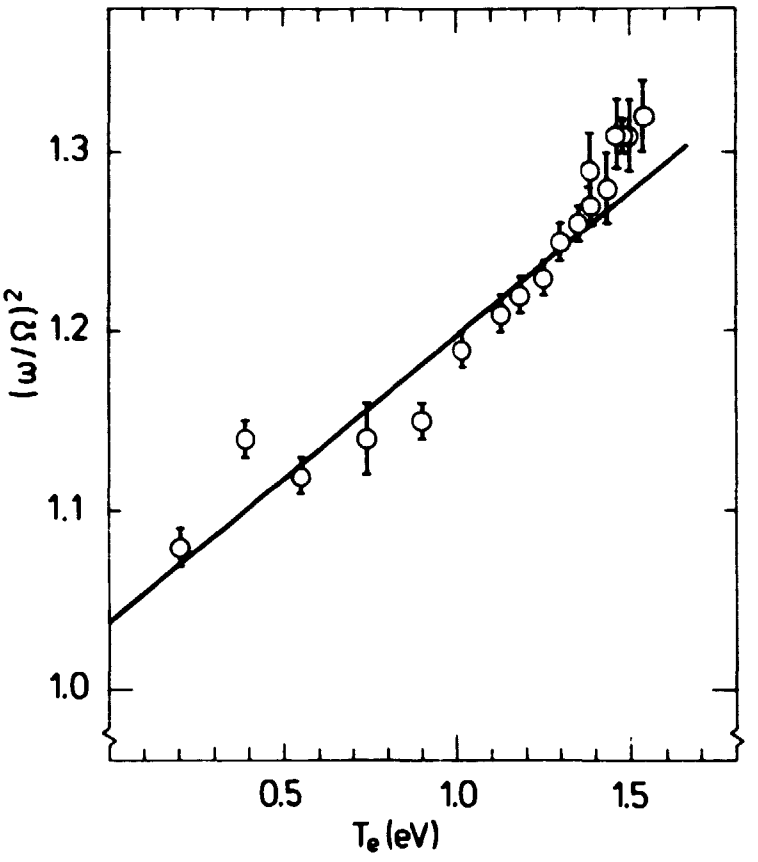

Fig. 10. Frequency versus electron temperature, T_e, for a constant beam energy, ϕ_B = 19 V.

6.3. Conclusion

From the general dispersion relation for electrostatic waves, a simplified dispersion relation was derived and for an ion-beam plasma the parameter range for instability of the ion-beam instability and the ion-cyclotron instability was found by numerical calculations. The electrostatic ion-cyclotron instability excited by an ion beam was observed experimentally. The frequency of the instability was shown to be consistent with a simplified dispersion relation derived from the fluid equations. By microwave heating of the plasma electrons and by using an electrostatic energy analyzer the dependence of the instability limits both with respect to the electron temperature and the beam velocity could be investigated. These were found to be in good agreement with simplified expressions derived from the general electrostatic dispersion relation.

ACKNOWLEDGEMENTS

The work reviewed in this report was carried out at the Physics Department of Risø National Laboratory. The author is grateful for the excellent working conditions provided. The main part of the work was performed in collaboration with colleagues from the plasma physics section and with visitors from other institutions. The author is very grateful to all these co-workers for their inspiring and encouraging co-operation. The author is especially indebted to N. D'Angelo, V.O. Jensen, P. Nielsen, H.L. Pécseli, J. Juul Rasmussen and N. Sato for their helpfulness and friendship. The critical reading of this manuscript by V.O. Jensen, J. Juul Rasmussen and J.P. Lynov is also appreciated, along with the skilled electronic assistance of K.-V. Weisberg and the technical assistance of M. Nielsen and B. Reher.

Part of this work was performed under the association Euratom-Risø National Laboratory.

REFERENCES

ANDERSEN, H.K., D'ANGELO, N., JENSEN, V.O., MICHELSEN, P. and NIELSEN, P. (1968). Phys. Fluids 11, 1177-1180.

ANDERSEN, S.A., JENSEN, V.O. and MICHELSEN, P. (1972). Rev. Sci. Instrum. 43, 945-947.

ANDERSEN, S.A., CHRISTOFFERSEN, G.B., JENSEN, V.O., MICHELSEN, P. and NIELSEN, P. (1971). Phys. Fluids 14, 990-998.

BAKER, D.R. (1972). Phys. Rev. Lett. 28, 1189-1192.

BAKER, D.R. (1973). Phys. Fluids 16, 1730-1739.

BUTCHELNIKOVA, N.S., SALIMOV, R.A. and EIDELMAN, Ju.I. (1966). Nucl. Fusion 6, 255-260.

BUZZI, J.M. (1974). Phys. Fluids 17, 716-723.

CASE, K.M. (1959). Ann. Phys. (N.Y.) 7, 349-364.

CHEN, F.F., ETIEVANT, C. and MOSHER, D. (1968). Phys. Fluids 11, 811-821.

CHRISTOFFERSEN, G.B. (1971). Risø Report No.250, 55-62.

CHRISTOFFERSEN, G.B. and PRAHM, L.P. (1973). Phys. Fluids 16, 708-710.

CHUNG, P.M., TALBOT, L. and TOURYAN, K.J. (1975). Electric Probes in Stationary and Flowing Plasmas: Theory and Application (Springer Verlag, Berlin), 150 pp.

DAKIN, D.R., TAJIMA, T., BENFORD, G. and RYNN, N. (1976). J. Plasma Phys. 15, 175-195.

D'ANGELO, N. (1968). Astrophys. J. 154, 401-403.

D'ANGELO, N. (1976). J. Geoph. Res. 81, 1779-1781.

DAWSON, J. (1961). Phys. Fluids 4, 869-874.

DRUMMOND, W.E. and ROSENBLUTH, M.N. (1962). Phys. Fluids 5, 1507-1513.

FRIED, B.D. and CONTE, S.D. (1961). The Plasma Dispersion Function (Academic Press, N.Y.), 419 pp.

FRIED, B.D. and GOULD, R.W. (1961). Phys. Fluids 4, 139-147.

GARY, S.P., ALEXEFF, I. and HSIEH, S.-L. (1976). Phys. Fluids 19, 1630-1634.

GOULD, R.W. (1964). Phys. Rev. 136A, 991-997.

HAMBERGER, S.M., JANCARIK, J., SHARP, L.E., ALDCROFT, D.A., and WETHERELL, A. (1971). In: Plasma Physics and Controlled Nuclear Fusion Research. Proceedings of the 4. International Conference held at Madison, USA, 17-23 June 1971. Vol. 2 (IAEA, Vienna) 37-53.

HASHMI, M. and VAN DER HOUVEN VAN OORDT, A.J. (1971). Risø Report No. 250, 27-32.

HATAKEYAMA, R., SATO, N., SUGAI, H. and HATTA, Y. (1977). Phys. Lett. 63A, 28-30.

HATAKEYAMA, R., SATO, N., SUGAI, H. and HATTA, Y. (1980). Plasma Phys. 22, 25-40.

HATTA, Y. and SATO, N. (1961). In: Proceedings of the 5. International Conference on Ionization Phenomena in Gases, Munich 28 August - 1 September, 1961. Edited by H. Maecker. Vol. 1 (North-Holland, Amsterdam) 478-484.

HENDEL, H.W., YAMADA, M., SEILER, S.W. and IKEZI, H. (1976). Phys. Rev. Lett. 36, 319-322.

HIRSHFIELD, J.L. and JACOB, J.H. (1968). Phys. Fluids 11, 411-413.

HIROSE, A., ALEXEFF, I. and JONES, W.D. (1970). Phys. Fluids 13, 2039-2044.

HSUAN, H., OKABAYASHI, M. and EJIMA, S. (1975). Nucl. Fusion 15, 191-194.

HSUAN, H.C.S. and JENSEN, V.O. (1973). Phys. Fluids 16, 1776-1778.

ISHIZUKA, H., ONO, H. and KOJIMA, S. (1974). J. Phys. Soc. Jpn. 36, 1158-1163.

JEFFREYS, H. and SWIRLES, B. (1962). Methods of Mathematical Physics, 3. ed. (University Press, Cambridge), 716 pp.

JENSEN, V.O. (1962). Risø Report No. 54, 14 pp.

JENSEN, V.O. (1976). Risø Report No. 322, 98 pp.

JENSEN, V.O. and LYNOV, J.P. (1979). Phys. Fluids 22, 1133-1140.

JENSEN, V.O. and MICHELSEN, P. (1972). Risø Report No. 257, 33 pp.

JENSEN, T.D., MICHELSEN, P. and RASMUSSEN, J.Juul (1978). Risø-M-2120, 8 pp.

KUHN, S. (1979). Plasma Phys. 21, 613-626.

LAFRAMBOISE, J.G. (1966). University of Toronto, Institute for Aerospace Studies, Report No. 100, AD-634596, 211 pp.

LAM, S.H. (1965). Phys. Fluids 8, 1002-1004.

LANDAU, L. (1946). J. Phys. USSR, 10, 25-34.

LANGMUIR, I. and KINGDON, K.H. (1925). Proc. Roy. Soc. 107, 61-79.

LEVINE, A.M. and KUCKES, A.F. (1966). Phys. Fluids 9, 2263-2266.

LIBOFF, R.L. (1962). Phys. Fluids 5, 963-980.

LITTLE, P.F. (1961). In: Proceedings of the 5th International Conference on Ionization Phenomena in Gases, Munich 28 August - 1 September 1961. Edited by H. Maecker. Vol. 2 (North-Holland, Amsterdam), 1440-1455.

LYNOV, J.P., MICHELSEN, P., PÉCSELI, H.L., RASMUSSEN, J.Juul, SAEKI, K. and TURIKOV, V.A. (1979). Phys. Scr. 20, 328-335.

MICHELSEN, P. (1971). Risø Report No. 250, 382-385.

MICHELSEN, P. (1980). In: Proceedings of the International Conference on Plasma Physics, Nagoya, Japan, April 7-11, 1980. Vol. 2 (Fusion Research Association of Japan), 122-137.

MICHELSEN, P., PÉCSELI, H.L. and RASMUSSEN, J. Juul (1977). In: Proceedings of the 13. International Conference on Phenomena in Ionized Gases 1977, Berlin, September 12-17, 1977, (Physical Society of the GDR), 781-782.

MICHELSEN, P., PÉCSELI, H.L. and RASMUSSEN, J. Juul (1978). Plasma Phys. 20, 45-57.

MICHELSEN, P., PÉCSELI, H.L., RASMUSSEN, J. Juul and SATO, N. (1976). Phys. Lett. 55A, 345-346.

MICHELSEN, P., PÉCSELI, H.L., RASMUSSEN, J. Juul and SCHRITTWIESER, R. (1979). Plasma Phys. 21, 61-73.

MICHELSEN, P. and PRAHM, L.P. (1971). Risø Report No. 250, 103-110.

MOTLEY, R.W. (1975). Q-Machines (Academic Press, N.Y.), 190 pp.

MOTLEY, R.W. and D'ANGELO, N. (1963). Phys. Fluids 6, 296-299.

NIELSEN, P. (1969). Risø Report No. 190, 35 pp.

PARKINSON, D. and SCHINDLER, K. (1969). J. Plasma Phys. 3, 13-20.

PÉCSELI, H.L. (1975). Phys. Scr. 11, 311-315.

PÉCSELI, H.L. (1974). Phys. Fluids 17, 378-383.

PÉCSELI, H.L. and PETERSEN, P.I. (1973). Risø Report No. 290, 17 pp.

PERKINS, F.W. (1976). Phys. Fluids 19, 1012-1020.

RASMUSSEN, J.Juul (1977). Risø-M-1950, 77 pp.

RYNN, N. and D'ANGELO, N. (1960). Rev. Sci. Instrum. 31, 1326-1333.

SATO, N., HATTA, Y., HATAKEYAMA, R. and SUGAI, H. (1974). Appl. Phys. Lett. 24, 300-302.

SATO, N. and SASAKI, A. (1972). J. Phys. Soc. Jpn. 32, 543-551.

SATO, N., SUGAI, H. and HATAKEYAMA, R. (1975). Phys. Rev. Lett. 34, 931-934.

SATO, N., SUGAI, H. and HATAKEYAMA, R. (1977). Plasma Phys. 19, 187-207.

SCHRITTWIESER, R. (1978). Phys. Lett. 65A, 235-238.

STIX, T.H. (1962). The Theory of Plasma Waves (McGraw-Hill, N.Y.), 283 pp.

STIX, T.H. (1973). Phys. Fluids 16, 1922-1926.

TSYTOVICH, V.N., STENFLO, L., WILHELMSSON, H., GUSTAVSON, H.-G. and ØSTBERG, K. (1973). Phys. Scr. 7, 241-249.

VAN KAMPEN, N.G. (1955). Physica 21, 949-963.

WEIBEL, E.S. (1970). Phys. Fluids 13, 3003-3006.

WEITZNER, H. (1964). Phys. Fluids 7, 476-477.

WHARTON, C., KORN, P., PRONO, D., ROBERTSON, S., AUER, P. and DUM, C.T. (1971). In: Plasma Physics and Controlled Nuclear Fusion Research 1971. Proceedings of the 4. International Conference held at Madison, USA, 17-23 June 1971. Vol. 2 (IAEA, Vienna), 25-37.

WONG, A.Y., D'ANGELO, N. and MOTLEY, R.W. (1962). Phys. Rev. Lett. 9, 415-416.

WONG, A.Y., MOTLEY, R.W. and D'ANGELO, N. (1964). Phys. Rev. 133A, 436-442.

YAMADA, M., SEILER, S. and HENDEL, H.W. (1977). Phys. Fluids 20, 450-458.

DANSK RESUMÉ

Undersøgelse af elektrostatiske ionbølger i et kollisionsfrit plasma

I den foreliggende rapport gennemgås en række publikationer vedrørende teoretiske og eksperimentelle undersøgelser af elektrostatiske ionbølger i et kollisionsfrit plasma. Det eksperimentelle arbejde er udført i Risøs Q-maskine.

Introduktionen af Q-maskinen i begyndelsen af tresserne blev et gennembrud for eksperimentel plasmafysik. I løbet af få år blev adskillige nye typer af plasmabølger og instabiliteter observeret. Hovedårsagen til Q-maskinens succes var dels at plasmaet kunne produceres uden store elektriske felter, dels at plasmaet var roligt og vedvarende, og endelig at plasmaparametrene dækkede et nyt og vigtigt område for plasmastudier.

Risøs Q-maskine blev opbygget i 1966-1967, og et stort antal plasmafænomener er siden blevet studeret i denne maskine. Nogle af disse eksperimenter er sammen med teoretiske betragtninger og beregninger publiceret i afhandlingerne, der er gengivet i appendices I-X i denne rapport, mens et resumé med kommentarer er givet i selve rapporten.

I kapitel 2 beskrives princippet i Q-maskinens virkemåde samt ionenergianalysatoren og Langmuirproben, der anvendes til at foretage målinger i plasmaet med. Plasmaet i Q-maskinen produceres ved, at alkalimetaldamp, som f.eks. cesiumdamp, ioniseres på en tantalplade opvarmet til omkring 2000 K. De producerede ioner danner, sammen med elektroner emitteret fra tantalpladen, et plasma, der holdes sammen i en søjle ved hjælp af et stærkt magnetfelt. Målinger af ionhastighedsfordelingsfunktionen ved hjælp af en ionenergianalysator og målinger af plasmapotentialet ved forskellige plasmaparametre omtales i appendix I.

I kapitel 3 diskuteres udbredelsen af lineære ion-akustiske bølger i et plasma, hvor ion- og elektrontemperaturen er af samme størrelsesorden, og hvor det antages, at hastighedsfordelingen for ioner både i nulte-orden og i perturbationen kan udtrykkes ved hjælp af en sum af Maxwellfordelinger. Eksperimenter og beregninger er beskrevet i appendices II and III. De eksakte løsninger til Vlasov-Poisson ligningssystemet viser sig at kunne beskrive de eksperimentelle resultater ganske godt. Det vises, at den almindeligvis brugte første-pol-approximation, giver resultater tæt på den eksakte løsning, når fordelingsfunktionerne er drivende Maxwellfordelinger. Dette forklarer, hvorfor mange eksperimentelle observationer af ion-akustiske bølger synes at være i overensstemmelse med en første-pol-approximation.

I kapitel 4 og appendices IV beskrives eksperimenter af ion-akustiske bølgers udbredelse i en tæthedsgradient, produceret ved at omgive plasmasøjlen med et negativt forspændt rør. Mens bølger med bølgelængde kortere end e-foldningslængden af tæthedsgradienten udbreder sig uændret, udviser bølger med lange bølgelængder en hydrodynamisk vækst kvalitativt i overensstemmelse med en teori baseret på en fluidummodel.

Kapitel 5 omhandler beregninger af ion-akustiske bølger i et plasma, der gennemstrømmes af en ionstråle. Det diskuteres især hvad randbetingelserne for bølgeexcitationen kan betyde for udbredelsen. I tilfælde af at bølgen exciteres ved en hastighedsmodulation, viser det sig, at bølgeamplituden i et vist område af rummet kan vokse selv i et stabilt plasma. De teoretiske resultater har vist sig at være i god overensstemmelse med målinger. Nærmere detaljer findes i appendices V-VII.

Kapitel 6 og appendices VIII-X omhandler målinger og beregninger af elektrostatiske ioncyklotronbølger. Fra den generelle dispersionsrelation beregnes en simplificeret dispersionsrelation, og for et ionstråleplasma beregnes parameterområdet for ionstråleinstabiliteter og ioncyklotroninstabiliteter numerisk. Den elektrostatiske ioncyklotroninstabilitet exciteret af en ionstråle er observeret eksperimentelt. Tærskelværdier

af både ionstrålehastighed og af elektrontemperatur for excitation af instabiliteten er målt og sammenlignet med teoretiske resultater.

APPENDIX A

As shown in III, the solution to Eq. 3.2 with the boundary condition $f(x = 0,v,t) = g(v)e^{-i\omega t}$ can be written as

$$n(x) = \frac{1}{\pi}\int_0^\infty \frac{1}{k}\,\mathrm{Im}\left[M_b\left(\frac{\omega}{k}\right)\right]e^{ikx}dk,$$

where

$$M_b\left(\frac{\omega}{k}\right) \equiv \frac{\frac{\omega}{k}\,\fint_{-\infty}^{\infty}\frac{g(v)}{v-\omega/k}dv}{1 - \frac{c_s^2}{n_o}\,\fint_{-\infty}^{\infty}\frac{f_o'(v)}{v-\omega/k}dv}$$

The symbol $\fint_{-\infty}^{\infty}$ means integration below the pole $v = \frac{\omega}{k}$. Im [ ], means the imaginary part of [ ], and $n = \int_{-\infty}^{\infty} g(v)dv$. If we assume that $g(v)$ and $f_o(v)$ are both drifting Maxwellians with a drift velocity V_o, and if we introduce $U_o = \frac{V_o}{c_i}$, $q = \frac{c_i k}{\omega}$, and $\xi = \frac{x\omega}{c_i}$ we get:

$$n(\xi) = \frac{1}{\pi}\int_0^\infty \frac{1}{q}\,\mathrm{Im}\left[\frac{\frac{1}{q}\,Z\left(\frac{1}{q} - U_o\right)}{1 - \frac{\theta}{2}\,Z'\left(\frac{1}{q} - U_o\right)}\right]e^{i\xi q}dq,$$

where Z is the plasma dispersion function (Fried and Conte 1961). For large values of ξ the only contribution to the integral comes from a very small q, and therefore we can use the asymptotic expansion for $Z(\zeta) \sim i\sqrt{\pi}\exp(-\zeta^2) - \frac{1}{\zeta}$ (Fried and Conte 1961). i.e. for $q \to 0$ we have

$$M_b(q) \sim -\frac{1}{q}\,\mathrm{Im}\left(\frac{q - i\sqrt{\pi}\,\exp(-q^{-2})}{1 + \frac{1}{2}\theta q^2 + i\theta\sqrt{\pi}\,\frac{1}{q}\exp(-q^{-2})}\right) \sim (1+\theta)\,\frac{\sqrt{\pi}}{q}\exp(-q^{-2}).$$

For the density we get for $\xi \to \infty$

$$n(\xi) \sim \frac{1+\theta}{\sqrt{\pi}} \int_0^\infty \frac{1}{q^2}\,\exp[-(q^{-2} + i\xi q)]\,dq.$$

This integral can be evaluated by using the method of stationary phase (Jeffreys and Swirles 1962). If we substitute

$$\frac{1}{q} = \xi^{1/3} z$$

we get

$$n(\xi) \sim \frac{1+\theta}{\sqrt{\pi}}\xi^{1/3} \int_0^\infty \exp[-\xi^{2/3}(z^2 + \frac{i}{z})]\,dz. \qquad \text{(A-1)}$$

For large values of ξ the main contribution to the integral is from the neighbourhood of stationary points $z = z_o$ (saddle points) determined by

$$\frac{df(z)}{dz}\Big|_{z = z_o} = 0, \qquad f(z) = z^2 + \frac{i}{z}$$

i.e., by $2z - iz^{-2} = 0$

with the solutions $z_o = (\frac{i}{2})^{1/3}$. Since we have

$$\lim_{R\to\infty} R \int_{\theta=0}^{\pi/6} \exp[-\xi^{2/3}(R^2 e^{i2\theta} - \frac{i}{R} e^{-i2\theta})]d\theta = 0,$$

the integration path can be changed for the integral (A-1) to run from 0 to infinity along a line in the complex plane through the saddle point, $z_o = (\sqrt{3}+i)2^{4/3}$. In the vicinity of z_o $f(z)$ can be expanded into a Taylor series:

$$f(z) \simeq f(z_o) + f'(z_o)(z-z_o) + \frac{1}{2}f''(z_o)(z-z_o)^2 + \ldots$$

where

$$f(z_o) = \frac{3}{2^{5/3}} (1 + i\sqrt{3})$$

$$f'(z_o) = 0; \quad f''(z_o) = 6,$$

and we get

$$n(\xi) \sim \frac{1+\theta}{\sqrt{\pi}} \xi^{1/3} \int_o^\infty \exp\left\{-\xi^{2/3}[f(z_o) + \frac{1}{2}f''(z_o)(z-z_o)^2]\right\} dz$$

$$= \frac{1+\theta}{\sqrt{\pi}} \xi^{1/3} \exp[-\xi^{2/3} f(z_o)] \int_o^\infty \exp[-\xi^{2/3} \frac{1}{2}f''(z_o)(z-z_o)^2] \, dz.$$

Since the main contribution to the integral comes from the region close to z_o we can write

$$n(\xi) \sim \frac{1+\theta}{\sqrt{\pi}} \xi^{1/3} \exp[-\xi^{2/3} f(z_o)] \int_{-\infty}^\infty \exp[-\xi^{2/3} \frac{1}{2}f''(z_o)(z-z_o)^2] \, dz$$

$$= \frac{1+\theta}{\sqrt{\pi}}\ \xi^{1/3}\ \exp[-\xi^{2/3}\ f(z_o)]\ \sqrt{\frac{2\pi}{\xi^{2/3} f''(z_o)}}$$

$$= \frac{1+\theta}{\sqrt{3}}\ \exp[-\xi^{2/3} \cdot 3 \cdot 2^{-5/3}(1 + i\sqrt{3})],$$

which is the asymptotic evolution of $n(\xi)$.

APPENDICES

I - X

Reprinted from *Printed in U.S.A.*

THE PHYSICS OF FLUIDS VOLUME 14, NUMBER 3 MARCH 1971

Determination and Shaping of the Ion-Velocity Distribution Function in a Single-Ended *Q* Machine

S. A. ANDERSEN, V. O. JENSEN, P. MICHELSEN, AND P. NIELSEN*
Danish Atomic Energy Commission, Research Establishment Risö, Roskilde, Denmark
(Received 13 March 1970; final manuscript received 2 July 1970)

An electrostatic energy analyzer with a resolution better than 0.03 eV was constructed. This analyzer was used to determine the ion-velocity distribution function at different densities and plate temperatures in a single-ended *Q* machine. In all regions good agreement with theoretical predictions based on simple, physical pictures is obtained. It is shown that within certain limits the velocity distribution function can be shaped; double-humped distribution functions have been obtained. The technique used here is suggested as an accurate method for determination of plasma densities within 10% in single-ended *Q* machines.

I. INTRODUCTION

In recent years many experiments have been performed in order to study the propagation properties of density perturbations in single-ended *Q* machines. The phase velocity and damping characteristics of grid-excited, ion-acoustic waves have been examined by Doucet and Gresillon[1] and by Sato *et al.*[2] Reports of work on ion-wave echoes in single-ended *Q* machines have been published by Ikezi *et al.*[3] and by Baker *et al.*[4] Finally, the propagation of short density pulses has been studied by Andersen *et al.*[5,6] All the experiments mentioned above were performed in order to test theoretical predictions based on the linearized, collisionless Boltzmann equation. The density perturbations studied in these experiments were generated by a grid placed in the plasma column. In order to make quantitative comparisons between the experimental results and the theoretical predictions it is essential to know the undisturbed ion-velocity distribution function, $f(v)$, and the initial velocity distribution of the ions in the perturbation. The latter point has been stressed very clearly by Hirschfield and Jacob,[7] and experiments performed in order to determine the velocity distribution function in the perturbation have been reported by Andersen *et al.*,[8] and more recently by Ikezi and Taylor.[9] A few measurements of the undisturbed distribution function in plasmas in single-ended *Q* machines have also been reported.[5,10]

In this paper we describe a rather accurate measurement of $f(v)$ as a function of plasma density, temperature of the hot Ta plate, and distance from the Ta plate. The method used to determine $f(v)$ further allows us to measure the plasma potential as a function of the parameters mentioned above. In this paper we also demonstrate that we can shape $f(v)$ within certain limits; e.g., we can construct a double-humped distribution function which appears to be interesting for the study of Landau growth. As a by-product of our work we obtained a fairly accurate method of determination of the plasma density.

II. EXPERIMENTAL SET-UP

A schematic drawing of the single-ended *Q* device used in this experiment is shown in Fig. 1. The plasma is produced by surface ionization of a beam of cesium atoms from oven A on the hot tantalum plate ($\sim$ 2500°K) and is confined radially by a uniform, axial magnetic field of intensity up to 10 000 G. The plasma column is 3 cm in diameter and up to 1.2 m long; in the experiments to be described in this paper it ends at an ion-energy analyzer movable along the axis. A copper tube 5 cm in diameter and 15 cm long is placed round the plasma near the hot tantalum plate. This tube is connected with Cs oven B and indirectly heated from the hot plate and provides a spatially limited region with high neutral Cs pressure in the plasma column. In the work of Andersen[11] this tube was used for differential cooling of the plasma ions. A third Cs oven, C, is placed at the far end of the column. By means of this oven we can obtain a cloud of neutral Cs far away from the hot plate. The vacuum system, consisting of a stainless-steel tube (not shown in Fig. 1), is cooled to −20°C in order to reduce the Cs background pressure. In operation the vacuum system is pumped down to below 10^{-5} Torr.

A detailed drawing of the analyzer is shown in Fig. 2. This analyzer closely resembles the one described by Buzzi *et al.*[10] It consists of a brass housing 38 mm long and 22 mm in diameter. A hole 8 mm in diameter in one end of the housing is covered by a copper mesh, 35 μm thick and with

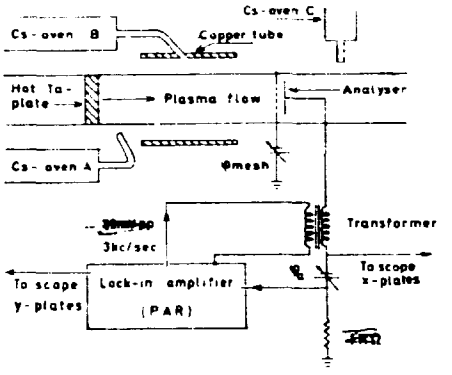

FIG. 1. Schematics of the experimental set-up.

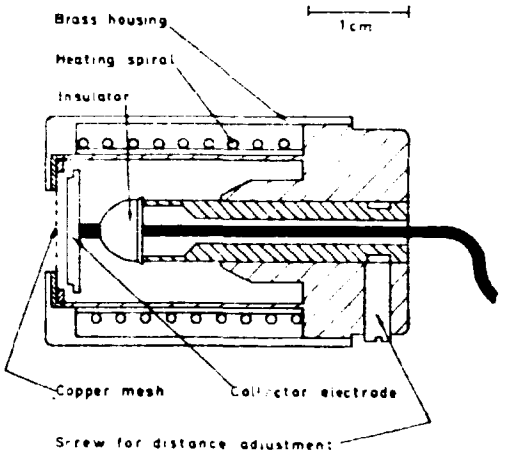

FIG. 2. Detailed drawing of the electrostatic analyzer.

40 000 25 μm × 25 μm holes per cm^2. A collector electrode is placed at a variable distance d (up to 1.2 mm) behind the mesh. In order to avoid cesium condensation on the mesh–collector system the analyzer can be heated electrically to about 500°C by a heating spiral.

In operation the analyzer is placed in the plasma as indicated in Fig. 1. The mesh and the whole housing is biased negatively (−6 to −10 V) with respect to the earth in order to reflect the electrons. The distribution of ion energies parallel to the magnetic field lines is determined by measurement of the current voltage characteristic of the collector plate. If we assume that the analyzer resolution function is very narrow, then the ion current to the collector plate as a function of collector voltage, φ_a, is given by

$$I(\varphi_a) = enA \int_{v_{min}}^{\infty} vf(v)\, dv, \qquad (1)$$

where A is the effective mesh area, n is the ion density, and $f(v)$ is the ion-velocity distribution function. The minimum velocity, v_{min}, accepted by the collector is given by $\frac{1}{2}mv_{min}^2 = e(\varphi_a - \varphi_{pl})$, φ_{pl} being the plasma potential and m the ion mass. By differentiation of (1) with respect to φ_a we get

$$\frac{dI(\varphi_a)}{d\varphi_a} \begin{cases} \propto f\left[v = \left(\frac{2e(\varphi_a - \varphi_{pl})}{m}\right)^{1/2}\right] & \text{for } \varphi_a \geq \varphi_{pl}, \\ = 0 & \text{for } \varphi_a < \varphi_{pl}. \end{cases} \qquad (2)$$

Thus, we get

$$f\left[v = \left(\frac{2e(\varphi_a - \varphi_{pl})}{m}\right)^{1/2}\right]$$

directly by differentiation of the collector current-voltage characteristic with respect to φ_a.

The electrical circuit shown schematically in Fig. 1 is arranged to show this differentiated characteristic on a scope. Through the transformer a 3 kc/sec 0.03 V peak-to-peak voltage from the generator in the Princeton Applied Research lock-in amplifier is added to the collector dc voltage, φ_a. The ac current to the collector is measured by its corresponding voltage drop across the 1 kΩ resistor. The part of this voltage which is in-phase with the transformer voltage is proportional to $dI(\varphi_a)/d\varphi_a$. (The out-of-phase part is determined by the capacity and self-induction in the circuit.) The lock-in amplifier is adjusted to measure the in-phase part, which is displayed on the scope as a function of φ_a. Thus, the scope simply displays $dI(\varphi_a)/d\varphi_a$ as a function of φ_a.

A calculation of the width of the analyzer resolution function is very complicated. Longitudinal energy loss or gain by deflection of the ion orbits in the holes in the mesh will widen the resolution function, so will changes in the collector work function over the surface. Such changes might be caused by inhomogeneities in the collector material or by variation in the thickness of the Cs layer covering the collector. Also instabilities in the space charge layer round the mesh might broaden the resolution function. We obtained an upper limit for the width of the resolution function experimentally. Figure 3 shows an example of a differentiated characteristic obtained by means of the technique described above at a rather low density ($n \approx 10^8$ cm^{-3}) and with Cs oven B heated. As will be discussed below, the distribution function of the plasma generated on the Ta plate at this low density is close to a truncated Maxwellian with a minimum velocity given by $\frac{1}{2}mv_{min}^2 = e(\varphi_{hp} - \varphi_{pl}) = e\varphi_0$. This truncated Maxwellian corresponds to the wide right-hand peak in Fig. 3. When the ions pass the neutral Cs cloud in

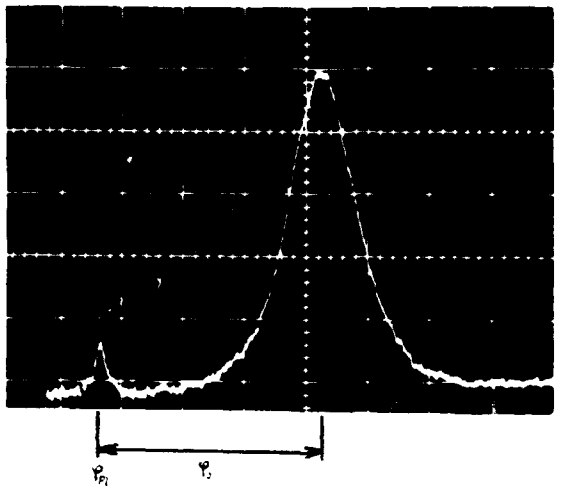

FIG. 3. Typical example of differentiated analyzer characteristic

$$f\left[v = \left(\frac{2e(\varphi_a - \varphi_{pl})}{m}\right)^{1/2}\right].$$

Sweep 0.5 V large div. Analyzer positioned at $x = 26$ cm, Ta plate at $x = 0$. $n \approx 10^8$ cm^{-3}.

the copper tube, some of them will undergo charge exchange and leave cold (tube temperature $\sim$500°K) ions behind. These ions are formed in a region with plasma potential and are therefore accepted by the analyzer when φ_a is close to and a little above φ_{pl}. The narrow left-hand peak in Fig. 3 corresponds to the contribution from these cold ions. From the positive slope of this peak, which theoretically should be vertical, we can get an upper limit for the width of the analyzer resolution function. The width has been measured at different densities and temperatures and always found to be less than 0.03 eV. The width of the curves of the form (2) measured in this experiment is typically around 2–3 V; therefore, it is justifiable to neglect the influence of a finite width of the resolution function in writing (1).

To find $f(v)$ from (2) and curves like the one shown in Fig. 3, one has to know φ_{pl}. As already mentioned, the cold charge exchange ions are formed in a region with plasma potential. Therefore, the position of the left-hand side of the narrow peak on curves like the one in Fig. 3 determines φ_{pl}.

At high densities the width of the resolution function will increase owing to space-charge-limited current. An upper pessimistic limit for the allowed collector current density is given by Child's law

$$I_{max} = \frac{2}{9}\epsilon_0\left(\frac{2e}{m}\right)^{1/2} d^{-2}(\varphi_a - \varphi_{mesh})^{3/2}. \qquad (3)$$

In the experiments, $\varphi_a - \varphi_{mesh}$ was around 5 V, and the distance d between mesh and collector was around 0.1 mm; so the maximum allowed current density is calculated to be $I_{max} \approx 0.1$ mA/cm^2. In all our experiments the collector current density was kept below this value, and no sign of space charge limitation was seen.

In all experiments the plasma column ended at the analyzer housing, which was kept on a negative voltage in order to reflect all electrons. Thus, the electron cloud in thermal contact only with the hot tantalum plate will take on a temperature, T_e, equal to the temperature, T_{hp}, of the hot plate.

All the measurements to be reported in this paper were performed with B fields around 8000 G. Variation of the magnetic field had little influence on the results.

III. RESULTS OF MEASUREMENTS

By means of the technique just described the ion-velocity distribution function was measured at various plate temperatures and ion densities. The presentation of the results is divided into three parts: low-density region, medium-density region, and high-density region.

A. Low-Density Region ($n \lesssim 10^8$ cm^{-3})

This region is characterized by ion–ion mean free paths long compared with the length of the machine. The distribution function, therefore, does not change appreciably along the plasma column. As already pointed out[10,12] in this case one would expect the ion distribution function to be a truncated Maxwellian with a minimum velocity corresponding to the potential drop, $\varphi_0 (= \varphi_{hp} - \varphi_{pl})$, at the tantalum plate.

In normalized form a truncated Maxwellian is written

$$f(v) = \begin{cases} \left(\frac{2m}{\pi T_e}\right)^{1/2} \frac{1}{1 - \operatorname{erf}(e\varphi_0/T_e)^{1/2}} \exp\left(-\frac{mv^2}{2T_e}\right) \\ \qquad\qquad \text{for } v \geq \left(\frac{2e\varphi_0}{m}\right)^{1/2}, \qquad (4) \\ 0 \qquad\qquad \text{for } v < \left(\frac{2e\varphi_0}{m}\right)^{1/2}. \end{cases}$$

Throughout this paper temperatures are measured in energy units.

In Fig. 3 a typical picture of the differentiated analyzer characteristic (2) is shown. As already mentioned, the main peak corresponds to the contribution of the main plasma, while the small left-hand peak is made up of ions formed by charge exchange in the neutral Cs cloud in the copper tube. In this series of experiments the Cs oven B was

only slightly heated so that only a few charge exchange ions were formed. The contribution from these ions was only used to determine the plasma potential. As is clearly seen from the picture, and as was also noticed by Buzzi *et al.*,[10] the left-hand wing of the main peak is not upright as would be expected if the distribution function were a truncated Maxwellian. Buzzi *et al.*[10] explain this smoothing out as being caused by zero relative velocity Coulomb collisions. Experimentally, we have found that the shape of the left wing in this low-density region is nearly independent of distance between the Ta plate and the analyzer and of the density. We would therefore suggest that the smooth shape is at least in part caused by variation, either in the Ta plate work function or in temperature over the surface. Variation in the work function is to be expected because the Ta plate does not form a single crystal, and it is known that the work function depends on the orientation of the surface with respect to the crystal axis. The variation in plate temperature has been measured by means of a pyrometer to be about 100°C.

We define the effective ion temperature by

$$T' = m \int_{-\infty}^{\infty} (v - v_d)^2 f(v)\, dv, \qquad (5)$$

where the drift velocity

$$v_d = \int_{-\infty}^{\infty} v f(v)\, dv.$$

Because of the smooth shape of the experimental curves the effective temperature calculated from these curves will be higher than that calculated from (4).

Photographs like the one shown in Fig. 3 were taken with the analyzer placed at different distances from the hot plate. Inspection of these photographs show that the distribution function becomes slightly wider at long distances, and the noise level increases. The broadening of the distribution function is probably caused by the noise.

With the analyzer 5 cm from the end of the copper tube traces like the one shown in Fig. 3 have been taken. From these we checked the following two expected plasma features.

Although the effective parallel ion temperature decreases as the ion flow is accelerated through the potential drop, φ_0, the plate temperature can be deduced from the negative slope of the main peak on the differentiated characteristics.[10] In semilogarithmic plots the right-hand wings of the curves are linear over one decade. From the slope of these

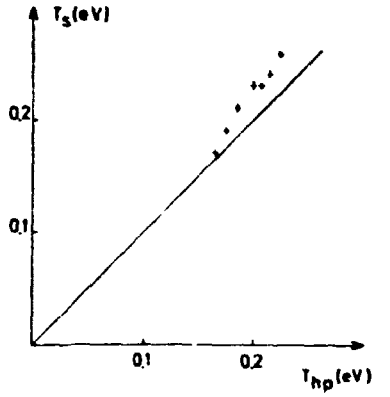

FIG. 4. Plate temperature T_s deduced from the slope of the differentiated characteristics as a function of the plate temperature, T_{hp}.

plots the temperature T_s was deduced. The crosses in Fig. 4 show the results of such measurements as a function of the plate temperature T_{hp}. The straight line shows the expected dependence (slope 45°). The plate temperature was measured by means of a pyrometer. The good agreement in Fig. 4 allows us to conclude that the ions are formed with a parallel temperature equal to that of the hot plate.

From a simple physical picture the variation of φ_0 with plate temperature can be calculated. The Richardson electron emission current density from the hot plate is given by

$$I_R = A\left(\frac{T_{hp}}{\kappa}\right)^2 \exp\left(-\frac{ew}{T_{hp}}\right), \qquad (6)$$

where κ is the Boltzmann constant, $A = 120\text{A/cm}^2\,^\circ\text{K}^2$, and w is the plate work function (=4.1 V). If we assume the electron distribution function to be a Maxwellian, we have the balance equation

$$I_R \exp\left(-\frac{e\varphi_0}{T_{hp}}\right) = \frac{1}{4} en\langle v_e\rangle = en\left(\frac{T_e}{2\pi m_e}\right)^{1/2}, \qquad (7)$$

where m_e is the electron mass.

From (6) and (7) and by using $T_{hp} = T_e$ we get

$$\varphi_0 = \frac{T_{hp}}{e} \ln\left(\frac{(2\pi)^{1/2} m_e^{1/2} A T_{hp}^{3/2}}{en\kappa^2}\right) - w. \qquad (8)$$

In the experiment the argument of the logarithm is around 10^{12} and only varies by a factor of less than 10. Therefore, the logarithm itself is around 28 and can be considered constant. In Fig. 5, (8) has been verified. The crosses are experimental points obtained by measuring φ_0 on traces like the one in Fig. 3. The straight line has been drawn through $(0, -w)$ and the majority of the experimental points. The slope of the straight line differs from that pre-

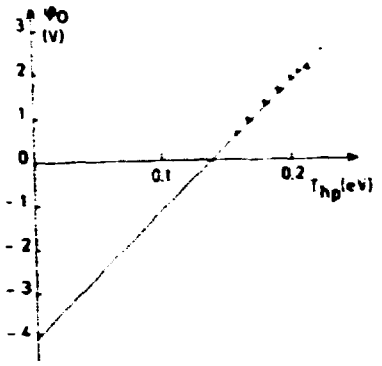

FIG. 5. Potential drop φ_0 at the hot plate as a function of plate temperature. The crosses are the experimental points deduced from traces like the one shown in Fig. 3. The full line shows the expected slope given by formula (8). $n \approx 10^9$ cm^{-3}.

dicted by (8) by less than 5%. Similar results were obtained by Buzzi *et al.*[10]

B. Medium-Density Region (10^9 cm^{-3} $\lesssim n \lesssim$ 5 × 10^9 cm^{-3})

This region is characterized by ion–ion mean free paths comparable to the length of the plasma column. The distribution function is close to a truncated Maxwellian at the hot plate and changes to approach a drifting Maxwellian along the column. This change was studied experimentally by means of the energy analyzer.

The plasma flow is governed by the following three conservation laws:

Mass flow

$$n(x)v_d(x) = c_1; \tag{9}$$

Momentum flow

$$nm\int_{-\infty}^{\infty} v^2 f(v)\,dv + nT_\perp = c_2; \tag{10}$$

Energy flow

$$\frac{1}{2}nm\int_{-\infty}^{\infty} v^3 f(v)\,dv + nv_dT_\perp + nv_dT_\parallel = c_3. \tag{11}$$

x is the coordinate along the flow and $x = 0$ at the hot plate. $f(v)$ is the normalized velocity distribution function, which is a function of x. $T_\perp(x)$ is the perpendicular ion temperature, which equals $T_{\perp p}$ at $x = 0$. c_1, c_2, and c_3 are constants along the flow and can be calculated from the conditions near $x = 0$.

In deriving the conservation equations, interactions between electrons and ions caused by Coulomb collisions were neglected, while allowance was made for ion–ion collisions. Also interaction between ions and electrons as a result of all kinds of instabilities was neglected. The electrons are assumed to act on the ion flow only through a static electric field, which, because of quasineutrality, is given by

$$E = -\frac{T_\parallel}{e}\frac{1}{n}\frac{dn}{dx}. \tag{12}$$

Upon introduction of the effective temperature T' given by (5), (9) and (10) combine to give

$$\frac{v_d^2}{T_\parallel/m} - \frac{c_2 - c_1 v_d}{c_1 T_\parallel} + 1 + \frac{T'}{T_\parallel} = 0. \tag{13}$$

In a T'–v_d diagram (13) corresponds to a family of parabolas, one for each value of c_2/c_1. c_1 and c_2 were calculated from (9) and (10) on the assumption that $f(v)$ for $x = 0$ is a truncated Maxwellian of the form (4). It is found that c_2/c_1 is only a function of $(e\varphi_0/T_\parallel)^{1/2}$. In Fig. 6 experimentally interesting parts of the parabolas of the form (13) are drawn for five values of $(e\varphi_0/T_\parallel)^{1/2}$.

The curve tm is drawn through points in the diagram calculated from (5) for $f(v)$ as truncated Maxwellians of the form (4). As the plasma flows away from the hot plate, the distribution function approaches a drifting Maxwellian of the form

$$f(v) = \left(\frac{m}{2\pi T}\right)^{1/2}\exp\left(-\frac{m(v - v_d)^2}{2T}\right). \tag{14}$$

By insertion of (14) into (5) and (11) and by the use of (13), points in the diagram have been calculated. The curve dm is drawn through these points. It is interesting to note that in the limit of large $v_d(T_\parallel/m)^{-1/2}$ this curve approaches $T'/T_\parallel = \frac{2}{3}$ asymptotically. The physical explanation of this is as follows: Owing to the large expansion in the sheath at the hot plate the longitudinal temperature drops almost to zero. As the thermal energy in the

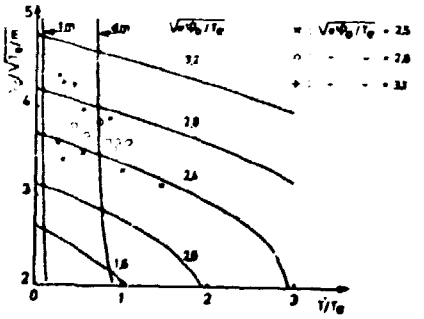

FIG. 6. Diagram showing the evolution along the column of the ion-flow parameters T' and v_d. Full curves (parabolas) show solutions to (13) for different values of $(e\varphi_0/T_\parallel)^{1/2}$. Curves tm and dm represent $[T'/T_\parallel, v_d(T_\parallel/m)^{-1/2}]$ values for truncated Maxwellians and drifting Maxwellians, respectively. Points with the same signature are obtained by moving the analyzer along the column.

two perpendicular degrees of freedom is shared between all three degrees of freedom, the resulting temperature will be ⅔ of the original perpendicular temperature.

In an experiment where density and plate temperature are kept constant, i.e., $e\varphi_0/T_e$ is constant, we would expect to find values of $[T'/T_e, v_d(T_e/m)^{-1/2}]$ near the line tm in Fig. 6 when the analyzer is close to the hot plate where the distribution function is close to a truncated Maxwellian. As the analyzer is moved along the column, the distribution function will eventually change into a drifting Maxwellian. In the diagram we therefore expect to follow a parabola and, when full Maxwellization is obtained, to find points at the line dm.

Experiments were performed for three values of $e\varphi_0/T_e$. From characteristics like the one shown in Fig. 3, T'/T_e and $v_d(T_e/m)^{-1/2}$ were calculated on a digital computer. The value of φ_0 is determined from the characteristics taken nearest to the hot plate in the same way as indicated in Fig. 3. The experimentally obtained values are shown as points in Fig. 6. For each value of $e\varphi_0/T_e$ it is found that the points move in the direction of larger T'/T_e when the analyzer moves away from the hot plate. In the figure we notice that no points are found on the curve tm. This can be explained by the fact that the distribution functions near the hot plate are not truncated Maxwellians, but smooth functions as already discussed in Sec. IIIA. In the same way we can understand that points are found on the right-hand side of line dm. When we start with an effective temperature higher than that of a truncated Maxwellian near the hot plate, there is an excess of thermal energy present in the flow. This will give rise to increased temperature at the point where complete Maxwellization is reached.

We find agreement between theory and experiments in this medium-density region satisfactory. However, it should be pointed out that our measurements do not follow the theoretical calculations so closely as to permit us to exclude that part of the change in the distribution function is caused by instabilities.

C. High-Density Region ($n \gtrsim 5 \times 10^9$ cm^{-3})

This region is characterized by ion–ion mean free paths short compared with the length of the plasma column. The distribution function is, therefore, always very close to a Maxwellian.

In the low- and medium-density regions the plasma potential was determined by means of a few ions formed by charge exchange in the neutral Cs cloud in the copper tube. Such charge-exchange processes are also expected to take place in the neutral Cs cloud formed by oven A in front of the hot plate even when the copper tube and oven B are kept cold or removed. The approximate number of charge-exchange processes occurring in this cloud can be estimated as follows: The flux of neutrals from oven A is given approximately by

$$F_n \approx n_n\left(\frac{2T_{oven}}{m}\right)^{1/2}, \tag{15}$$

where n_n is the neutral density. Similarly, the plasma flux is given by

$$F_{Pi} \approx n\left(\frac{2e\varphi_0}{m}\right)^{1/2}. \tag{16}$$

The neutrals from the oven hit the hot plate at an angle of about 45°, and it is known that only about half the neutrals become ionized on the hot plate; therefore, $F_n \approx 3F_{Pi}$. By combining (15) and (16) and using $T_{oven} \approx 0.05$ eV and $\varphi_0 \approx 1.3$ V (see Fig. 5) we get $n_n \approx 15n$. The charge-exchange cross sections, σ_{ce}, at low energies have been measured by Dreicer *et al.*[13] to be $\sim 3 \times 10^{-12}$ cm^2. The length L of the neutral cloud is about 10 cm. The probability for an ion to pass through the neutral cloud without undergoing charge exchange is

$$P(n) = \exp(-n_n\sigma_{ce}L) \approx \exp(-n/2 \times 10^{10}). \tag{17}$$

It is seen that for plasma densities lower than about 10^{10} cm^{-3} very few ions will undergo charge exchange in the neutral cloud at the hot plate. In the experiments with low and medium densities described in Secs. IIIA and B no sign of such charge exchange was seen. For densities $n \gtrsim 10^{10}$ cm^{-3}, where according to (17) charge-exchange processes are of importance, the mean free path for 90° deflection as a result of Coulomb collisions is short compared with the length of the plasma column ($L_{mfp} \approx 10$ cm at $n = 10^{10}$ cm^{-3}). The distribution function for $n \gtrsim 10^{10}$ cm^{-3} is, therefore, always expected to be a Maxwellian.

The temperature and drift velocity of this resulting distribution function are determined by the following three processes: (a) production and acceleration of primary ions at the surface of the hot Ta plate; (b) production of slow charge exchange ions in the neutral Cs cloud in the vicinity of the Ta plate; and finally (c) Maxwellization through ion–ion collisions within a distance of a few ion–ion mfp from the Ta plate. If only processes (a) and (b) took place, we would expect a double-humped dis-

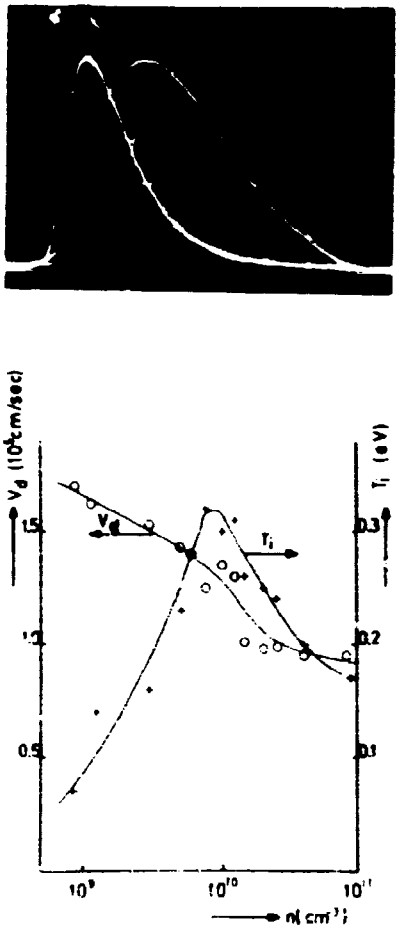

FIG. 7. (a) Examples of distribution functions measured at different densities. a, $n \approx 3 \times 10^9$ cm^{-3}; b, $n \approx 8 \times 10^9$ cm^{-3}; c, $n \approx 3 \times 10^{10}$ cm^{-3}. $T_{h_p} \approx 2400$°K. Analyzer positioned at $x = 62$ cm. Sweep 0.5 V/large div (amplitude gain varied from curve to curve). (b) Experimental values of drift velocity and ion temperature as functions of density.

tribution function similar to that shown in Fig. 3, where charge-exchange ions were produced artificially in the Cs cloud confined in the copper tube. In process (a) the acceleration of the primary ions is determined by the plate temperature and the flux of neutral Cs from oven A. In process (b) the production of slow charge-exchange ions is determined mainly by the Cs flux. We therefore expect the resulting distribution function to depend on the Ta plate temperature and especially on the density. For densities at which the production of charge exchange ions begins to be comparable to the production of primary ions one would expect the drift velocity to decrease; similarly, Maxwellization of the double-humped distribution function will lead to an increase in temperature. At very high densities, at which all ions undergo charge exchange, the distribution function is very narrow, and an ion temperature close to that of the neutral cloud is to be expected.

Experimentally, we have measured the velocity distribution function at different densities and constant plate temperature ($T_{h_p} \approx 0.21$ eV). As we expected, no variation in the distribution function is found when the energy analyzer is moved along the the column. Figure 7(a) shows a few examples of the distribution function (2) taken for different n values. From curves like the ones in Fig. 7(a), the drift velocity v_d and the temperature T_i have been deduced, and the result is shown in Fig. 7(b) as a function of n. We see that the drift velocity decreases with density, and that the temperature reaches a maximum around $n \approx 10^{10}$ cm^{-3}. This is in agreement with the qualitative discussion just given.

IV. SHAPING OF THE DISTRIBUTION FUNCTION

A few attempts to shape the ion velocity distribution function in Q machines have been reported in the literature. Andersen[11] introduced the copper tube shown in Fig. 1 in order to perform differential cooling of the plasma ions by collisions with the neutrals in the Cs cloud. He measured the propagation properties of an ion-acoustic wave launched in the downstream direction and found that the phase velocity and the damping of such a wave decreased with increasing density in the neutral cloud. This was indirect proof of the cooling since Landau's theory predicts that the phase velocity and the damping will decrease with decreasing ion temperature. For a plasma density ($n \sim 1.5 \times 10^8$ cm^{-3}) we have measured the ion velocity distribution on the downstream side of the tube at different neutral densities. The neutral density was varied by simply varying the temperature of Cs oven B. Figure 8 shows three examples; (a) is obtained at a rather low neutral density at which only a small part of the ions formed at the hot plate undergoes charge exchange in the tube. As the neutral density is increased, more charge-exchange processes take place, and distribution functions like the one in (b) are obtained. For very high neutral densities all ions undergo charge exchange, and we are left with a cold plasma with small drift velocities as shown in (c). Note that we are able to produce "double-humped" distribution functions as in (a) and (b). This kind of distribution function appears to be interesting because it should be suitable for the study of Landau growth.

In a few experiments attempts were made to cool the ions in a Q machine simply by introduc-

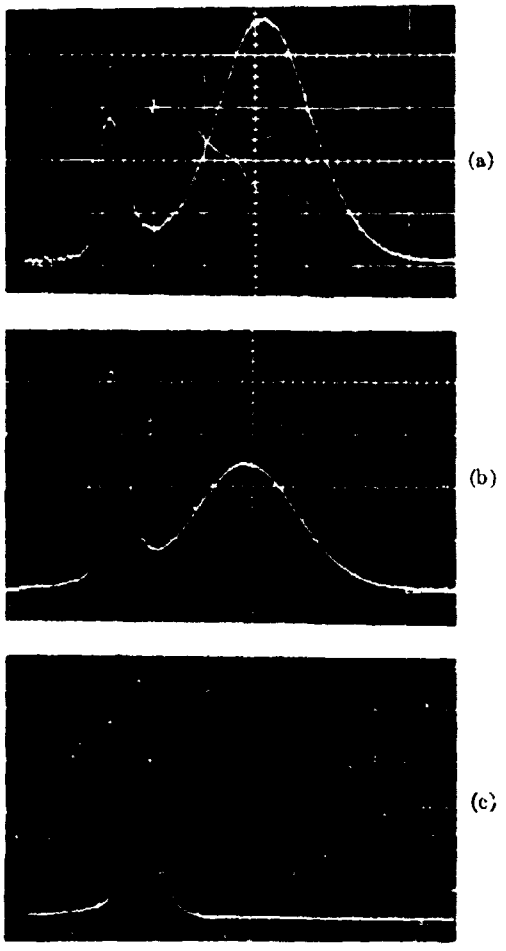

FIG. 8. Examples of distribution functions obtained at different neutral Cs pressures in the copper tube. a, Rather low Cs pressure; b, medium Cs pressure; c, high Cs pressure. $n \approx 1.5 \times 10^{8}$ cm^{-3}. Analyzer positioned at $x = 26$ cm. Sweep 0.5 V/large div.

ing a rather high pressure of an inert gas into the plasma.[1,14,15] We have examined this method of cooling with the analyzer. Figure 9 shows how the distribution function changes with distance in the case where $n \approx 10^{9}$ cm^{-3}, and $p_{\text{neutral}} = 2 \times 10^{-4}$ Torr of argon. In a similar way Fig. 10 shows the distribution functions obtained at a fixed position at three different argon pressures. We note that this method of cooling gives a distribution function which depends very much on distance from the hot plate and on argon pressure, and which is generally *not* a Maxwellian.

Finally, it should be mentioned that we have used the energy analyzer to check some earlier results obtained with a supersonic plasma wind tunnel.[16] This device is essentially a single-ended Q machine, where the magnetic field is reshaped to form a magnetic Laval nozzle.

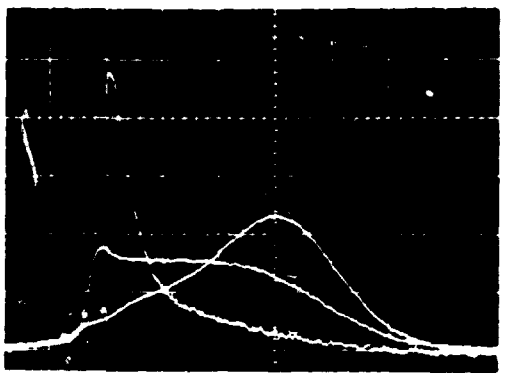

FIG. 9. Distribution functions at three positions along the column in partly ionized plasma. a, $x = 26$ cm; b, $x = 56$ cm; c, $x = 106$ cm. Argon background pressure 2×10^{-4} Torr. Plate temperature 2400 K. Sweep 0.5 V large div. $n \approx 10^{9}$ cm^{-3}.

The measurements were performed in a plasma that was cooled by charge exchange in the neutral cloud in the copper tube. The "throat" of the nozzle was about 5 cm from the downstream end of the tube shown in Fig. 1. The distribution function was measured with the analyzer placed 80 cm from the nozzle. The plasma potential at this position was determined by means of ions formed by charge exchange in a neutral Cs cloud from oven C (see Fig. 1). The measurements show that Mach numbers $[M = v_i/(T_i/m_i)^{\frac{1}{2}}]$ up to 3 and electron ion temperature ratios, T_e/T_i, up to 4 are easily obtained. These measurements agree with our earlier results.

It should be noted that high Mach numbers ($M \sim 4$) and high temperature ratios ($T_e/T_i \sim 6$) are already present in the single-ended Q machine with a straight magnetic field at low and medium densities. These numbers can be deduced from Fig. 6. In this case the high Mach numbers are

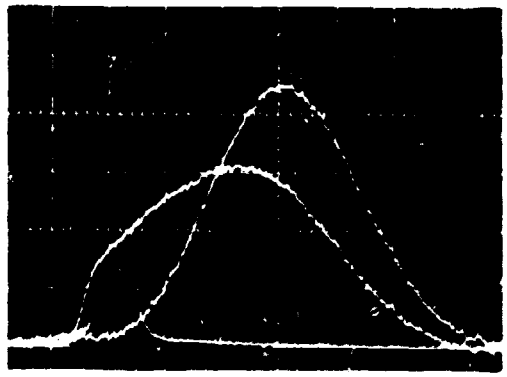

FIG. 10. Distribution functions for three argon background pressures. a, $P_A = 5 \times 10^{-5}$ Torr; b, $P_A = 10^{-4}$ Torr; c, $P_A = 5 \times 10^{-4}$ Torr. Analyzer positioned at $x = 76$ cm. $n \approx 10^{9}$ cm^{-3}. Plate temperature 2400°K. Sweep 0.5 V/large div.

caused by acceleration through the potential drop, φ_s, at the hot plate.

V. CONCLUSION

In this paper we have described a low-energy electrostatic analyzer suitable for determination of ion velocity distribution functions in single-ended Q machines. The analyzer was used to measure the distribution function at different plate temperatures and densities. The measured functions agree reasonably well with predictions based on simple theoretical pictures.

From a theoretical point of view, knowledge of the distribution function is very important. Especially, all calculations based on the Vlasov equation require accurate knowledge of this function. For instance it is well known that the damping (Landau damping) of longitudinal waves is proportional to $df(v)/dv$ at v = the phase velocity of the wave. A weak point in many wave experiments reported in the literature has been lack of knowledge of the exact shape of the velocity distribution function. As seen from this paper, the distribution function varies greatly with density, plate temperature, and neutral pressure. In order that accurate knowledge of this function may be obtained in future experiments, we therefore suggest that the function be measured directly, for instance by means of a technique like the one described here, rather than deduced from our results.

Accurate measurements of the velocity distribution function as described here also raised the possibility of accurate density measurements. By combination of the velocity distribution function with the total ion flux, which can be determined by measuring the ion current to a negatively biased plate in the column, the density can be deduced. We believe that density measurements correct to within less than 10% can be obtained. Such measurements would seem to be very interesting for the calibration of other methods.

The analyzer described here can also be used for ac measurements, i.e., it also allows us to determine the ion velocity distribution as a function of time in different kinds of wave measurements. This opens the possibility of studying the very interesting concept of wave particle interaction directly. Some preliminary work of this kind has already been performed.[6]

The "double-humped" distribution function obtained by means of the neutral cloud in the copper tube may make it possible to study Landau growth.

ACKNOWLEDGMENTS

The authors want to thank O. Rasmussen for discussions on the theoretical part of Sec. IIIB. Further, we thank K.-V. Weisberg for help with the electronic equipment, B. Reher for building the analyzer, and he and M. Nielsen for help in maintaining the Q device.

---

* Present address: The University of Texas at Austin, Austin, Texas 78712.

[1] H. J. Doucet and D. Gresillon, in *Plasma Physics and Controlled Nuclear Fusion Research* (International Atomic Energy Agency, Vienna, 1969), Vol. I, p. 659; Phys. Letters, 28A, 257 (1968); Phys. Fluids 13, 773 (1970).

[2] N. Sato, H. Ikezi, Y. Yamashita, and N. Takahashi, Phys. Rev. Letters 20, 837 (1968); N. Sato, H. Ikezi, N. Takahashi, and Y. Yamashita, Phys. Rev. 183, 278 (1969).

[3] H. Ikezi, N. Takahashi, and K. Nishikawa, Phys. Fluids 12, 853 (1969).

[4] D. R. Baker, N. R. Ahern, and A. Y. Wong, Phys. Rev. Letters 20, 318 (1968).

[5] H. K. Andersen, S. A. Andersen, V. O. Jensen, P. Michelsen, and P. Nielsen, in *Proceedings of the International Conference on Physics of Quiescent Plasmas*, Paris (Ecole Polytechnique, Paris, 1969), Vol. I, p. 55.

[6] S. A. Andersen, V. O. Jensen, P. Michelsen, and P. Nielsen, Phys. Letters 32A, 413 (1970).

[7] J. L. Hirshfield and J. H. Jacob, Phys. Fluids 11, 411 (1968).

[8] S. A. Andersen, V. O. Jensen, and P. Nielsen, Phys. Fluids 12, 2694 (1969).

[9] H. Ikezi and R. J. Taylor, Phys. Rev. Letters 22, 923 (1969); J. Appl. Phys. 41, 738 (1970).

[10] I. M. Buzzi, H. J. Doucet, and D. Gresillon, in *Proceedings of the International Conference on Physics of Quiescent Plasmas*, Paris (Ecole Polytechnique, Paris, 1969), Vol. III, p. 149.

[11] S. A. Andersen, Risö Report No. 188, Risö (1969).

[12] A. V. Gurevich, R. A. Salimov, and N. S. Buchel'nikova, Akademiya Nauk SSSR, Novosibirsk, Institut Yadernoi Fiziki, Preprint 208 (1968).

[13] H. Dreicer, D. B. Henderson, D. Mosher, F. E. Wittman, and K. Wolfsberg, in *Proceedings of the International Conference on Physics of Quiescent Plasmas*, Paris (Ecole Polytechnique, Paris, 1969), Vol. III, p. 11.

[14] F. P. Zhan, E. Guilino, M. Hashmi, and N. D'Angelo, Phys. Fluids 10, 1116 (1967).

[15] H. K. Andersen, N. D'Angelo, V. O. Jensen, P. Michelsen, and P. Nielsen, Phys. Fluids 11, 1177 (1968).

[16] S. A. Andersen, V. O. Jensen, P. Nielsen, and N. D'Angelo, Phys. Fluids 12, 557 (1969).

THE PHYSICS OF FLUIDS VOLUME 16, NUMBER 2 FEBRUARY 1973

Propagation of density perturbations in a collisionless Q-machine plasma

P. Michelsen and H. L. Pécseli

Danish Atomic Energy Commission, Research Establishment Risø, Roskilde, Denmark

(Received 1 June 1972)

The evolution of the ion velocity distribution function is calculated by means of the linearized Vlasov equation for the case where the initial perturbation consists of a steplike density discontinuity. Some characteristic features in the solution are caused by wave–particle interaction. These features are found experimentally by perturbing the plasma in a single-ended Q machine by means of a grid immersed in the plasma column. The perturbed ion distribution function is measured with an electrostatic energy analyzer.

I. INTRODUCTION

The propagation of steplike discontinuities through a collisionless plasma has been treated theoretically by numerous authors, among others Mason,[1] Sakanaka *et al.*,[2] Gurevich *et al.*,[3] and Korn *et al.*[4] For electron–ion temperature ratios $T_e/T_i \gtrsim 4$, theory predicts shock formation, a feature seen experimentally by Vanek *et al.*,[5] Taylor *et al.*,[6] and Korn *et al.*[4] Special interest is taken there in the gradual steepening of the density and flux fronts.

In our case $T_e/T_i \simeq 1.5$ and $\Delta n \ll n_0$ (Δn is the density in the perturbation, n_0 is that of the main plasma). We used a linear approach to the problem and found that the motion is self-similar, and thus no shock is formed.

Since the maximum obtainable information is given by the perturbed distribution function rather than by the perturbed density, our main concern was a comparison of an analytical expression and measurements of the ion velocity distribution function.

II. THEORY

We used the linearized ion Vlasov equation. Assuming a Boltzmann distribution for the electrons

$$n_e = n_0 \exp(e\varphi/\kappa T_e), \qquad T_e = \text{const},$$

and quasineutrality at all times, we get the well-known equation[7]

$$\frac{\partial f(x,v,t)}{\partial t} + v\frac{\partial f(x,v,t)}{\partial x} = c_s^2 \frac{df_0(v)}{dv}\frac{\partial n(x,t)}{\partial x} \tag{1}$$

with $c_s^2 = \kappa T_e/m_i$.

For convenience, we put

$$\int_{-\infty}^{\infty} f_0(v)\,dv = 1, \qquad \int_{-\infty}^{\infty} f(x,v,t)\,dv = n(x,t).$$

Equation (1) is to be solved with the initial condition

$$f(x,v,t=0) = \Delta n[1-\epsilon(x)]g(v), \tag{2}$$

where $\epsilon(x)$ is Heaviside's step function:

$$\int_{-\infty}^{\infty} g(v)\,dv = 1.$$

Andersen *et al.*[7] have found the solution to Eq. (1) with the initial condition $f(x,v,t=0) = \Delta n\, g(v)\delta(x)$:

$$n(x,t) = (\Delta n/t)h(x/t), \tag{3}$$

$$f(x,v,t) = \frac{\Delta n}{t}g(v)\delta\left(v-\frac{x}{t}\right) + \frac{\Delta n}{t}c_s^2\frac{df_0(v)}{dv}\frac{h(x/t)}{v-(x/t)}, \tag{4}$$

where

$$h(\gamma) = \pi^{-1}\,\mathrm{Im}\left[\left(P\int_{-\infty}^{\infty}\frac{g(v)}{v-\gamma}\,dv + i\pi g(\gamma)\right) \times\left(1-c_s^2 P\int_{-\infty}^{\infty}\frac{f_0'(v)}{v-\gamma}\,dv - i\pi c_s^2 f_0'(\gamma)\right)^{-1}\right]. \tag{5}$$

Equations (3) and (4) are valid provided that the denominator in (5)—which, in fact, is the dielectric function of the plasma—has no zeros in the upper half of the complex γ plane. That is, $f_0(v)$ must be a suitable distribution such as a Maxwellian.

We get the solution to Eq. (1) with condition (2) simply by superposition

$$n(x,t) = \int_0^{\infty}\frac{\Delta n}{t}h\left(\frac{x+\eta}{t}\right)d\eta = \Delta n\int_{x/t}^{\infty}h(\gamma)\,d\gamma \tag{6}$$

and

$$f(x,v,t) = \int_0^{\infty}\frac{\Delta n}{t}g(v)\delta\left(v-\frac{x+\eta}{t}\right)d\eta + c_s^2\Delta n\int_0^{\infty}\frac{f_0'(v)}{t}\frac{h[(x+\eta)/t]}{v-[(x+\eta)/t]}\,d\eta$$

$$= \Delta n\, g(v)\delta\left(v-\frac{x}{t}\right) + c_s^2\Delta n\, f_0'(v)\int_{x/t}^{\infty}\frac{h(\gamma)}{v-\gamma}\,d\gamma. \tag{7a}$$

The last integral is singular for $v \geq x/t$ so we must prescribe the proper way of integration. This amounts

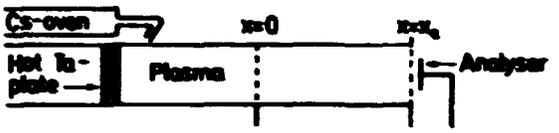

FIG. 1. Schematic diagram of the Q machine.

to finding $K(v)$ in the following, rewriting of Eq. (7a):

$$f(x,v,t)=\Delta n\, g(v)\epsilon\left(v-\frac{x}{t}\right)+c_s^2\Delta n\, f_0'(v) \times P\int_{x/t}^{\infty}\frac{h(\gamma)}{v-\gamma}\,d\gamma+K(v)\epsilon\left(v-\frac{x}{t}\right).$$

Now,

$$(t,v)=(t_1,v_1) \quad \text{and} \quad x\to\infty \Rightarrow f(x,v,t)\to 0,$$

$$(t,v)=(t_1,v_1) \quad \text{and} \quad x\to-\infty \Rightarrow f(x,v,t)\to\Delta n\, g(v_1),$$

so

$$K(v)=-c_s^2\Delta n\, f_0'(v)P\int_{-\infty}^{\infty}\frac{h(\gamma)}{v-\gamma}\,d\gamma.$$

In other words

$$f(x,v,t)=c_s^2\Delta n f_0'(v)P\int_{x/t}^{\infty}\frac{h(\gamma)}{v-\gamma}\,d\gamma +\left[\Delta n\, g(v)-c_s^2\Delta n\, f_0'(v)P\int_{-\infty}^{\infty}\frac{h(\gamma)}{v-\gamma}\,d\gamma\right]\epsilon\left(v-\frac{x}{t}\right); \quad (7b)$$

$f(x,v,t)$ is not defined for $v=x/t$. We notice that both (6) and (7b) are self-similar, i.e., they depend on x/t only. The first term in (7a) is the solution for freely streaming particles, the second is the contribution of collective interaction. The total ion flux in the perturbation,

$$F(x,t)=\int_{-\infty}^{\infty}vf(x,v,t)\,dv,$$

is found by using the fact that F must be self-similar $[F(x/t)]$ since f is self-similar. The Vlasov equation reduces to

$$\frac{\partial f(y,v)}{\partial y}(v-y)=c_s^2 f_0'(v)\frac{dn(y)}{dy} \quad \text{with} \quad y\equiv\frac{x}{t}.$$

Integration with respect to v gives

$$\frac{dF(y)}{dy}-y\frac{dn(y)}{dy}=0,$$

since

$$\int_{-\infty}^{\infty}f_0'(v)\,dv=0.$$

Using (6) we get $dF(y)/dy=-y\Delta n h(y)$. We must require $F(\infty)=0$. Thus,

$$F\left(\frac{x}{t}\right)=\Delta n\int_{x/t}^{\infty}\gamma h(\gamma)\,d\gamma. \quad (8)$$

III. EXPERIMENTAL SETUP

A cesium plasma is produced by surface ionization on a hot tantalum plate (2200 °K) in a single-ended Q machine (Fig. 1). The plasma is confined by a uniform, axial magnetic field at intensity 0.6 T. The density n_0 is approximately 2×10^9 cm^{-3}. The electron temperature is assumed to be that of the hot plate. The plasma column is 3 cm in diameter, 50 cm long, and ends on an electrostatic energy analyzer consisting of a collector behind a fine copper mesh.[8] The mesh potential is negative with respect to the plasma potential φ_{pl} in order to reflect all the electrons.

As a function of the collector potential φ_c, the collector current is proportional to

$$I(\varphi_c)\sim\int_{v_{min}}^{\infty}v[n_0 f_0(v)+f(x,v,t)]\,dv, \quad (9)$$

$$v_{min}=[(2e/m_i)(\varphi_c-\varphi_{pl})]^{1/2}.$$

With the collector potential constant and below φ_{pl} we get the total ion current to the collector

$$\int_0^{\infty}v(n_0 f_0+f)\,dv.$$

This is almost equal to the total ion flux (8) because the ions have a drift velocity that is high compared with their thermal velocity.

The plasma perturbation is introduced by means of a grid placed in the column at $x=0$, which is 25 cm from the hot plate. The grid consists of a thin nickel mesh with 400 0.5×0.5 mm² holes per cm². The optical transparency is about 90%. At a time $t=0$, the grid potential φ is switched from $\varphi_0<\varphi_f$ to φ_f (φ_f is the floating potential). For $t<0$ the grid absorbs some of the ions so the density between the hot plate and the grid is $n_0+\Delta n$, while it is n_0 behind the grid. φ_0 is chosen so that $\Delta n\simeq 0.1 n_0$. Figure 2 shows the ion current.

The ion velocity distribution function is determined by differentiating (9) with respect to φ_c.

We get

$$\frac{dI(\varphi_c)}{d\varphi_c}\propto n_0 f_0\left(v=\left[\frac{2e}{m_i}(\varphi_c-\varphi_{pl})\right]^{1/2}\right) +f\left(x_a,v=\left[\frac{2e}{m_i}(\varphi_c-\varphi_{pl})\right]^{1/2},t\right),$$

where x_a is the analyzer position.

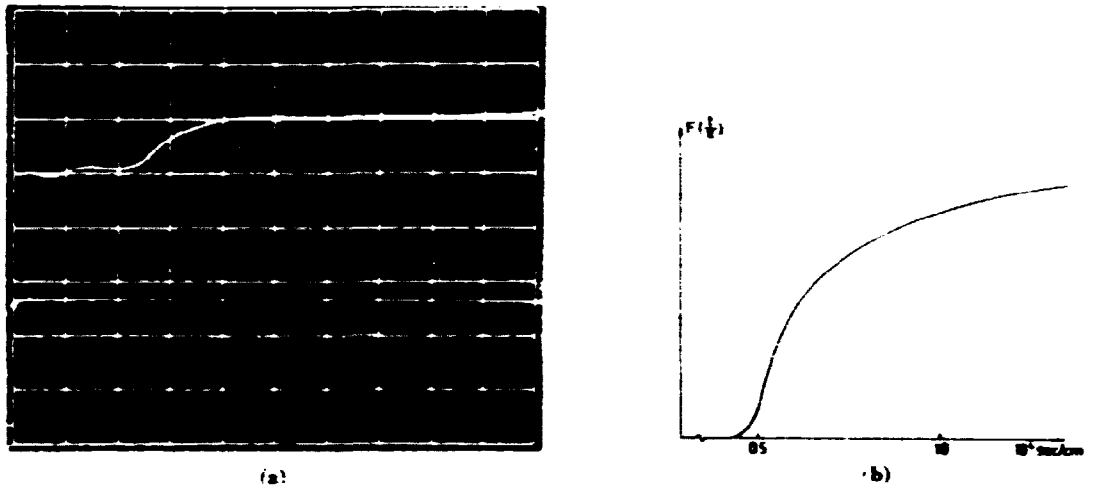

(a) (b)

FIG. 2 (a). The total ion current to the analyzer, $x_a = 10$ cm; 20 μsec/large div. (b) Calculated ion flux as a function of t/x.

The time-independent part $f_0(v)$ is measured by using the circuit described in Ref. 8, and by keeping the grid potential constant at φ_0. By changing the grid potential to φ_0 we measure $g(v)+f_0(v)$. $g(v)$ is found by subtraction as described in Ref. 9. (See Figs. 3 and 4.)

The plasma potential is measured by charge exchange as described in Ref. 10.

The velocity distribution function $f(x, v, t)$ of the particles in the perturbation is measured with the analyzer coupled to the circuit described in Ref. 2. This circuit is designed in such a way that for a chosen velocity v_a the perturbed velocity distribution function $f(x_a, v_a, t)$ is displayed on an oscilloscope as a function of time. For improvement of the signal noise ratio 10^4–10^5 pulses are analyzed, and the average signal is obtained by means of a Princeton applied Research waveform eductor. The pulses are generated by applying a 200-Hz square-wave signal to the grid.

IV. CONCLUSIONS AND DISCUSSION

There is general agreement between the experimentally obtained curves Figs. 5(a)–(e), and the calculated ones in Fig. 5(f). The local maximum at $t = \tau_a$ x_a, Figs. 5(a)–(c), and the local minimum, Fig. 5(e), are due to the right-hand term in Eq. (1) and can be taken as experimental proof of wave–particle interaction. Figure 5(d) shows no significant extremum because $f_0'(v) \simeq 0$ for this velocity. Some discrepancies between the calculated and the experimental curves can be noted. We believe that these can be explained by the following:

(1) $f_0(v)$ and $g(v)$ are assumed to be Maxwellians in the calculations. The measured ones deviate slightly from Maxwellians.

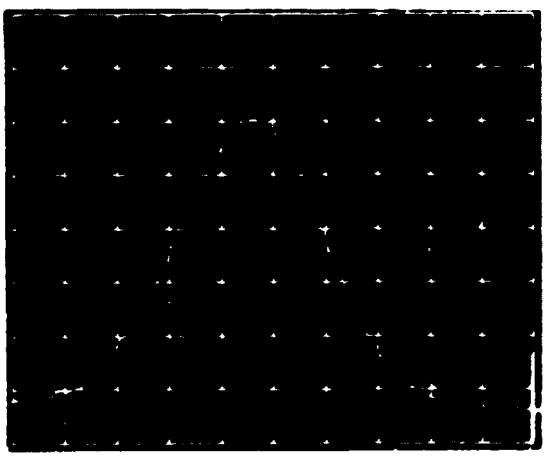

FIG. 3. The time-independent part of the ion velocity distribution function $f_0(v)$. 0.5 V/large div.

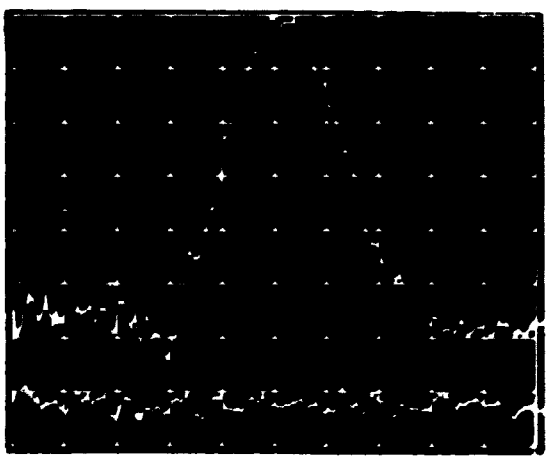

FIG. 4. The perturbation $g(v)$. The inherent noise of the circuit is shown. 0.5 V/large div.

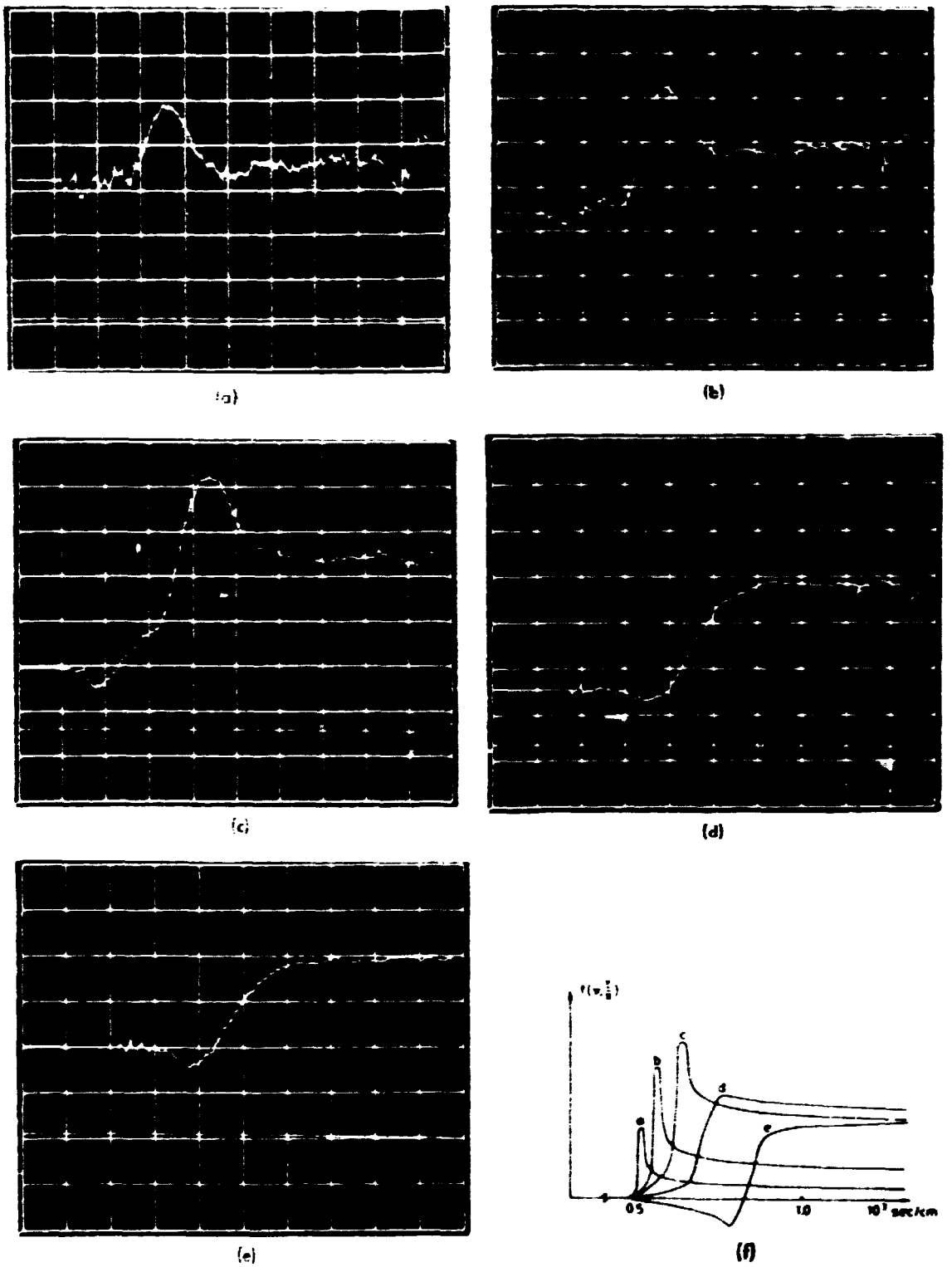

FIG. 5. The ion velocity distribution function $f(x_0, v, t)$ in the perturbation; $x_0 = 6$ cm; 10 μsec/large div. (a) $v_0 = 1930$ m/sec; (b) $v_0 = 1760$ m/sec; (c) $v_0 = 1590$ m/sec; (d) $v_0 = 1420$ m/sec; (e) $v_0 = 1220$ m/sec; (f) calculated results. The letters written on the curves correspond to experimental curves (a) through (e).

(2) Our grid gives only an approximation to the initial condition (1).

(3) In the calculations we considered the analyzer resolution with

$$\frac{\Delta I(\varphi_a)}{\Delta\varphi_a} \sim \frac{\Delta I(\varphi_a)}{\Delta v_a} \sim \int_{v_{min}}^{\infty} f(x, v, t)\, dv, \tag{10}$$

$$v_{min}^2 = \left[2e(\varphi_a \pm \Delta\varphi_a - \varphi_{pl})/m_e\right]^{1/2}.$$

This seems to be a fairly good approximation at low velocities. We know of no direct way of measuring the resolution properties of the analyzer except at very low velocities.[3]

(4) In the derivation of (7a) we neglected the change in the plasma potential associated with the pulse. This change is given by

$$\Delta\varphi_{pl}(t) \simeq \alpha T_e/e\left[n(x_a, t)/n_e\right], \tag{11}$$

where $n(x_a, t)$ is given by (6). Rigorously, the signal $S_{an}(t)$ displayed on the scope is written

$$S_{an}(t) \simeq \int_{v_{min}}^{\infty} v f_e + f_i\, dv,$$

$$v_{min}^2 = \left[2e(\varphi_a \pm \Delta\varphi_a - \left[\varphi_{pl} + \Delta\varphi_{pl}(t)\right])/m_e\right]^{1/2}.$$

By considerations analogous to those in Ref. 2 we get an additional term to Eq. (10) which at worst, can amount to 20% of (10).

Since $n(x_a, t)$ is a monotonic function of t, this term cannot cause *local* extrema like those in Figs. 5(a–c, e).

Finally, we must mention that the linear assumption seems to be well satisfied. We varied the ratio between the initial density perturbation and the density of the main plasma $\Delta n/n_e$ up to about 1, without seeing any change in the curve shape. Therefore, we may conclude that nonlinearities are not important for propagation of ion waves in a collisionless plasma as long as the temperature ratio $T_e/T_i \simeq 1$.

ACKNOWLEDGMENT

The authors want to thank V. O. Jensen for helpful discussions.

[1] R. J. Mason, Phys. Fluids 13, 1042 (1970).
[2] P. H. Sakanaka, C. K. Chu, and T. C. Marshall, Phys. Fluids 14, 611 (1971).
[3] A. V. Gurevich, L. V. Pariiskaya, and L. P. Pitaevskii, Zh. Eksp. Teor. Fiz. 54, 891 (1968) [Sov. Phys.-JETP 27, 476 (1968)].
[4] P. Korn, T. C. Marshall, and S. P. Schlesinger, Phys. Fluids 13, 517 (1970).
[5] V. Vanek and T. C. Marshall, in *Proceedings of the 3rd International Conference on Quiescent Plasmas* (Danish Atomic Energy Commission, Riso, Denmark, 1971), p. 136.
[6] R. J. Taylor, D. R. Baker, and H. Ikezi, Phys. Rev. Letters 24, 206 (1970).
[7] S. A. Andersen, G. B. Christoffersen, V. O. Jensen, P. Michelsen, and P. Nielsen, Phys. Fluids 14, 980 (1971).
[8] S. A. Andersen, V. O. Jensen, P. Michelsen, and P. Nielsen, Phys. Fluids 14, 728 (1971).
[9] G. B. Christoffersen, in *Proceedings of the 3rd International Conference on Quiescent Plasmas* (Danish Atomic Energy Commission, Riso, Denmark, 1971), p. 55.
[10] S. A. Andersen, G. B. Christoffersen, V. O. Jensen, and P. Michelsen, Plasma Phys. 14, 202 (1972).

Investigation of ion acoustic waves in collisionless plasmas

G. B. Christoffersen, V. O. Jensen, and P. Michelsen

Danish Atomic Energy Commission, Research Establishment Risø, Roskilde, Denmark

(Received 6 February 1973; final manuscript received 9 October 1973)

The Green's functions for the linearized ion Vlasov equation with a given boundary value are derived. The propagation properties of ion acoustic waves are calculated by performing convolution integrals over the Green's functions. For T_e/T_i less than about 3 it is concluded that the collective interaction is very weak and that the propagation properties are determined almost completely by freely streaming ions. The wave damping, being due to phase mixing, is determined by the width of the perturbed distribution function rather than by the slope of the undisturbed distribution function at the phase velocity as concluded from normal mode calculations.

I. INTRODUCTION

During the last ten years many experiments on ion-acoustic waves propagating through steady state, collisionless plasmas have been performed[1-5]. The aim of most of this work has been to compare the results with calculations based on the linearized Vlasov equation and thereby verify the validity of that equation and the methods used to solve it. For the propagation of ion waves along the magnetic lines of force, the linearized Vlasov equation for the ions is

$$\frac{\partial f(x,v,t)}{\partial t} + v\frac{\partial f(x,v,t)}{\partial x} + \frac{E(x,t)q}{m_i}\frac{df_0(v)}{dv} = 0, \quad (1)$$

where $f_0(v)$ is the zero-order ion velocity distribution function, and $f(x,v,t)$ is the perturbed ion velocity distribution function. q and m_i are the charge and the mass of the ions, respectively.

By assuming that the electrons behave as an isothermal fluid and that quasi-neutrality prevails we get that the electric field is given by

$$E(x,t) = -\frac{\kappa T_e}{q}\frac{1}{n_0}\frac{\partial n(x,t)}{\partial x}. \quad (2)$$

Here, κ is Boltzmann's constant, and T_e is the electron temperature. n_0 is the zero-order density given by $n_0 = \int_{-\infty}^{\infty} f_0(v)\,dv$.

Combining (1) and (2) gives the ion Vlasov equation in the form

$$\frac{\partial f(x,v,t)}{\partial t} + v\frac{\partial f(x,v,t)}{\partial x} = c_e^2\frac{1}{n_0}\frac{\partial n(x,t)}{\partial x}\frac{df_0(v)}{dv}, \quad (3)$$

where

$$n(x,t) = \int_{-\infty}^{+\infty} f(x,v,t)\,dv, \quad c_e^2 = \kappa T_e/m_i. \quad (4)$$

The term on the right-hand side of Eq. (3) is the most interesting term since it describes the collective interaction between the electric field associated with a density perturbation [see Eq. (2)] and ions in the background plasma with the velocity distribution function $f_0(v)$. The two terms on the left-hand side alone describe ions streaming freely through space without any interaction with the plasma. The collective interaction term is peculiar to plasmas; a similar term is not found in the Boltzmann equation used to describe other many-body systems (normal gases, neutrons in a fission reactor, etc.).

The technique normally used in solving Eq. (3) for propagation of ion acoustic waves was given by Landau.[6] In this technique the dielectric function, $\varepsilon(k,\omega)$, is calculated from the Vlasov equation, and the dispersion relation is then given by the equation $\varepsilon(k,\omega) = 0$. From Eqs. (3) and (4)[7] we obtain

$$\varepsilon(k,\omega) = 1 - c_e^2\frac{1}{n_0}\int_{-\infty}^{+\infty}\frac{f_0(v)}{v-\omega/k}\,dv, \quad (\mathrm{Im}\,\omega/k > 0). \quad (5)$$

A solution (ω', k') to the dispersion relation indicates that the plasma can transmit a wave which is often called a natural mode or normal mode of the type $\exp[i(\omega' t - k' x)]$. This wave is damped (Landau damping) or grows depending on the sign of the imaginary part of ω' or k'.

Quantitative agreements between experiments with grid excited ion-acoustic waves in a Q machine and calculations based on the procedure mentioned here were first reported by Wong *et al.*[1] Because $\varepsilon(k,\omega)$, as given in (4), depends on $f_0(v)$, a quantity which only appears in the collective term in the Vlasov equation, the results of these experiments were taken as indications of the importance of this term.

Calculations of the propagation properties of waves based on the technique just mentioned have been criticized by various authors.[8-13] Hirschfield and Jacob[13] showed that "the interpretation of experiments on the spatial Landau damping is complicated by the contribution of the free-streaming, initially perturbed particles". They considered an electrostatic wave excited by a grid in a steady-state plasma. By assuming a simple interaction mechanism between grid and plasma they calculated the velocity distribution function in the density perturbation at the grid. With this distribution as the boundary value they solved the Vlasov equation without the collective interaction term and found that the wave propagates and damps away very much the same way as when calculated by the normal mode method described above. In this case the damping is caused by phase mixing of the freely streaming particles in the perturbation excited at the grid. The normal mode technique ignores this effect [the boundary value does not appear in the expression for $\varepsilon(k,\omega)$]. Therefore, the experimental results cannot be taken as proof of collective interaction.

The difference between the normal mode method and that of Hirschfield and Jacob can most readily be clarified as follows: A formal solution of Eqs. (3) and (4) for a case where a wave is excited at $x = 0$ can be obtained by using the "method of characteristics", i.e., by integrating along the unperturbed orbits $x' - x = v(t' - t)$ in an (x', t') diagram. For the perturbed velocity distribution function we get

$$f(x,v,t) = g(x' = 0, v, t') + c_r^2 \frac{1}{n_0}\frac{1}{v} f_0(v) \int_0^{x} \frac{\partial n(x',t')}{\partial x'} dx', \quad (v > 0), \tag{6}$$

$$f(x,v,t) = c_r^2 \frac{1}{n_0}\frac{1}{v} f_0(v) \int_{\infty}^{x} \frac{\partial n(x',t')}{\partial x'} dx', \quad (v < 0).$$

The perturbed density is obtained by inserting Eq. (6) into Eq. (4). In Eq. (6), $g(x' = 0, v, t')$ is the distribution function in the perturbation generated by the exciter at $x = 0$. The particles in the g function move freely in the x direction and, therefore, also contribute to the perturbation for $x > 0$. The integral terms in Eq. (6) clearly stem from collective interaction.

The normal mode technique neglects the g function and only considers the collective interaction terms in Eq. (6). Hirschfield and Jacob neglect the last terms and show that the g term alone gives results very similar to those obtained from a normal mode treatment. Offhand, one cannot say which term is the most important one in an actual experimental situation. In the limit of very low electron temperature ($c_r \to 0$), the integral terms disappear and the normal mode technique is evidently incorrect. At high electron temperature the collective forces become strong [see Eq. (2)]and the g term will become unimportant. For an actual case one has to calculate solutions to Eqs. (3) and (4); such calculations require knowledge of $f_0(v)$ as well as of $g(x = 0, v, t)$.

In this paper we report on exact calculations of wave properties obtained for situations realizable in single-ended Q machines and some other steady-state plasmas.

We also present experimental results which agree with theory. The work presented here is essentially a continuation of an earlier work[12] in which we solved Eqs. (3) and (4) for an initial value where the perturbed velocity distribution function at $t = 0$ has the form $g(v)\delta(x)$; i.e., we found the Green's function for the equations with a given initial value. This situation was approximated experimentally by applying short pulses to a grid in a single-ended Q machine. Measurements of $f(x,v,t)$ and $n(x,t)$ showed very good agreement with the calculations. It was concluded that in Q machines where $T_e \approx T_i$, the freely streaming g term is much more important than the collective term; a clear-cut signature of the last term for $v > 0$ in Eq. (6) could only be seen in measurements of the perturbed velocity distribution function, $f(x,v,t)$.

In the case of waves treated in this paper, $g(x = 0, v, t)$ is an oscillating function of the type $g(v)\exp(i\omega t)$.[14] We obtain the solution to the wave problem by calculating the Green's functions for Eqs. (3) and (4) with a given boundary value and then by performing a normal convolution integration over time. The solutions of the equations for Q machine plasmas ($T_e \approx T_i$) again show that the contribution from the collective term is very weak and scarcely noticeable in any experiment. Only if $T_e \gtrsim 3T_i$ can collective effects be expected to be seen in measurements of $f(x,v,t)$, and not in density measurements. Our experimental results agree with the calculations.

The paper is organized as follows. In Sec. II we present the mathematical procedure used to solve the equations. A few theoretical results are shown in Sec. III, where we also give a brief discussion of the physical mechanisms explaning these results. Section IV describes the experimental setup and the results obtained. Finally, in Sec. V we give a general discussion and present our conclusions.

Fragments of the work described in this paper have been described elsewhere.[14-18]

II. THEORETICAL RESULTS

The experimental situation is as follows: The plasma is generated at the hot plate of a single-ended Q machine. It flows from the plate along a constant magnetic field through a biased grid at $x = 0$. At grid potential, ϕ_0, the one-dimensional ion velocity distribution function for the downstream plasma, as measured by an electrostatic energy analyser,[19] is $f_0(v)$. When the grid potential is changed by a small amount, $\Delta\phi$, the velocity distribution function is $f_0(v) + g(v)$. For sufficiently small values of $\Delta\phi$, the shape of $g(v)$ is independent of $\Delta\phi$ while the amplitude is proportional to $\Delta\phi$.[14] Therefore, it is clear that both $f_0(v)$ and $g(v)$ equal zero for $v < 0$. In our case, then the integral term for $v < 0$ in Eq. (6) vanishes. However, from a mathematical point of view it simplifies the analysis if $g(v)$ and $f_0(v)$ are analytic functions in the whole complex v plane. This means, of course, that $g(v)$ and $f_0(v)$ cannot be equal to zero for all negative v's, but we assume that the values of the two functions for v negative are so small that for physical reasons they can be neglected. Drifting Maxwellians of the type $\exp[-(v - v_d)^2/c_i^2]$ with $v_d \gtrsim 2.5c_i$ fulfill this requirement. The numerical calculations reported in the next section are performed for such $f_0(v)$ and $g(v)$ functions.

At this point we would point out that we cannot specify $g(v)$ for $v < 0$ because we also have to satisfy the condition that no particles are coming from infinity [$f(x \to \infty, v < 0, t) = 0$]. If however $f_0(v)$ is small for $v < 0$, it follows that $g(v)$ must also be small for negative v's.

In the experiment the wave is generated by superimposing an oscillating potential $\Delta\phi\exp(-i\omega t)$ on the dc voltage ϕ_0 of the grid. The boundary value for which we have to solve Eqs. (3) and (4) is therefore,

$$f(x = 0, v, t) = g(v)\exp(-i\omega t) \tag{7}$$

and

$$n(x = 0, t) = \exp(-i\omega t)\int_{-\infty}^{\infty} g(v)\,dv. \tag{8}$$

Here, we integrate from $-\infty$ to ∞ but in accordance with the preceding remarks the contribution to the density from particles moving with negative velocity is negligible. In this way the calculation is reduced to a pure boundary

value problem. The general case where $f_0(v) \neq 0$ for $v < 0$ is more complicated, but can, for instance, be solved as a mixed initial value-boundary value problem as done by Weitzner.[10]

The use of the linearized equation is justified by the fact that in the experiment $n(x = 0, t) \ll n_0$.

In the calculations we use a Green's function technique and first calculate the time and space dependence of perturbations generated by short pulses, $[\delta(t)]$, applied to the grid, and then perform a convolution integration over time to obtain the response to an oscillating potential on the grid.

We introduce the δ function as follows

$$\delta(t) = \lim_{\alpha \to 0} \frac{1}{\pi} \frac{\alpha}{\alpha^2 + t^2}. \tag{9}$$

To find the Green's function for the density, $n_G(x, t)$, and that for the distribution function, $f_G(x, v, t)$, we solve Eqs. (3) and (4) with the boundary conditions

$$f_G(x = 0, v, t) = g(v) \frac{1}{\pi} \frac{\alpha}{\alpha^2 + t^2} \tag{10}$$

and

$$n_G(x = 0, t) = \int_{-\infty}^{\infty} g(v) \frac{1}{\pi} \frac{\alpha}{\alpha^2 + t^2} dv \equiv \eta \frac{1}{\pi} \frac{\alpha}{\alpha^2 + t^2}, \tag{11}$$

and let $\alpha \to 0$ in the solutions. In solving the equations we apply a Laplace transformation in space, $f(k) = \int_0^{\infty} \exp(ikx) f(x)\, dx$, and a Fourier transformation in time, $f(\omega) = \int_{-\infty}^{\infty} \exp(-i\omega t) f(t)\, dt$. Doing this we find the results

$$\begin{aligned} n_G(k, \omega) &= \frac{1}{ik} \exp(-\alpha|\omega|) \left(\frac{\eta c_e^2}{n_0} \int_{-\infty}^{\infty} \frac{f_0'(v)}{v - \omega/k} dv - \int_{-\infty}^{\infty} \frac{v g(v)}{v - \omega/k} dv \right) \left(1 - \frac{c_e^2}{n_0} \int_{-\infty}^{\infty} \frac{f_0'(v)}{v - \omega/k} dv \right)^{-1} \\ &= -\frac{1}{ik} \exp(-\alpha|\omega|) \left[\eta + \frac{\omega}{k} \int_{-\infty}^{\infty} \frac{g(v)}{v - \omega/k} dv \left(1 - \frac{c_e^2}{n_0} \int_{-\infty}^{\infty} \frac{f_0'(v)}{v - \omega/k} dv \right)^{-1} \right] \\ &\equiv \frac{1}{ik} \exp(-\alpha|\omega|) N\left(\frac{\omega}{k}\right), \end{aligned} \tag{12}$$

and

$$\begin{aligned} f_G(k, v, \omega) &= \frac{1}{ik} \exp(-\alpha|\omega|) \left(\frac{c_e^2}{n_0} N\left(\frac{\omega}{k}\right) \frac{f_0'(v)}{v - \omega/k} - \frac{v g(v)}{v - \omega/k} + \frac{c_e^2 \eta}{n_0} \frac{f_0'(v)}{v - \omega/k} \right) \\ &= \frac{1}{ik} \exp(-\alpha|\omega|) \left(- \frac{v g(v)}{v - \omega/k} - \frac{c_e^2}{n_0} \frac{f_0'(v)}{v - \omega/k} \frac{\frac{\omega}{k} \int_{-\infty}^{\infty} \frac{g(v)}{v - \omega/k} dv}{1 - (c_e^2/n_0) \int_{-\infty}^{\infty} dv\, f_0'(v)/[v - (\omega/k)]} \right) \\ &\equiv \frac{1}{ik} \exp(-\alpha|\omega|) M\left(v, \frac{\omega}{k}\right). \end{aligned} \tag{13}$$

To transform $n_G(k, \omega)$ and $f_G(k, v, \omega)$ back to time and space variables we have to perform the integrations

$$n_G(x, t) = \frac{1}{4\pi^2} \int_{-\infty+i\delta}^{+\infty+i\delta} \exp(-ikx) \times \int_{-\infty}^{\infty} \exp(i\omega t) n_G(k, \omega)\, d\omega\, dk \tag{14}$$

and

$$f_G(x, v, t) = \frac{1}{4\pi^2} \int_{-\infty+i\delta}^{+\infty+i\delta} \exp(-ikx) \times \int_{-\infty}^{\infty} \exp(i\omega t) f_G(k, v, \omega)\, d\omega\, dk, \tag{15}$$

where δ is a positive number assuring that the integration path in the k plane runs above all singularities in $n_G(k, \omega)$ and in $f_G(k, v, \omega)$. Since ω only takes real values in the integrations in Eqs. (14) and (15), it is clear that $n_G(k, \omega)$ and $f_G(k, v, \omega)$ are singular on the real k axis. However, by defining $n_G(k, \omega)$ and $f_G(k, v, \omega)$ for real k values by the analytic continuation of the functions, we can avoid the singularities on the real axis. Furthermore, $n_G(k, \omega)$ and $f_G(k, v, \omega)$ also have singularities in the positive imaginary part of the k plane if there exist k values in this plane for which the denominator of $N(\omega/k)$ equals zero. We assume that the denominator of $N(\omega/k)$ has no zero for $\mathrm{Im}\, k > 0$; later, we shall show that this assumption holds as long as we confine ourselves to treat $f_0(v)$ functions which only have stable solutions in a normal mode treatment of the wave problem.[6,12]

The v integrations in $N(\omega/k)$ have poles for $v = \omega/k$. For $\mathrm{Im}\, k > 0$, the pole lies above the real v axis if $\omega < 0$ and below if $\omega > 0$. Therefore, the analytic continuation

of $n_G(k,\omega)$ and $f_G(k,v,\omega)$ for real k is obtained by prescribing that the v integration path shall run below the pole for $\omega < 0$ and above for $\omega > 0$. We therefore define

$$N(\omega/k) = \begin{cases} N_b(\omega/k) & \text{for } \omega < 0 \\ N_a(\omega/k) & \text{for } \omega > 0 \end{cases} \tag{16}$$

and

$$M(v,\omega/k) = \begin{cases} M_b(v,\omega/k) & \text{for } \omega < 0 \\ M_a(v,\omega/k) & \text{for } \omega > 0, \end{cases} \tag{17}$$

where the subscript b indicates that the v integration path runs below the pole and the subscript a indicates that it runs above the pole.

Having defined the analytic continuations of $n_G(k,\omega)$ and $f_G(k,v,\omega)$, we can go to the limit $\delta = 0$ in Eqs. (14) and (15) and rewrite Eq. (14) in the form

$$\begin{aligned} n_G(x,t) = {} & \frac{1}{4\pi^2 i} \\ & \times \left[\int_{-\infty}^{0-}\int_{-\infty}^{0-} \frac{1}{k}\exp(i\omega t + \alpha\omega - ikx) N_b\left(\frac{\omega}{k}\right) d\omega\, dk \right. \\ & + \int_{-\infty}^{0-}\int_{0+}^{\infty} \frac{1}{k}\exp(i\omega t - \alpha\omega - ikx) N_a\left(\frac{\omega}{k}\right) d\omega\, dk \\ & + \int_{0+}^{\infty}\int_{-\infty}^{0-} \frac{1}{k}\exp(i\omega t + \alpha\omega - ikx) N_b\left(\frac{\omega}{k}\right) d\omega\, dk \\ & \left. + \int_{0+}^{\infty}\int_{0+}^{\infty} \frac{1}{k}\exp(i\omega t - \alpha\omega - ikx) N_a\left(\frac{\omega}{k}\right) d\omega\, dk \right]. \end{aligned} \tag{18}$$

By substituting $k = \omega/u$ after some simple algebra we get

$$\begin{aligned} n_G(x,t) = {} & -\frac{1}{4\pi^2 i}\left\{ \int_{-\infty}^{\infty} \frac{1}{u} N_b(u) \right. \\ & \times \int_{-\infty}^{0-} \exp\left[-i\omega\left(\frac{x}{u} + i\alpha - t\right)\right] d\omega\, du \\ & \left. - \int_{-\infty}^{\infty} \frac{1}{u} N_a(u) \int_{0+}^{\infty} \exp\left[-i\omega\left(\frac{x}{u} - i\alpha - t\right)\right] d\omega\, du \right\}. \end{aligned} \tag{19}$$

Performing the ω integration we immediately get

$$\begin{aligned} n_G(x,t) = {} & \frac{1}{4\pi^2}\left(\frac{1}{t + i\alpha}\int_{-\infty}^{\infty} N_a(u)\left(u - \frac{x}{t + i\alpha}\right)^{-1} du \right. \\ & \left. + \frac{1}{t - i\alpha}\int_{-\infty}^{\infty} N_b(u)\left(u - \frac{x}{t - i\alpha}\right)^{-1} du \right). \end{aligned} \tag{20}$$

To proceed we note that $N_a(u)$ is analytic in the half-u plane in which $\mathrm{Im}\, u \le 0$ and $N_b(u)$ is analytic for $\mathrm{Im}\, u \ge 0$. This is assured by the analytic continuation of the function as described here and because the denominators in N_a and N_b are assumed to have no zeros in the half-planes where the two functions are defined. The denominator in N_b is the classical dielectric function for the plasma [see Eq. (5)]. This function is known[12] to have no zeros in the half-plane in which it is defined for $f_0(v)$ functions which are stable in a normal mode treatment.

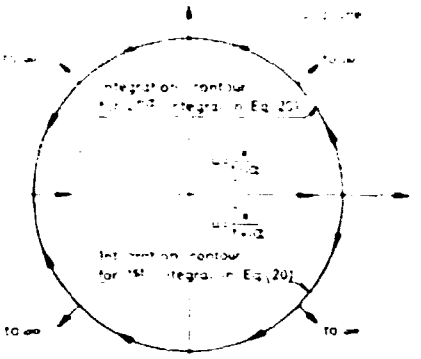

FIG. 1. Integration contours.

Similarly, as also shown in Ref. 12, the denominator of N_a has no zeros in the half-plane where it is defined as long as we only consider Landau-stable $f_0(v)$ functions. Finally, it is clear from the definitions of the N functions in Eq. (12) that $N_{a,b}(u) \to 0$ for $|u| \to \infty$ in the two half-planes where the N functions are defined. Thus, in calculating the integrals in (20) we can use Jordan's lemma and change the integration paths to closed half-circles as indicated in Fig. 1. The integrand in the first integral in (20) has a pole at $u = x/t + i\alpha$, i.e., within the integration contour; similarly, the integrand in the last integral has a pole at $u = x/t - i\alpha$ within the integration contour for this integral. Using residue calculations we thus get

$$n_G(x,t) = \frac{1}{2\pi i}\left[\frac{1}{t + i\alpha} N_a\left(\frac{x}{t + i\alpha}\right) - \frac{1}{t - i\alpha} N_b\left(\frac{x}{t - i\alpha}\right) \right]. \tag{21}$$

By going to the limit $\alpha \to 0$ we get

$$n_G(x,t) = \frac{1}{2\pi i}\frac{1}{t}\left[N_a\left(\frac{x}{t}\right) - N_b\left(\frac{x}{t}\right) \right] \tag{22}$$

and because $N_a(x/t) = N_b^*(x/t)$ for real x/t we get

$$n_G(x,t) = -\frac{1}{\pi}\frac{1}{t}\,\mathrm{Im}\, N_b\left(\frac{x}{t}\right). \tag{23}$$

Equation (23) is the Green's function for the perturbed density obtained from Eqs. (3) and (4) with the boundary conditions (10) and (11). Equation (23) differs from the corresponding function [Eq. (12)] in Ref. 12 only by the term

$$\frac{\eta c_e^2}{n_0}\int_{-\infty}^{\infty} \frac{f_0'(v)}{v - \omega/k}\, dv$$

in the definition of N in Eq (12). This difference is caused by the fact that in Ref. 12 the Green's function was found for an initial value problem, while here it is for a boundary value problem. The case treated here is more relevant to grid-excited perturbations in Q machines.

To calculate $f_G(x,v,t)$ from (15) we proceed in a way similar to that used in the $n_G(x,t)$ calculations. Thus, we obtain, in analogy with Eq. (21)

$$f_G(x,v,t) = \frac{1}{2\pi i}\left[\frac{1}{t + i\alpha} M_a\left(v, \frac{x}{t + i\alpha}\right) \right.$$

$$- \frac{1}{t - i\alpha} M_b\left(v, \frac{x}{t - i\alpha}\right)\Bigg]. \quad (24)$$

By inserting the M functions given by Eqs. (17) and (13) into Eq. (24) we get

$$f_G(x,v,t) = \frac{1}{2\pi i}\frac{c_r^2}{n_0} f_0'(v)\left(\frac{N_b(x/t + i\alpha)}{vt + i\alpha v - x} - \frac{N_b(x/t - i\alpha)}{vt - i\alpha v - x}\right)$$
$$- \frac{vg(v)}{2\pi i}\left(\frac{1}{vt + i\alpha v - x} - \frac{1}{vt - i\alpha v - x}\right)$$
$$+ \frac{1}{2\pi i}\frac{c_r^2}{n_0}\eta f_0'(v)\left(\frac{1}{vt + i\alpha v - x} - \frac{1}{vt - i\alpha v - x}\right). \quad (25)$$

After some simple algebra we go to the limit $\alpha = 0$ and use the definition of the δ function in Eq. (9) and the well-known definition of the principal value

$$P\frac{1}{y - a} = \lim_{\alpha \to 0} \frac{y - a}{(y - a)^2 + \alpha^2}. \quad (26)$$

Doing this we get

$$f_G(x,v,t) = \left\{vg(v) - \frac{c_r^2}{n_0} f_0'(v)\left[\mathrm{Re}\ N_b\left(\frac{x}{t}\right) + \eta\right]\right\}$$
$$\times \delta(x - vt) + \frac{c_r^2}{n_0} f_0'(v)\,\mathrm{Im}\ N_b\left(\frac{x}{t}\right)\frac{1}{\pi} P\frac{1}{x - vt}. \quad (27)$$

Equation (27) is the Green's function for the perturbed ion velocity distribution function. The difference between this function and the corresponding one derived in a somewhat different way in Ref. 12 is again caused by different choices of initial conditions.

Having the Green's function for the perturbed density and ion velocity distribution function, it is simple to calculate the response for any signal applied to the grid. Here, we consider the case where an oscillating potential as $\exp(-i\omega t')$ is applied to the grid and calculate the propagation properties of the wave generated thereby.

The density, $n(x,t)$, in the wave as a function of x and t is given by

$$n(x,t) = \int_{-\infty}^{t} \exp(-i\omega t') n_G(x, t - t')\,dt', \quad (28)$$

which, with the substitution $t - t' = \tau$ and with the use of (23), can be rewritten

$$n(x,t) = -\exp(-i\omega t)\int_0^\infty \frac{1}{\pi\tau}\exp(i\omega\tau)\,\mathrm{Im}\ N_b\left(\frac{x}{\tau}\right)d\tau$$
$$= \exp(-i\omega t)\frac{1}{\pi}\int_0^\infty \frac{1}{v}\exp\left(i\omega\frac{x}{v}\right)\mathrm{Im}\ N_b(v)\,dv. \quad (29)$$

To obtain the last term in Eq. (29) we have introduced $v = x/\tau$. Inspection of Eq. (12) shows directly that $N_b(v) \to 0$ for $v \to 0$; therefore, there is no problem at the lower limit of the integral in Eq. (29). The same expression for $n(x,t)$ was derived by using different arguments elsewhere.[15] The modulus of the complex integral in Eq. (29) gives the amplitude of the density in a wave as a function of x. Similarly, the argument of the integral is the phase of the wave measured with respect to the phase of the wave exciter.

A similar calculation of the perturbed ion velocity distribution in a wave gives

$$f(x,v,t) = \exp(-i\omega t)\left(\exp\left(i\omega\frac{x}{v}\right)\right.$$
$$\times\left\{g(v) - \frac{c_r^2}{n_0}\frac{1}{v} f_0'(v)[\mathrm{Re}\ N_b(v) + \eta]\right\}$$
$$\left. - \frac{c_r^2}{n_0} f_0'(v)\frac{1}{\pi} P\int_0^\infty \frac{1}{v}\frac{\mathrm{Im}\ N_b(v)}{v - v}\exp\left(i\omega\frac{x}{v}\right)dv\right). \quad (30)$$

Again, the modulus of the complex term in the large parenthesis in Eq. (30) represents the amplitude of the perturbed ion velocity distribution function and the argument gives the phase. The same formula for $f(x,v,t)$ was obtained in Ref. 15.

A computer code has been produced which allows us to calculate the Green's functions (23) and (27) and the amplitude and phase of the wave function (29) and (30). The code calculates the quantities mentioned for cases where $f_0(v)$ and $g(v)$ are drifting Maxwellians of the form

$$f_0(v) \propto \exp[-(v - v_d)^2/c_i^2] \quad (31)$$

and

$$g(v) \propto \exp[-(v - v_{d_g})^2/c_n^2]. \quad (32)$$

c_i is related to the ion temperature through $c_i^2 = 2\kappa T_i/m_i$ and similarly $c_n^2 = 2\kappa T_n/m_i$. The propagation properties can be calculated for various values of the parameters T_e/T_i, v_d/c_i, v_{d_g}/c_i, and T_i/T_n.

III. DISCUSSION OF NUMERICAL RESULTS

In this section we show and discuss a few results obtained from calculating the Green's functions given in Eqs. (23) and (27), and the wave propagation properties in Eqs. (29) and (30). We have chosen to present the calculations for a situation where the parameters in Eqs. (31) and (32) have the following values: $v_d/c_i = 3$, $v_{d_g}/c_i = 3$, and $T_i/T_n = 1$. Such values can be obtained in single-ended Q machines.[19] To show the effect of changing the electron to ion temperature ratio we have performed the calculations for various values of T_e/T_i. In an experiment performed in order to check the Green's functions[12] one can apply short pulses to a grid and measure the response as a function of time from a probe at some fixed position. We therefore present the calculated Green's function as a function of the dimensionless time, tc_i/x, rather than as a function of distance. The Green's functions, $f_G(x,v,t)$, as given in Eq. (27) are singular for $x = vt$. Experimentally, these functions can be measured by means of an electrostatic energy analyzer[12] which necessarily has a finite resolution. The signal $S_G(x,v_a,t)$ which we obtain from the analyzer when it is adjusted to measure a velocity v_a is therefore given by

$$S_G(x,v_a,t) \propto \frac{1}{v_a}\int_0^\infty v f_G(x,v,t)\exp[-(v - v_a)^2/v_r^2]\,dv. \quad (33)$$

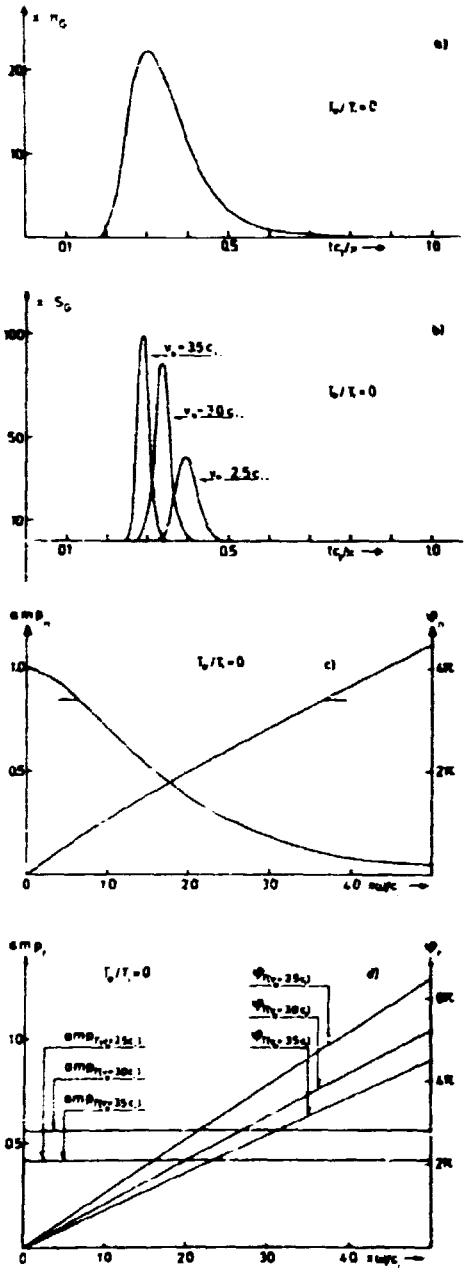

FIG. 2. Propagation through plasma with cold electrons, $T_e/T_i = 0$. (a) The Green's function for the density. (b) The analyzer signal $S_G(x, v_a, t)$ [see Eq. (33)] calculated for various v_a values. (c) Amplitude and phase of wave density. (d) Amplitude and phase of perturbed ion velocity distribution function in a wave.

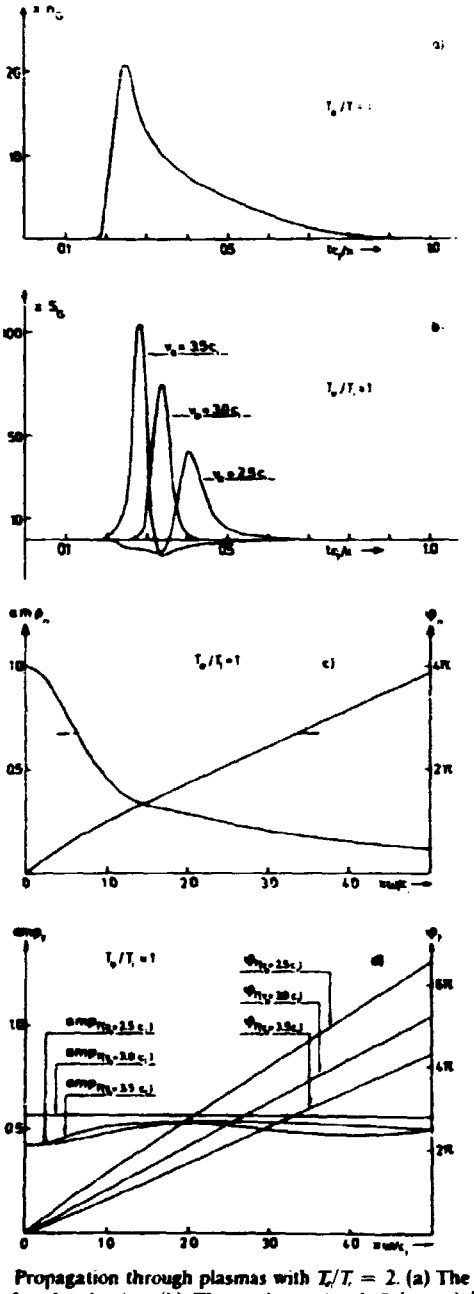

FIG. 3. Propagation through plasmas with $T_e/T_i = 2$. (a) The Green's function for the density. (b) The analyzer signal $S_G(x, v_a, t)$ [see Eq. (33)]calculated for various v_a values. (c) Amplitude and phase of wave density. (d) Amplitude and phase of perturbed ion velocity distribution function in a wave.

This equation is obtained under the assumption that the resolution of the analyzer is a Gaussian of the type $\exp[-(v-v_a)^2/v_r^2]$. The functions, S_G, shown in Figs. 2–4 are obtained for the case where $v_r = c_s/4$.

The curves amp_n and ϕ_n showing the amplitude and the phase of the density, respectively, are calculated directly from Eq. (29) as functions of the dimensionless parameter $\omega x/c_s$. Similarly, the amplitude amp_f and the phase ϕ_f of the perturbed distribution function in a wave are calculated from Eq. (30), also as functions of $\omega x/c_s$.

Figure 2 shows the results obtained for the case of freely streaming ions where $T_e/T_i = 0$. In Fig. 2(a) we present the Green's function, n_G, for the density and in Fig. 2(b) the S_G function calculated for three v_a values. Figures 2(c) and (d) show the amplitude and the phase of the density and of the distribution function in a wave, respectively. The wave damping in this case is clearly caused by phase-mixing of freely streaming ions.

In Fig. 3 we show the corresponding curves obtained for the case $T_e/T_i = 1$. We notice that the most significant difference between the curves in Fig. 2 and the ones in Fig. 3 is the undershoot seen on the S_G curves in Fig. 3(b). This undershoot, which is a clear-cut signature of the collective interaction term in Eq. (3), was demonstrated experimentally in Ref. 12 and a physical explanation was

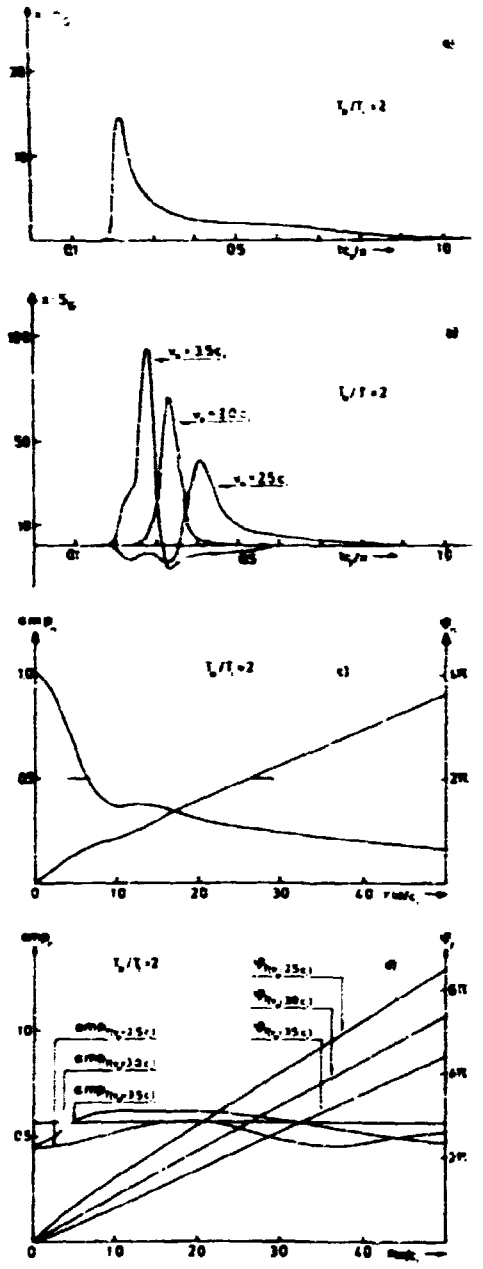

FIG. 4. Propagation through plasmas with $T_e/T_i = 2$. (a) The Green's function for the density. (b) The analyzer signal $S_a(x, v_a, t)$ [see Eq. (33)] calculated for various v_a values. (c) Amplitude and phase of wave density. (d) Amplitude and phase of perturbed ion velocity distribution function in a wave.

given in Ref. 20. The curves in Fig. 3(c) and (d), showing the wave characteristics, are so similar to the corresponding ones in Figs. 2(c) and (d) that it seems unlikely that collective interaction in ion-acoustic waves can be demonstrated experimentally if $T_e \lesssim T_i$. The damping is, in this case, of course, partly due to phase mixing and partly to collective interaction.

The curves in Fig. 4 are calculated for $T_e/T_i = 2$. Here, we note a tendency in the n_G curve to show two maxima. This is a significant change in comparison with the corresponding results in Fig. 2(a) and 3(a). The physical reason for this splitting up has been discussed in some detail in Ref. 16. The two maxima in the n_G curve are responsible for the tendency of the amp$_n$ curve in Fig. 4(c)

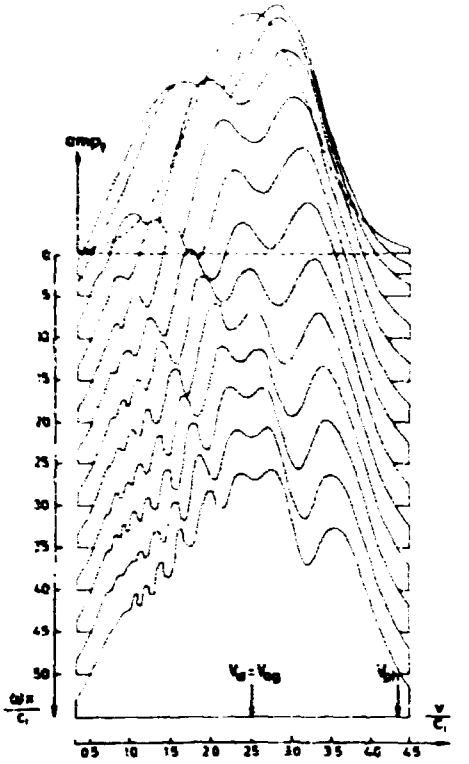

FIG. 5. Curves showing the amplitude of the perturbed ion velocity distribution function at various positions calculated for a plasma where $T_e/T_i = 3$, $v_a = v_{ds} = 2.5c_s$, and $T_i/T_e = 1$.

to oscillate with distance. This oscillation can be understood physically as a beating between two damped waves propagating with velocities corresponding to the velocity of the two maxima in the n_G curve.[16,17] We also note a clear difference between the amp$_f$ curve in Fig. 4(d) and that in Fig. 2(d). This difference is also a clear sign of collective interaction. In Fig. 5 we show examples of amp$_f$ curves calculated as functions of v/c_s at various $\omega x/c_s$ values for the case where $T_e/T_i = 3$, $v_d = v_{ds} = 2.5c_s$, and $T_i/T_e = 1$. The very characteristic oscillations of the curves are explained physically in Refs. 17 and 18. An experimental observation of these oscillations would constitute a clear-cut sign of collective interaction in ion acoustic waves.

More extensive discussions of the physical mechanism explaining the results obtained by calculating the Green's function and the wave characteristics are given in Refs. 15–18, and 20. It should be noted that the calculations in Refs. 16 and 20 are based on the Green's functions of Ref. 12 which were obtained for an initial value problem. A comparison between the Green's functions of Ref. 12 and those obtained for a boundary value problem in this paper shows that the functions are very similar and that they have the same characteristic dependences of the parameters. Therefore, the discussions given in Refs. 16 and 20 are also valid for waves treated as a boundary value problem.

IV. EXPERIMENTAL RESULTS

In this section we describe measurements of the perturbed ion velocity distribution in ion waves in a single-ended Q machine. The experimental setup is shown

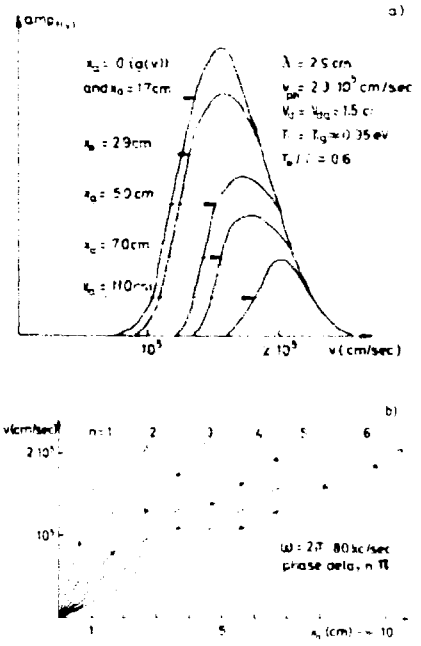

FIG. 6: Experimental set up.

schematically in Fig. 6. The plasma is produced by surface ionization of a beam of cesium atoms from the Cs oven on the hot tantalum plate ($\simeq 2500°K$) and is radially confined by a uniform, magnetic field of an intensity up to 1 T. The plasma column is 3 cm in diameter and it ends at an electrostatic ion energy analyzer[19] at $x = x_a$. In the experiments to be described here the plasma density, n_0, is less than $10^9 cm^{-3}$, i.e., the plasma can be considered as being collisionless. The vacuum system consists of a stainless steel tube (not shown in Fig. 6) which is cooled to $-20°C$ to reduce the Cs background pressure. In operation the pressure is below 10^{-5} Torr. The plasma waves studied in this work were excited by a grid at $x = 0$. The grid consists of a thin nickel mesh with 400 0.5×0.5 mm² holes per cm².

The experimental procedure is as follows: First, the desired undisturbed ion velocity distribution function, $f_0(v)$, is obtained by adjusting the temperature of the hot plate and the density of the Cs beam. The grid is biased to a potential ϕ_0 which is close to the floating potential and $f_0(v)$ is measured by the analyzer by using the technique described in Ref. 19. The grid potential is now changed by a small amount $\Delta\phi$ to $\phi_0 + \Delta\phi$ and the velocity distribution $f_0(v) + g(v)$ is measured. The function $g(v)$ can then be obtained by using the technique described in Ref. 14.

Now the grid is connected to the oscillating signal $[\exp(i\omega t)]$ of a lock-in amplifier as shown in Fig. 6. Thereby a wave with frequency ω is launched; this wave is analyzed by the electrostatic analyzer. For the measurements of the perturbed velocity distribution function, the circuit shown in Fig. 6 was used. The analyzer grid is biased negatively with respect to the plasma potential ϕ_{pl} in order to reflect all electrons. The collector plate is connected to a sweep-box which varies the plate potential ϕ_a slowly and linearly with time as indicated in the figure. The time varying part of the ion current to the collector plate, when biased to ϕ_a, is given by

$$I(\phi_a, t) = qA \int_{v_{min}}^{\infty} v f(x_a, v, t)\, dv, \tag{34}$$

where $\frac{1}{2}mv_{min}^2 = q(\phi_a - \phi_{pl})$ and A is the effective mesh area. By changing the variable: $v^2 = (2q/m)(\phi - \phi_{pl})$, Eq. (34) becomes

$$I(\phi_a, t) = \text{const} \int_{\phi_a - \phi_{pl}}^{\infty} f(x_a, \phi, t)\, d\phi; \tag{35}$$

this is the signal led from the sweep-box to the lock-in amplifier in Fig. 6. The lock-in amplifier amplifies the part of this signal which oscillates with the frequency ω and thus produces a signal

$$S(\phi_a) = \frac{1}{\Delta T}\int_0^{\Delta T} I(\phi_a, t)\exp[i(\omega t - \theta_0)]dt$$

$$= \frac{\text{const}}{\Delta T}\int_0^{\Delta T}\exp[i(\omega t - \theta_0)]dt \int_{\phi_a - \phi_{pl}}^{\infty} f(x_a, \phi, t)\, d\phi. \tag{36}$$

θ_0 is a phase angle adjustable on the amplifier. $S(\phi_a)$ is led to the differential unit and differentiated with respect to time. The output signal, which is led to the y plates of the scope and displayed as a function of ϕ_a, is

$$\frac{dS(\phi_a)}{dt} = \frac{dS(\phi_a)}{d\phi_a}\frac{d\phi_a}{dt}$$

$$= -\frac{\text{const}}{\Delta T}\frac{d\phi_a}{dt}\int_0^{\Delta T}\exp[i(\omega t - \theta_0)]\, f(x_a, \phi_a - \phi_{pl}, t)dt$$

$$\propto \left| f\left[x_a, v = \left(\frac{2q(\phi_a - \phi_{pl})}{m}\right)^{1/2}\right]\right|$$

$$\times \exp\{i[\theta(\phi_a - \phi_{pl}) - \theta_0]\}. \tag{37}$$

$d\phi_a(t)/dt$ is a constant because $\phi_a(t)$ as generated by the sweep-box is proportional to time. The electric circuit only works the way discussed if the time constants for differentiation, integration, voltage sweeping, and for the wave are chosen properly.

Experimental measurements of $\text{amp}_f = |f(x_a, v = (2q(\phi_a - \phi_{pl})/m)^{1/2})|$ and of $\phi_f = \theta(\phi_a - \phi_{pl})$ are obtained by varying θ_0 on the lock-in amplifier until amp_f as displayed on the oscilloscope reaches its maximum value for a given ϕ_a. As seen from Eq. (37) it is possible to convert the measured quantities, amp_f and ϕ_f, into functions of velocity only if the effective analyzing potential, $\phi_a - \phi_{pl}$, is known. Experimentally, we have determined ϕ_{pl} by utilizing the technique described in Ref. 19.

In Fig. 7 we show experimental results obtained for a situation where $f_0(v)$ and $g(v)$ were found to be close to Maxwellian distribution functions with drift velocities $v_d = v_{dg} = 1.5c_s$, $T_i = T_g \simeq 0.35$ eV, and $T_i/T_e \simeq 0.6$. The density $n_0 \simeq 10^9 cm^{-3}$ and the frequency, $\omega/2\pi$, applied to the exciting grid was 80 kc/sec. The phase velocity and

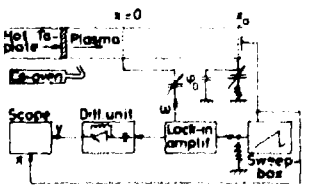

FIG. 7. Experimental results obtained in measurements on an ion acoustic wave with frequency 80 kc/sec. (a) The amplitude of the perturbed ion velocity distribution function measured at various positions. (b) The phase delay of $f(x_a, v)$ measured at various positions.

the damping of the wave density were determined in the conventional way by measuring the amplitude and the phase of the ion saturation current ($\phi_s = \phi_{sc}$) to the analyzer collector at various positions. The phase velocity was found to be $v_{ph} = 2.3 \times 10^5$ cm sec corresponding to a wavelength $\lambda = 2.9$cm. The wave amplitude damps with an e^{-1} – folding length of approximately one wavelength.

In Fig. 7(a) we present measurements of amp_{n_i} as functions of v obtained at various analyzer positions. Figure 7(b) shows experimentally obtained phase relations. At different x_s positions we have found those v values for which $f(x_s, v)$ is delayed $n \times \pi$ with respect to the phase of the exciter (n is an integer). The results shown in the figure constitute an experimental verification of the phase relation $\exp(i\omega x_s/v_s)$, which is obtained directly from Eq. (30) by going to the limit $c_s = 0$, i.e., in the limit where collective interaction can be ignored. The small discrepancy ($\approx 10\%$) between the phase relation obtained from Eq. (30) and the experimental points can be explained by the uncertainty in the experimental determination of ϕ_{sc}, which causes an uncertainty in the calculation of v [see Eq. (37)].

According to Eq. (30), amp_{n_i} should be equal to $g(v)$ and independent of x_s if $c_s = 0$. The experimental results in Fig. 7(a) show a strong damping of amp_{n_i} with distance x_s, especially for low v values. By using the following arguments based on freely streaming ions this damping can be explained by the finite resolution of the analyzer. The ions are released from the grid with the velocity distribution function $g(v)\cos\omega t$. At $x = x_s$ the analyzer measures amp_{n_i} at the time $t_s = x_s/v_s$. At this time however, there are also ions present at x_s with the velocity v, and they are partly accepted by the analyzer because of its finite resolution expressed by $\exp[-(v - v_s)^2/v_r^2]$. The ions with velocity v were released from the grid at $t = t_s - x_s/v$. Therefore, the analyzer adjusted to measure at the velocity v_s gives a signal

$$S_{v_s} \propto \int_0^\infty v g(v) \cos\left[\omega\left(\frac{x_s}{v_s} - \frac{x_s}{v}\right)\right] \exp[-(v - v_s)^2/v_r^2]\, dv. \tag{38}$$

By assuming v_r to be small compared with v_s, $vg(v)$ can be considered as a constant and $v_s^{-1} - v^{-1} \simeq (v - v_s)/v_s^2$. After some simple algebra one gets

$$S_{v_s} \propto \exp\left[-\left(\frac{\omega x_s v_r}{2v_s^2}\right)^2\right]. \tag{39}$$

This expression explains the very strong damping measured at low v_s values.

Measurements such as the ones described here have been performed at various frequencies and densities, and with different $f_0(v)$ and $g(v)$ functions. The conclusions from all the measurements are that *no* sign of collective interaction could be demonstrated. This is what would be expected from the theoretical work of Secs. II and IV. It should be mentioned that similar measurements leading to the same conclusions were reported by Ikezi and Taylor.[21,22]

Further, we have heated the electrons in order to reach a T_e/T_i value around 3. The heating technique used has been described by Christoffersen and Prahm.[23] At these high-temperature ratios the characteristic oscillations in amp_{n_i} shown in Fig. 5 can be expected. We were not able to detect these oscillations experimentally. We believe that the reason is that the resolution of the analyzer is not sufficiently good.

V. DISCUSSION AND CONCLUSIONS

In this paper we have calculated the Green's functions for the linearized ion Vlasov equation for a known boundary value problem. The Green's functions for the density as well as for the perturbed velocity distribution function are obtained, and they are always found to take the self-similar form, $n_{i_1}(x, t) = (1/t)h_{n_i}(x/t)$. The functions, $h_{n_i}(x/t)$, depend on the boundary value, $g(v)$, and on the dielectric properties of the plasma, which in turn depend on T_e and on the undisturbed ion velocity distribution function $f_0(v)$.

The Green's function for the density, $n_{i_1}(x, t)$, varies weakly with T_e/T_i as long as $T_e/T_i \lesssim 3$ (see Figs. 2, 3, and 4). Furthermore, it should be noted that the Green's function for the density obtained for the case where $T_e \neq 0$ could also be obtained for $T_e = 0$ if another $g(v)$ was assumed. The $g(v)$ function needed in order to produce a $n_{i_1}(x, t)$ function of a given form for a case without collective interaction can be calculated from Eqs. (12), (16), and (23) with $T_e = 0$. It is therefore clear that to demonstrate collective effects in a measurement of $n_{i_1}(x, t)$ would require a detailed knowledge of the boundary value function $g(v)$. In an actual experimental situation such knowledge is very difficult to obtain and it can, therefore, be concluded that it is very unlikely that collective effects can be demonstrated in measurements of $n_{i_1}(x, t)$.

For $T_e \neq 0$, the Green's functions for the perturbed velocity distribution function, $f_{i_1}(x, v, t)$, show the same characteristic features [the undershoots seen in Figs. 3(b) and 4(b)] which are clearly caused by collective interaction. The experimental observations of these features reported in Ref. 12 are therefore a clear demonstration of collective effects.

The propagation characteristics for locally excited ion acoustic waves were calculated by performing convolution integrals of the Green's functions. The calculations show that waves are, in general, damped. For $T_e = 0$, the damping is clearly caused solely by phase mixing of freely streaming ions and therefore the ratio, δ/λ, between the damping length and the wavelength is roughly given by $v_{ph}/\Delta v$ where Δv is the width of the $g(v)$ function. For $T_e \neq 0$, collective interaction plays a role in the wave damping. It should, however, be noted that by assuming the proper $g(v)$ function, one can get the same Green's function for the density for $T_e = 0$ as the one we get for $T_e \neq 0$. We can also obtain the same amp_{n_i} curve for the case where $T_e = 0$ as the one we obtain for $T_e \neq 0$. We may therefore conclude that density measurements in a wave are equally unlikely to demonstrate collective interaction as are measurements of $n_{i_1}(x, t)$. We can further point out that for the case $T_e \neq 0$, the damping ratio, δ/λ, is roughly determined by the width of the $n_{i_1}(x, t)$ function divided by the phase velocity of the wave. This

statement is in contradiction to the results obtained in a normal mode treatment where it is found that the damping is determined by the slope of the $f_0(v)$ function at $v = v_{ph}$. Our results suggest that some calculations of stability problems based on a normal mode treatment probably ought to be reconsidered. In this respect it should be noted that by using the Green's functions obtained in this work it has been possible to show rigorously that an exponentially damped wave of the normal mode form $\exp[-i(\omega t - kx)]$($\mathrm{Im}\, k > 0$) is *not* a possible solution to the Vlasov equation (3) for all values of v.[24] Further, it should be noted that Estabrook and Alexeff[25] have recently integrated the Vlasov equation numerically and found results that confirm our statement that collective interaction in ion acoustic waves is negligible.

Our calculations of the perturbed velocity distribution function in a wave show that the effect of collective interaction is very weak unless $T_e \gtrsim 3T_i$. At these relatively high values of the electron temperature, characteristic oscillations in amp.$_{(v)}$, as seen in Fig. 5, occur. These oscillations have not been seen experimentally, but the observations of them would constitute a clear signature of the collective effect in ion acoustic waves.

As a last remark it should be emphasized that in our treatment we have assumed the perturbed velocity distribution function at the boundary to take the form $g(v)\exp(-i\omega t)$. We believe that this assumption holds for grid-excited waves in single-ended Q machines as long as $\omega \ll \omega_{pi}$.[12] At higher frequencies the potential around the grid varies significantly during the transit time for an ion moving through the sheath around the grid. Therefore, the g function will most likely also become a function of time, i.e., take the form $g[v, \exp(i\omega t)]$, which means that higher harmonics are generated. As long as we are only concerned with the fundamental mode this will not change the main features of our results.

The experimental results reported in this paper are in agreement with our statement that collective effects are negligible in ion-acoustic waves if $T_e \lesssim 3T_i$.

ACKNOWLEDGMENTS

The authors want to thank A. S. Jensen for pointing out the possibility of using the technique in Sec. II for performing the inverse Laplace Fourier transformations. The helpful discussions and assistance with the numerical computations of H. C. S. Hsuan, H. Pécseli, P. I. Petersen, and L. P. Prahm are acknowledged. Finally, we would like to thank M. Nielsen and B. Reiner for help in the experiments and for maintaining the Q device.

[1] A. Y. Wong, R. M. Motley, and N. D'Angelo, Phys. Rev. 133, A436 (1964).
[2] N. Sato, H. Ikezi, N. Takahashi, and Y. Yamashita, Phys. Rev. 183, 278 (1969).
[3] P. Korn, T. C. Marshall, and S. P. Schlesinger, Phys. Fluids 13, 517 (1970).
[4] H. J. Doucet and D. Gresillon, Phys. Fluids 13, 773 (1970).
[5] G. Joyce, K. Lonngren, I. Alexeff, and W. D. Jones, Phys. Fluids 12, 2592 (1969).
[6] L. D. Landau, J. Phys. USSR 10, 25 (1946).
[7] V. O. Jensen, Risø Report No. 54 (1962).
[8] R. W. Gould, Phys. Rev. 136, A991 (1964).
[9] H. Weitzner, Phys. Fluids 6, 1123 (1963).
[10] H. Weitzner and D. Dobrott, Phys. Fluids 11, 152 (1968).
[11] H. Weitzner, in *Magnetic-Fluid and Plasma Dynamics*, edited by H. Grad (American Mathematical Society, Providence, Rhode Island 1967) p. 127.
[12] S. A. Andersen, G. B. Christoffersen, V. O. Jensen, P. Michelsen, and P. Nielsen, Phys. Fluids 14, 990 (1971).
[13] J. L. Hirshfield and J. H. Jacob, Phys. Fluids 11, 411 (1968).
[14] G. B. Christoffersen, in *Proceedings of the Third International Conference on Quiescent Plasmas* (Danish Atomic Energy Commission, Risø, Denmark, 1971), p. 55.
[15] G. B. Christoffersen, V. O. Jensen, and P. Michelsen, in *Proceedings of the Third International Conference on Quiescent Plasmas* (Danish Atomic Energy Commission, Risø, Denmark, 1971) p. 63.
[16] V. O. Jensen, in *Proceedings of the Third International Conference on Quiescent Plasmas* (Danish Atomic Energy Commission, Risø, Denmark, 1971), p. 87.
[17] V. O. Jensen and P. Michelsen, Risø Report No. 257, 1972.
[18] G. B. Christoffersen, V. O. Jensen, and L. P. Prahm, in *Proceedings of the Fifth European Conference on Controlled Fusion and Plasma Physics* (Euratom CEA, Grenoble, 1972), Vol. I, p. 175
[19] S. A. Andersen, V. O. Jensen, P. Michelsen, and P. Nielsen, Phys. Fluids 14, 728 (1971).
[20] S. A. Andersen, V. O. Jensen, P. Michelsen, and P. Nielsen, Phys. Lett. A32, 413 (1970).
[21] H. Ikezi and R. J. Taylor, Phys. Lett. 22, 923 (1969).
[22] H. Ikezi and R. J. Taylor, Phys. Fluids 13, 2348 (1970).
[23] G. B. Christoffersen and L. P. Prahm, Plasma Phys. 14, 1140 (1972).
[24] H. C. S. Hsuan and V. O. Jensen, Phys. Fluids 16, 1776 (1973).
[25] K. Estabrook and I. Alexeff, Phys. Rev. Lett. 29, 573 (1972).

VOLUME 34, NUMBER 19 PHYSICAL REVIEW LETTERS 12 MAY 1975

Damping-Growth Transition for Ion-Acoustic Waves in a Density Gradient

N. D'Angelo
Danish Space Research Institute, Lyngby, Denmark, and Danish Atomic Energy Commission Research Establishment Risø, Roskilde, Denmark

and

P. Michelsen and H. L. Pécseli
Association EURATOM-Atomenergikommissionen, Danish Atomic Energy Commission Research Establishment Risø, Roskilde, Denmark

(Received 18 February 1975)

A damping-growth transition for ion-acoustic waves propagating in a nonuniform plasma (e-folding length for the density l_n) is observed at a wavelength $\lambda \sim 2\pi l_n$. This result supports calculations performed in connection with the problem of heating of the solar corona by ion-acoustic waves generated in the solar photosphere.

The behavior of ion-acoustic perturbations propagating, along a density gradient, in a highly ionized, nonuniform plasma is of considerable interest in astrophysics and in geophysics. One example of this effect is provided by the problem of coronal heating.

Heating of the solar corona through Landau damping of ion-acoustic perturbations generated in the photosphere was discussed previously.[1,2] In the solar corona *two competing effects* have, in general, to be considered. One is the Landau *damping* of the ion-acoustic perturbations in a plasma of approximately equal ion and electron temperatures ($T_i \approx T_e$), and the other is a *growth* in the relative wave amplitude ($\tilde{n}/n$) when the perturbations move outward to more and more tenuous regions. A fair guess[1,2] was that Landau damping should be the dominant effect for wavelengths shorter than the scale height of the corona, whereas growth should occur for longer wavelengths. Calculations[3,4] have shown that in an isothermal (and $T_i \approx T_e$) exponential atmosphere acted upon by the solar gravity, growth occurs for wavelengths $\lambda > 2\pi l_n$, where l_n is the scale height. For $\lambda < 2\pi l_n$ the ion-acoustic perturbations are Landau damped in much the same way as in a plasma of uniform density.

In the laboratory, the hydrodynamic behavior of ion-acoustic perturbations in a nonuniform plasma has been observed by Doucet, Jones, and Alexeff.[5] Since their plasma, however, had a T_e/T_i ratio $\gg 1$, Landau damping could not be an important process.

The present, preliminary report contains the (to the best of our knowledge) first experimental demonstration of a transition from (hydrodynamic) growth to (Landau) damping of ion-acoustic perturbations, as the wavelength is varied from below to above $\sim 2\pi l_n$. In a laboratory experiment the situation is, of course, different from that of the solar corona also in the sense that the zero-order density gradient cannot be produced by gravity. As explained below, the density gradient in the experiment was produced by a combination of an axial electric field and radial plasma losses. The overall agreement between our measurements and the results of the calculations performed for the case of an isothermal atmosphere held by gravity (Refs. 3 and 4) indicates that these results apply to ion-acoustic wave behavior in density gradients no matter how the gradients are produced.

The experiment was conducted in a cesium plasma column of a conventional, single-ended Q device,[6] in which $T_i \approx T_e$. The plasma density was generally in the range (1 to 5)$\times 10^9$ cm^{-3}, with the neutral gas pressure $\lesssim 10^{-5}$ mm Hg. A (variable) density gradient along the direction of the magnetic field lines was produced by surrounding a portion of the plasma column (~ 3 cm diameter) with a metal tube of 3.5 cm in diameter biased to -30 to -100 V with respect to the generating plate of the Q device (see, for instance, Roberson, Ratner, and Hirshfield[7]). Ion-acoustic waves were excited, in much the same manner as, e.g., by Wong, Motley, and D'Angelo,[8] by a grid immersed in the plasma (normal to the axis of the column) between the generating plate and the metal tube. The steepness of the axial density profile (density decreasing from grid to tube) could be varied by varying the negative tube bias, more negative voltages on the tube giving rise to steeper density profiles. For a fixed tube voltage, smaller values of the confining magnetic field

gave rise to steeper density profiles.

Measurements were performed by means of a Langmuir probe, movable over a distance of ~25 cm along the axis of the plasma column. The exposed surface of the probe was a flat metal disc, 5 mm in diameter, oriented normal to the column axis. The zero-order axial density profile is obtained most easily through a measurement of the probe floating-potential profile and the relation $\kappa T_e \partial n/\partial x = en\partial\varphi/\partial x$ [e.g., Refs. 6 and 8] between density and potential gradients. The same 5-mm-diam probe was used to measure the axial plasma flux as a function of position along the plasma column. The flux was observed to decrease as the probe was moved away from the generating plate, thus showing the presence of radial plasma losses. We believe that these losses are produced in part by an ion "scrape-off" (the Larmor radius can be as large as ~1 cm) and in part by enhanced radial diffusion. When the zero-order plasma behavior is analyzed on the basis of continuity and momentum equations, including a radial loss term, agreement is found with the measured zero-order quantities. Clearly, an axial density gradient is associated with an axial electric field, the electrons being in Boltzmann equilibrium.

The wave measurements were performed with the probe electrically floating, since $\tilde{n}/n = e\tilde{\varphi}/\kappa T_e$ for waves of the type we are here concerned with ($\tilde{n}$ is the perturbed density and $\tilde{\varphi}$ the perturbed potential). The results of the wave measurements are summarized in Fig. 1. At any frequency, f, the corresponding wavelength is indicated by a cross. Above $f \sim 2$ kHz the waves are damped as they propagate away from the grid, and δ_d (with triangles pointing upward) is the damping distance. Below $f \sim 2$ kHz the waves grow; δ_g (with triangles pointing downward) is the growth distance. The measurements of Fig. 1 were performed with a bias on the metal tube of −30 V, which corresponds to an e-folding length for the axial density profile of ~12 cm. The confining magnetic field was 2000 G.

We note the following from Fig. 1: (a) $f\lambda$ = const $= 1.2\times10^5$ cm sec, as expected for the phase velocity of ion-acoustic perturbations in this plasma. (b) For $f \geq 3$ kHz, the ratio $\delta_g/\lambda \sim 0.5$, independent of frequency (a well known feature of Landau-damped ion-acoustic waves, when $T_i \approx T_e$). (c) For $f \leq 1$ kHz, the growth distance δ_g is independent of frequency (for 350 Hz $\leq f \leq$ 1000 Hz), as predicted by the hydrodynamic model (e.g., Refs. 1–5). Also, $\delta_g = 2l_n$ ($2l_n = 24$ cm). (d) At f near 2 kHz, δ_g and δ_d become very large, as expected at the frequency of transition between growth and damping.

In order to fortify the results in Fig. 1, we show in Fig. 2 those obtained in a somewhat different experiment. The ratio, R, between the wave amplitude at a distance $x_2 = 19$ cm from the exciting grid and the wave amplitude at $x_1 = 5$ cm is plotted versus wave frequency. The numbers in brackets indicate the bias (in volts) on the metal tube. Remember that a more negative bias corresponds to a steeper axial density gradient. Clearly, as expected, the transition between growth and damping ($R = 1$) moves to lower fre-

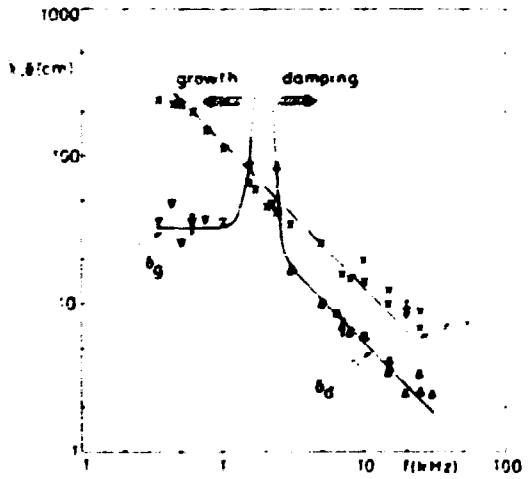

FIG. 1. The wavelength, λ, and the damping, δ_d, or growth, δ_g, distance versus the wave frequency, f. [$n = (1-5)\times10^9$ cm^{-3}, $B = 2000$ G.] The bias on the metal tube was −30 V.

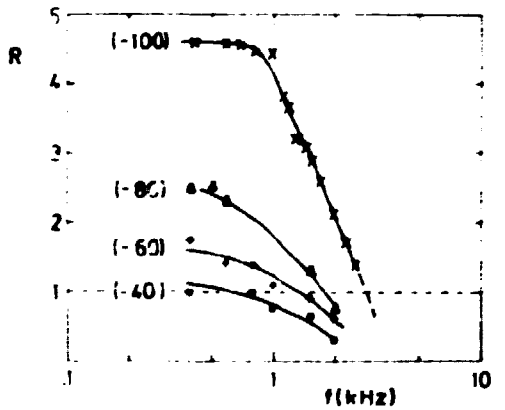

FIG. 2. The ratio, R, of wave amplitude at $x_2 = 19$ cm from the grid to the wave amplitude at $x_1 = 5$ cm versus the wave frequency. In brackets is the tube bias in volts [$n = (1-5)\times10^9$ cm^{-3}, $B = 3000$ G].

quencies as the steepness of the density profile is reduced. Note that in Fig. 2 the magnetic field strength differs from that in Fig. 1.

In addition, the relation between l_n and the (growth-damping) transition wavelength, λ_c, was observed to be $\lambda_c \simeq 2\pi l_n$, by varying l_n by a factor ~4. For instance, in the conditions of Fig. 2, values of $\lambda_c \simeq 40$, 70, 100, and 180 cm corresponded to values of $l_n \simeq 6$, 11, 18, and 25 cm, respectively.

Great care was exercised, particularly at the low-frequency end of the range of frequencies explored, to make sure that no wave reflection from the open end of the plasma column took place. This point was checked (a) by the actual wave phase measurements, which under all circumstances showed that we were indeed dealing with *propagating* waves, and (b) by altering the boundary conditions at the open end, without affecting the observed wave behavior. This fact is not surprising since the ions are not reflected from the end of the column.

It may be appropriate to mention here that, with the steepest density profiles ($V_{rad} \lesssim -100$ V), we have observed the generation of harmonics when a *growing* wave, in propagating away from the grid, produces a density modulation comparable with the zero-order density. This is due to a rectifier (or "diode") effect which occurs at $\tilde{n}/n \sim 100\%$ (the total density cannot become negative) and which may be looked upon, since $\tilde{v} \simeq C_s \tilde{n}/n$ ($\tilde{v}$ is the perturbed velocity and C_s the ion-acoustic speed), as the ejection, at the applied frequency, of plasma "blobs" from the low-density end of the column.

Finally a comment as to our results against the background of a controversy which has arisen in recent years among Q-machine workers (see Motley[9] for a summary), about the importance of phase-mixing of freely streaming particles versus collective interaction. The present results seem to emphasize the importance of collective interaction in ion-acoustic waves in inhomogeneous plasmas with $T_i \simeq T_e$. The hydrodynamic growth we have measured at low frequencies is mainly due to the interaction between the zero-order electric field associated with the density gradient and the particles in the wave perturbation. A pure "free-streaming" model does not appear to provide an immediate, adequate explanation of this result, since the zero-order distribution and the perturbed distribution at the grid must be equally affected by the radial losses. Note, however, that the concept of "free-streaming" has only been applied to uniform plasmas.

We thank M. Nielsen and B. Reher for their skillful technical assistance.

[1]N. D'Angelo, Astrophys. J. 154, 401 (1968).
[2]N. D'Angelo, Solar Phys. 7, 321 (1969).
[3]D. Parkinson and K. Schindler, J. Plasma Phys. 3, 13 (1969).
[4]C. H. Liu, J. Plasma Phys. 4, 617 (1970).
[5]H. J. Doucet, W. D. Jones, and I. Alexeff, Phys. Fluids 17, 1738 (1974).
[6]N. Rynn and N. D'Angelo, Rev. Sci. Instrum. 31, 1326 (1960).
[7]C. W. Roberson, A. S. Ratner, and J. L. Hirshfield, Phys. Rev. Lett. 31, 1041 (1973).
[8]A. Y. Wong, R. W. Motley, and N. D'Angelo, Phys. Rev. 133, A436 (1964).
[9]R. W. Motley, *Q-machines* (Academic, New York, 1975).

Ion Acoustic Waves in a Density Gradient

N. D'Angelo

Danish Space Research Institute, Lyngby, Denmark, and Research Establishment Risø, Roskilde, Denmark

and P. Michelsen and H. L. Pécseli

Association Euratom-AEK, Danish Atomic Energy Commission
Research Establishment Risø, Roskilde, Denmark

(Z. Naturforsch. **31 a**, 578–582 [1976]; received March 9, 1976)

A damping-growth transition for ion acoustic waves propagating in a non-uniform plasma (*e*-folding lengths for the density l_n) is observed at wavelengths $\lambda_c \approx 2\pi l_n$. The experiment, conducted in a *Q*-device, supports calculations performed in connection with the problem of solar corona heating.

I. Introduction

The propagation of ion acoustic waves in density gradients is of interest for plasmas in a gravitational field. Theoretical work based on a Vlasov model with special reference to the solar corona was performed by Parkinson and Schindler [1]. Liu [2] included also the effect of a magnetic field. A result of these investigations is the prediction of a (Landau) damping of the waves for wavelengths, λ, small compared to the *e*-folding length, l_n, of the density gradient while a growth in relative amplitude, $\tilde{n}/n_0$, is predicted for λ's much larger than l_n. The critical wavelength for the case where $T_i = T_e$ is $\lambda_c = 2\pi l_n$.

For high electron-to-ion temperature ratios, T_e/T_i, a fluid model is appropriate. In an experiment performed in a "diffusion plasma" with an imposed density gradient, Doucet et al. [3] found good agreement between experimental results and a simplified fluid picture for waves traveling from low density regions into regions of higher density.

In this paper we describe an experiment performed in the cesium plasma column of a conventional single ended Q-machine [4] in which $T_i \approx T_e$. In our case Landau damping of ion acoustic waves is an important process and the transition from damping to relative growth can be investigated. Although our plasma conditions are different from those considered by Parkinson and Schindler [1] and by Liu [2], our measurements reveal essentially the same features as resulted from their calculations.

Reprints requests to P. Michelsen, Danish Atomic Energy Commission, Research Establishment Risø, *4000-Roskilde*, Denmark

Preliminary results from our measurements are published in Reference [5]. The present paper, in addition to much more detailed results on wave measurements, contains a description of the zero order state.

II. Experimental Set-Up

The experiment was performed in a cesium plasma produced by surface ionization in a conventional single ended *Q*-machine [4]. The plasma column is ~ 3 cm in diameter and confined by a homogeneous $\boldsymbol{B}$ field of intensity ~ 2500 Gauss. Plasma densities are $1-5\times 10^9$ cm^{-3}, with temperatures $T_i \approx T_e \approx 2200$ °K. The neutral pressure is $\lesssim 10^{-5}$ mm Hg. Collisions are thus unimportant for the propagation of density perturbations. A (variable) density gradient along the direction of the $\boldsymbol{B}$ field is produced by surrounding a portion of the plasma column with a brass tube of length 15 cm and 3.5 cm inner diameter, biased to -30 volt to -100 volt with respect to the generating plate of the Q-device. This set-up is similar to the one described in Reference [6]. Ion acoustic waves are excited, in much the same manner as e.g. in Wong et al. [7], by a thin nickel mesh with ~ 140 0.8×0.8 mm^2 holes per cm^2 immersed in the plasma (normal to the axis of the column) between the hot plate and the brass tube. The plasma is terminated by a plate negatively biased in order to reflect all the electrons.

The steepness of the axial density profile (density decreasing from grid to tube) can be varied by varying the negative tube bias, more negative voltages on the tube giving rise to steeper density profiles. The tube has two effects on the plasma. First there is a lowering of the plasma potential, which causes an acceleration of the ions. The tube also gives rise to radial plasma losses by "scrape off" of ions (the Larmor radius being ~ 0.5 cm) or by ex-

citation of an instability which causes enhanced radial diffusion (for inst. a gravitational instability generated by the $E \times B$ rotation[8]). The resulting density gradient depends (apart from the tube voltage) on the magnetic field strength, lower B's giving rise to steeper profiles.

Measurements have been performed by means of a Langmuir probe, movable over a distance of ~ 25 cm along the axis of the plasma column, the exposed surface of the probe being a flat metal disc, 0.5 cm in diameter, oriented normal to the column axis. The zero order axial density profile is obtained most easily through a measurement of the probe floating potential and the relation [4, 7]

$$\varkappa T_e \, \partial n_0/\partial x = e \, n_0 \, \partial \Phi_0/\partial x \qquad (1)$$

between density and potential gradients (we consider the electrons as isothermal i.e. $T_e = \text{const}$). Figure 1a shows the measured potential profile for

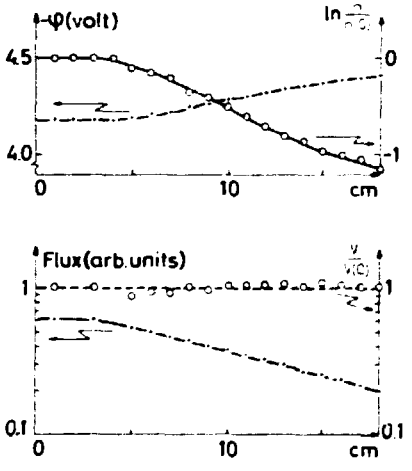

Fig. 1. a) Floating potential and density distribution along the column axis ($V_{tube} = -30$ V, $B = 2000$ gauss). b) Flux and axial velocity distribution for the same conditions of Figure 1 a.

one tube potential. Measurements of the total ion flux, nV, to the probe serve to determine the radial losses, $\mu_0(x)$, since

$$\frac{\partial (n_0 V_0)}{\partial x} = -\mu_0(x) \qquad (2)$$

in steady state conditions. Figures 1a and 1b show that $\mu_0(x) \cong n_0 \gamma$ where $\gamma = \text{constant}$, with good approximation. Finally we can determine the drift velocity $V_0(x)$ since we know the flux and density variation along the column axis (see Figure 1b). No large relative variation of $V_0(x)$ is expected with increasing x, since $V_0(x_0)$ is already larger than C_s (the sound speed) because of the sheath drop at the generating plate.

III. Wave Measurements

The wave measurements were performed using the Langmuir probe described in Section II. Only the relative fluctuations are of interest; thus all measurements were performed with the probe electrically floating since $\tilde{n}/n_0 \simeq e\tilde{\Phi}/\varkappa T_e$ ($\tilde{n}$ is the perturbed density, $\tilde{\Phi}$ the perturbed potential). The results of the wave measurements are summarized in Figure 2. During these measurements the bias of

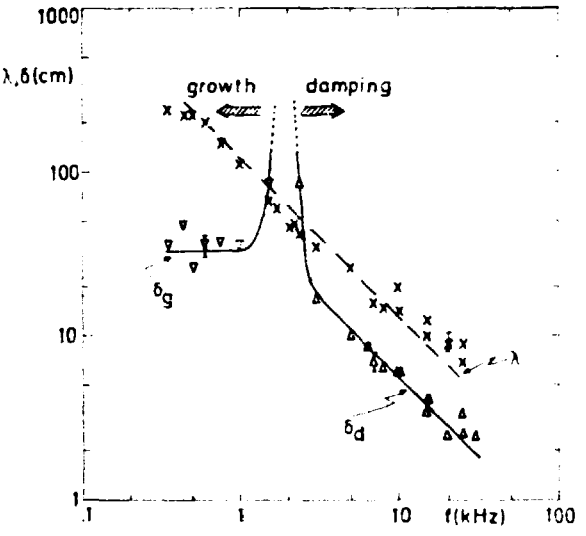

Fig. 2. The wavelength, λ, and the damping, δ_d, or growth, δ_g, distance vs. the wave frequency, f. ($n = 1-5 \times 10^9$ cm^{-3}, $B = 2000$ gauss). The bias on the metal tube is -30 volt.

the tube was -30 V and the confining magnetic field was 2000 Gauss. The e-folding length for the resulting axial density was ~ 12 cm. At any frequency, f, the corresponding wavelength is indicated by a cross. Above $f \sim 2$ kHz the waves are damped as they propagate away from the grid, and δ_d (triangles pointing upwards) is the damping distance. Below $f \sim 2$ kHz the relative amplitude of the waves increases with distance from the grid, and δ_g (triangles pointing downwards) is the growth distance. For $f \sim 2$ kHz we find $\delta \to \infty$ corresponding to undamped oscillations. We note from Figure 2:

a) $f\lambda = \text{const} \approx 1.2 \times 10^5$ cm/s, as expected for the phase velocity of ion acoustic perturbations in this plasma,

b) for $f \gtrsim 3$ kHz, the ratio $\delta_d/\lambda \simeq 0.5$, independent of frequency: a well known feature of Landau damped ion acoustic waves, when $T_i \cong T_e$,

c) for $f \lesssim 1$ kHz, the growth distance δ_g is independent of frequency as predicted by both a hydrodynamic[9] and a microscopic theory[1, 2] for the case of gravitationally held atmosphere.

In order to fortify the results in Fig. 2, we show in Figs. 3 and 4 those obtained in somewhat different

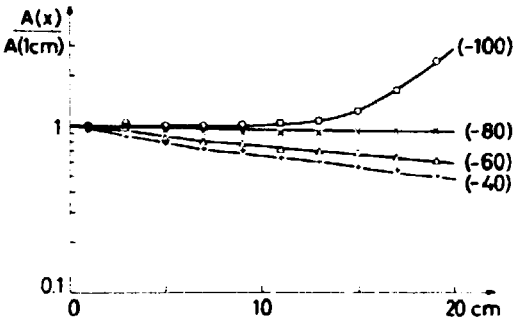

Fig. 3. Relative wave amplitude vs. axial distance for a fixed wave frequency, $f = 1.5$ kHz. Each curve refers to a different bias on the metal tube, the bias in volt being shown in brackets ($B = 3000$ gauss).

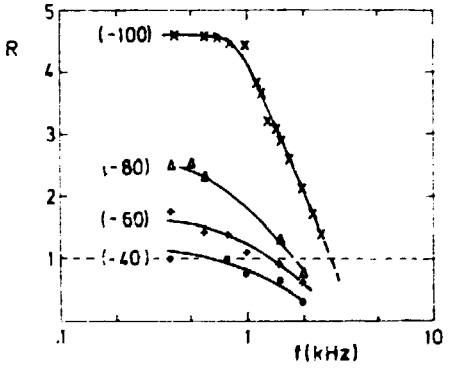

Fig. 4. The ration, R, of wave amplitude at $x_2 = 19$ cm from the grid to the wave amplitude at $x_1 = 5$ cm, vs. the wave frequency. In bracket is the tube bias in volt ($n = 1 - 5 \times 10^9$ cm^{-3}, $B = 3000$ gauss).

experiments. Figure 3 shows amplitude measurements as a function of x for a fixed frequency. The numbers in brackets indicate the bias of the metal tube (in volt). The transition between damping and relative growth is clearly demonstrated. Figure 4 shows the ratio, R, between the wave amplitude at a distance $x_2 = 19$ cm from the exciting grid and the wave amplitude at $x_1 = 5$ cm, plotted vs. frequency. The numbers in brackets indicate the tube bias in volts (more negative bias corresponding to a steeper axial density gradient). Clearly, as expected, the transition between growth and damping ($R = 1$) moves to lower frequencies as the steepness of the density profile is reduced.

Finally, in Fig. 5, by utilizing data from the measurements of Fig. 2 and Fig. 4, we show the

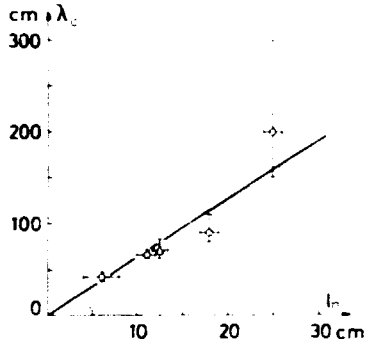

Fig. 5. The "critical" wavelength, λ_c, vs. the e-folding length of the axial density profile, l_n. The circles refer to the set of data in Fig. 4, the triangle to the data in Figure 2. The full line is the $\lambda_c = 2\pi l_n$ line.

observed relation between the e-folding length, l_n, for the density and the critical wavelength, λ_c. The full line represents the relation $\lambda_c = 2\pi l_n$.

In all the above measurements we assured ourselves that no wave reflection from the open end of the plasma column occurred. This point was checked by a) the actual wave phase measurements which showed that we were indeed dealing with propagating waves and b) by altering the boundary conditions of the "open" end (the one opposite to the hot plate), without affecting the observed wave behaviour.

It may be appropriate to mention here that nonlinearities were not observed in the above measurements. At extremely negative tube voltages ($V_{tube} \lesssim -100$ volt), however, pronounced harmonic generation was observed when a wave growing in relative amplitude was propagated. Typical results are shown in Figure 6. We explain this effect as follows. For these tube voltages radial losses are so strong that the unperturbed density on axis goes to zero within the tube (no plasma reaches the end plate). When $\tilde{n}/n_0 \sim 100\%$ the density gradient will have a rectifier (or "diode") effect (the total density cannot become negative), distorting the wave form and thus producing the harmonics. The wave form observed on an oscilloscope indeed showed a marked

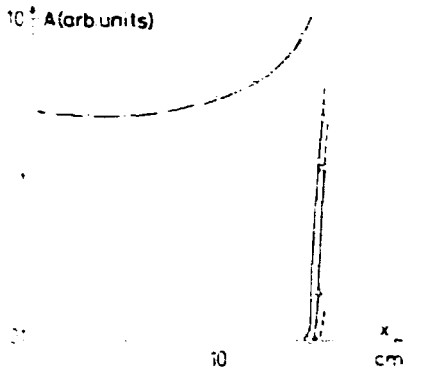

Fig. 6. Wave amplitude, at $f=1$ kHz, vs. axial distance, for $B=3000$ gauss and $V_{tube}=-150$ volt. At $x\simeq 14$ cm higher harmonics appear and grow (0, first harmonic; Δ, second harmonic; □, third harmonic).

flattening of the wave trough, thus supporting this interpretation. It is also interesting to note that, from measurements of the same type as for Fig. 1, we observe a very pronounced increase of $V_0(x)$ toward the "open" end of the colum, when V_{tube} 100 volt.

IV. Theory

As mentioned in the introduction the theoretical results for a gravitationally held atmosphere (Refs. [1, 2, 9]) do not apply directly to our experimental conditions. In the following we give a simplified fluid theory directly related to our experimental set-up, which takes into account a) the radial losses and b) the non-zero drift velocity. A fluid theory cannot substitute a correct microscopic analysis. It remains, however, essentially correct in describing the zero-order state and the wave phenomena at very long wavelengths [10, 11]. The wavelength regime with $\lambda \ll l_n$ is, on the other hand, correctly described by the usual Vlasov-Landau treatment for a homogeneous plasma.

Starting from the equations

$$\frac{\partial n}{\partial t}+\frac{\partial}{\partial x}(nV)=-\gamma n, \tag{3}$$

$$nm\frac{\partial V}{\partial t}+nmV\frac{\partial V}{\partial x}+z(T_i+T_e)\frac{\partial n}{\partial x}=0, \tag{4}$$

we obtain the linear equations

$$\frac{\partial \zeta}{\partial t}+\frac{\partial v}{\partial x}-\frac{\gamma V_0}{V_0^2-C_s^2}v+V_0\frac{\partial \zeta}{\partial x}=0, \tag{5}$$

$$\frac{\partial v}{\partial t}+V_0\frac{\partial v}{\partial x}+\frac{C_s^2\gamma}{V_0^2-C_s^2}v+C_s^2\frac{\partial \zeta}{\partial x}=0 \tag{6}$$

where $\zeta = n/n_0$ and $C_s^2=z(T_i+T_e)/m$. The term $-\gamma n$ with $\gamma=$ const accounts for the radial losses according to the discussion in Section II. To solve the Eqs. (5) – (6) we assume $V_0\sim$ const. In view of Fig. 1b this seems to be the best simplifying assumption. As already noted $V_0>C_s$ varies more slowly than n_0 and we are concerned with a solution for $\zeta = n/n_0(x)$. On the strength of this assumption we may apply elementary Fourier analysis and obtain

$$(\omega-k_r V_0)^2-k_i V_0^2-(k_r^2-k_i^2)C_s^2+\frac{k_i V_0\gamma C_s^2}{V_0^2-C_s^2}=0, \tag{7}$$

$$2k_i V_0(\omega-k_r V_0)+2k_r k_i C_s^2+\frac{k_r V_0\gamma C_s^2}{V_0^2-C_s^2}=0 \tag{8}$$

where k_r and k_i are the real and imaginary part of k, respectively, and ω is real corresponding to a boundary excitation. Using the zero order solution to (3)

$$n_0(x)=\frac{\text{const}}{V_0(x)}\exp\left\{-\gamma\int_0^x\frac{dx'}{V_0(x')}\right\} \tag{9}$$

we find $\gamma\cong V_0/l_n$ with the assumption of $V_0\sim$ const. Introducing this quantity in Eqs. (7) and (8) we obtain a numerical solution $\omega=\omega(k_r l_n)$ and $k_i=k_i(k_r)$, using the measured value of l_n. The calculations show that in the frequency range of interest k_i and ω/k_r are nearly constant, with $\omega/k_r\cong V_0+C_s$. If V_0 is determined from the measurements by using this relation, we find $V_0\cong 1.5\,C_s$ and with this value for V_0 we obtain $k_i l_n\cong 0.3$ or $\delta_g\cong 3\,l_n$, in good agreement with the results shown in Figure 2. (A cut-off frequency such as the one found in Ref. [3] does not appear in our calculations.) Near the damping-growth transition frequency these calculations do not hold.

For short wavelengths, as already remarked, the presence of the density gradient is unimportant and we expect the conventional Landau damping to be the dominant feature (see Section III).

A simple way of estimating the value of the transition wavelength, λ_c, is by noting that the growth-damping transition should occur at that wavelength for which the growth distance, δ_g (computed from fluid theory), equals the damping distance, δ_d (computed from the Vlasov-Landau theory for a uniform plasma). Since $\delta_d\cong 0.5\,\lambda$ and $\delta_g\cong 3\,l_n$, one obtains $\lambda_c\sim 6\,l_n$ (see Figure 5). It is also clear that

this simple argument applies to all cases in which there is competition between hydrodynamic growth and Landau damping, i.e. not only to the special case of a gravitationally hold atmosphere [1].

V. Conclusions

In this report we have presented measurements of ion acoustic wave propagation in a density gradient. The most interesting observation is that of a growth-damping transition at a critical wavelength, $\lambda_c \approx 2\pi L_n$. This result is in agreement with calculations performed on wave propagation in an isothermal atmosphere held by gravity [1, 2]. It thus appears that these calculations have a more general validity, i.e. they may apply independently of the particular way in which the density gradient is produced.

The relevance of the questions investigated in this report to the problem of the heating of the corona of the sun has already been noted [9]. Applications to problems where plasma expands from a finite region in space (e.g. laser produced plasmas) can be foreseen. As pointed out in Ref. [3] a similar experimental set-up may be convenient for generation of nonlinear ion waves of arbitray amplitude in a controlled manner. In order to see marked nonlinear effects our measurements show that the electron ion temperature ratio should be increased considerably (indeed in the experiment of Ref. [3] $T_e/T_i \gg 1$).

Acknowledgement

We thank M. Nielsen and B. Reher for their skilful technical assistance.

[1] D. Parkinson and K. Schindler, J. Plasma Phys. **3**, 13 [1969].
[2] C. H. Liu, J. Plasma Phys. **4**, 617 [1970].
[3] H. J. Doucet, W. D. Jones, and I. Alexeff, Phys. Fluids **17**, 1738 [1974].
[4] N. Rynn and N. D'Angelo, Rev. Sci. Instrum. **31**, 1326 [1960].
[5] N. D'Angelo, P. Michelsen, and H. L. Pécseli, Phys. Rev. Letters **31**, 1214 [1975].
[6] C. W. Roberson, A. S. Ratner, and J. L. Hirshfield, Phys. Rev. Letters **31**, 1041 [1973].
[7] A. Y. Wong, R. W. Motley, and N. D'Angelo, Phys. Rev. **133**, A 436 [1964].
[8] F. F. Chen, Phys. Fluids **9**, 965 [1966].
[9] N. D'Angelo, Astrophys. J. **154**, 401 [1968].
[10] H. Weitzner, Phys. Fluids **7**, 476 [1964].
[11] R. L. Liboff, Phys. Fluids **5**, 963 [1962].

Absolute and convective ion beam instability studied through Green's function

V. O. Jensen and P. Micheisen
Association Euratom-A.E.K. Danish Atomic Energy Commission, Research Establishment Risø, Roskilde, Denmark

Hulbert C. S. Hsuan*
Department of Electrical Engineering, University of Iowa, Iowa City, Iowa 52240

(Received 27 December 1973; final manuscript received 3 June 1974)

A Vlasov plasma with a double-humped, unstable ion velocity distribution function is considered. A δ function in space is assumed as the initial perturbation and the plasma response to this perturbation is calculated, i.e., the Green's function for the problem is found. The response can be divided into two parts: a self-similar, damped part of the form $t^{-1}h(x/t)$, and an unstable, exponentially growing part. The conditions for absolute and convective growth of the latter are discussed.

I. INTRODUCTION

During the past fifteen years great interest has been shown in the problem of growing waves in unstable plasmas. Sturrock[1,2] has performed pioneer work in this field by classifying the possible types of instabilities as evanescent, convective, or nonconvective (absolute) and by discussing the conditions under which the various types can be expected. Many authors[3-7] have considered unstable waves and described in detail various mathematical techniques used to treat the problem. In a recent paper, Rognlien and Self[8] include a review chapter on most of the work in this field; in their work references to many other interesting papers can be found.

Our interest in this problem is caused by the possibility of creating, in Q machines, a plasma with a double-humped ion velocity distribution function which is unstable to the ion acoustic wave mode.[9] This plasma provides the unique experimental possibility of following in detail the development in time and space of an instability which started as a narrow perturbation at $(x, t) = (0, 0)$. In this paper we present calculations based on the linearized Vlasov equation of the development of such a perturbation in an unstable plasma of the type obtainable in Q machines, i.e., we calculate the Green's function for the equations describing wave propagation through the plasma.

As is often found in this kind of treatment, some parts of the wavelength or frequency spectrum of the wave mode under consideration are unstable (growing) and other parts are stable (damped). In most treatments only the growing waves are considered because they are argued to be the predominant ones in the limit of large times or distances where experiments are most readily performed. We show that in a Q machine plasma it should be possible to detect the contribution from the stable waves and that from the unstable waves separately. The contribution from the stable waves dies away in a self-similar fashion as $t^{-1}h(x/t)$ as described elsewhere.[10,11] The contribution from the unstable waves is found to be absolutely unstable in some frames of reference and convective in others, and normally convective in the frame which follows the bulk of the self-similar stable wave contribution, as well as in the laboratory frame. We show that our results are in qualitative agreement with the experimental results of Baker[12,13] and that they therefore constitute an alternative explanation of his observations.

II. ANALYSIS

As in previous calculations[10,11] we describe the ions by their linearized Vlasov equation. We choose to model the electrons by a massless isothermal fluid. The electrons and the ions are coupled through the Poisson equation, and we consider a one-dimensional situation. Thus, our starting equations are

$$\frac{\partial f(x, v, t)}{\partial t} + v\frac{\partial f(x, v, t)}{\partial x} = \frac{c_e^2}{n_0}\frac{\partial n_e(x, t)}{\partial x}\frac{df_0(v)}{dv}, \tag{1}$$

$$\lambda_D^2\frac{\partial^2 n_e(x, t)}{\partial x^2} = n_e(x, t) - n_i(x, t), \tag{2}$$

and

$$n_i(x, t) = \int_{-\infty}^{\infty} f(x, v, t)dv. \tag{3}$$

Here,

$$c_e^2 = \kappa T_e/m_i, \quad n_0 = \int_{-\infty}^{\infty} f_0(v)dv$$

is the uniform unperturbed density for both ions and electrons, $\lambda_D = (\epsilon_0\kappa T_e/n_0e^2)^{\frac{1}{2}}$ is the electron Debye length, and $n_e(x, t)$ is the perturbed electron density.

Let us consider the response of the system to an initial perturbation with an ion velocity destribution

$$f(x, v, t = 0) = g(v)\frac{1}{\pi}\frac{\alpha}{x^2 + \alpha^2}, \tag{4}$$

where α is a scale length representing the size of the initial perturbation. This form of the initial perturbation is chosen for mathematical convenience since $\pi^{-1}\alpha(\alpha^2 + x^2)^{-1}$ is a normal representation of a delta function, $\delta(x)$, in the limit of α going to zero.

We use a standard Laplace-Fourier transform technique to solve (1)–(3) with initial condition (4). The transform is defined so that

$$F(k, \omega) = \int_{-\infty}^{\infty}\exp(-ikx)\int_0^{\infty}\exp(i\omega t)F(x, t)\,dt\,dx$$

and

$$F(x,t) = (2\pi)^{-2}\int_{\alpha}^{\alpha+i\infty}\exp(ikx)\int_{-\infty}^{\infty}\exp(-i\omega t)F(k,\omega)\,d\omega\,dk,$$

where $F(x,t)$ can be any of the three functions: $f(x,v,t)$, $n_e(x,t)$, or $n_i(x,t)$. The integral contour in the ω plane indicated by the index α runs above any of the poles of $F(k,\omega)$. The following relation can be shown, in general, from the reality condition, i.e., from the condition that $F(x,t)$ has to be a real quantity.

$$F(-k^*,-\omega^*) = [F(k,\omega)]^*,$$

where the asterisk * denotes the complex conjugate. With this relation it is easy to prove that

$$F(x,t) = \frac{1}{2\pi^2}\,\mathrm{Re}\int_{0}^{\infty+i\alpha}\int_{-\infty}^{\infty}F(k,\omega)\exp(-i\omega t+ikx)\,d\omega\,dk.$$

Re stands for the "real part of."

Straightforward algebra leads to the relation

$$n_e(k,\omega) = -\frac{i}{k}\left(\frac{I(\omega/k)}{1+(k\lambda_D)^2-P(\omega/k)}\right)e^{-\alpha k},$$

where $I(\omega/k)$ is related to the initial condition through

$$I\left(\frac{\omega}{k}\right) = \int_{\alpha}^{\infty+i\alpha}\frac{g(v)}{v-(\omega/k)}\,dv, \tag{5}$$

and where $P(\omega/k)$ is related to the plasma properties through

$$P\left(\frac{\omega}{k}\right) = \frac{\omega_p^2}{n_0}\int_{-\infty}^{\infty+i\alpha}\frac{f_0'(v)}{v-(\omega/k)}\,dv. \tag{6}$$

For $n_e(x,t)$ we get

$$n_e(x,t) = \frac{1}{2\pi^2}\,\mathrm{Im}\int_{0}^{\infty+i\alpha}\int_{\alpha}^{\infty+i\alpha}k\,\frac{1}{1+(k\lambda_D)^2-P(\omega/k)}\,I(\omega/k)\times\exp(-i\omega t+ikx-\alpha k)\,d\omega\,dk, \tag{7}$$

where Im represents the "imaginary part of."

In Ref. 10 we obtained an expression similar to (7) except for the $(k\lambda_D)^2$ term. This term only enters here because of our use of the Poisson equation (2) rather than the quasineutrality condition assumed in the former work. In Ref. 10 we considered stable plasmas, i.e., plasmas for which the equation

$$1+(k\lambda_D)^2-P(\omega/k) = 0 \tag{8}$$

has no solutions in the complex ω plane for which $\mathrm{Im}\omega > 0$. By using this we could move the ω integration path down to the real axis, and we found that the density always took the self-similar form $t^{-1}h(x/t)$. In this paper we consider unstable plasmas for which (8) has only one solution, $\omega(k)$, with $\mathrm{Im}\omega > 0$ for a fixed k. This solution is found for k values in the interval $0 < k < k_m$ and $\mathrm{Im}\omega(0) = \mathrm{Im}\omega(k_m) = 0$.[3] Using this we can write (7) in the form

$$n_e(x,t) = n_{es}(x,t) + n_{eu}(x,t), \tag{9}$$

where

$$n_{es}(x,t) = \frac{1}{2\pi^2}\,\mathrm{Im}\int_{0}^{\infty}\int_{\alpha}^{\infty+i\alpha}k\,\frac{1}{1+(k\lambda_D)^2-P(\omega/k)}\,I(\omega/k)\times\exp(-i\omega t+ikx-\alpha k)\,d\omega\,dk \tag{10}$$

and

$$n_{eu}(x,t) = \mathrm{Re}\,\frac{1}{\pi}\int_{0}^{\infty+i\alpha}\left[\frac{I(\omega/k)}{k[\partial P(\omega/k)/\partial\omega]}\right]_{\omega=\omega(k)}\times\exp[-i\omega(kt+ikx-\alpha k)]\,dk. \tag{11}$$

In (11) the function $\omega(k)$ is to be determined by (8). The stable contribution, $n_{es}(x,t)$, is essentially of the form obtained in Ref. 10. The unstable contribution, $n_{eu}(x,t)$, is of the general type treated by several authors.[1–3] In the following we discuss the two contributions separately.

A. The stable contribution

Since $P(\omega/k)$ and $I(\omega/k)$ are known functions as given by (5) and (6), $n_{es}(x,t)$ can be calculated by numerical computation from (10). This computation, however, is rather involved because we have to perform a triple integration over k, ω, and v for each (x,t) value for which we want to calculate n_{es}. Rather than performing such integrations, we show that in the limit of large t, where experiments are most likely to be possible, the $(k\lambda_D)^2$ term in the denominator is of no importance and can therefore be neglected, which simplifies (10) considerably. To neglect the $(k\lambda_D)^2$ term is equivalent to assuming quasineutrality rather than using (2).[10]

In (10) we substitute $v_p = \omega/k$ and find

$$n_{es}(x,t) = \frac{1}{2\pi^2}\,\mathrm{Im}\int_{0}^{\infty}\int_{-\infty}^{\infty}\frac{I(v_p)}{1+(k\lambda_D)^2-P(v_p)}\times\exp\left[-ikt\left(v_p-\frac{x+i\alpha}{t}\right)\right]dv_p\,dk. \tag{12}$$

This form suggests an asymptotic expansion of $n_{es}(x,t)$ in terms of t^{-1}. We substitute $y = kt$ and expand $n_{es}(k,v_p) = I(v_p)[1+(k\lambda_D)^2-P(v_p)]^{-1}$ in terms of t^{-1} as follows:

$$n_{es}(k,v_p) = n_{es}(0,v_p)+\left(\frac{y}{t}\right)^2\frac{\partial n_{es}}{\partial(k^2)}\bigg|_{k^2=0}+O\left(\frac{1}{t^4}\right) = \frac{I(v_p)}{1-P(v_p)}-\left(\frac{y}{t}\right)^2\lambda_D^2\frac{I(v_p)}{[1-P(v_p)]^2}+O\left(\frac{1}{t^4}\right).$$

Equation (12) can now be rewritten as

$$n_{es}(x,t) = \frac{1}{2\pi^2 t}\,\mathrm{Im}\int_{0}^{\infty}\int_{-\infty}^{\infty}\frac{I(v_p)}{1-P(v_p)}\times\exp\left[-iy\left(v_p-\frac{x+i\alpha}{t}\right)\right]dv_p\,dy+\frac{1}{2\pi^2}\frac{\lambda_D^2}{t}\times\mathrm{Im}\left\{\frac{\partial^2}{\partial x^2}\int_{0}^{\infty}\int_{-\infty}^{\infty}\frac{I(v_p)}{[1-P(v_p)]^2}\times\exp\left[-iy\left(v_p-\frac{x+i\alpha}{t}\right)\right]dv_p\,dy\right\}+O\left(\frac{1}{t^3}\right). \tag{13}$$

In writing the second term in (13) we make use of the fact that

$$\int_0^\infty (y/t)^2 \exp(iyx/t)\,dy$$

can be replaced by

$$-\partial^2/\partial x^2 \int_0^\infty \exp(iyx/t)\,dy.$$

Performing the y integration we obtain

$$n_{es}(x,t) = \frac{1}{2\pi^2} \times \mathrm{Im}\int_\kappa \frac{I(\tau_p)}{[1-P(\tau_p)]i(\tau_p-[(x+i\alpha)/t]\}}\,d\tau_p + \frac{1}{2\pi^2}\frac{\lambda_D^2}{t}\,\mathrm{Im}\left(\frac{\partial^2}{\partial x^2} \times \int_\kappa \frac{I(\tau_p)}{[1-P(\tau_p)]i(\tau_p-[(x+i\alpha)/t]\}}\,d\tau_p\right) + O\left(\frac{1}{t^5}\right). \tag{14}$$

By closing the τ_p integration paths around the upper half of the τ_p plane we get, by means of residue calculations,

$$n_{es}(x,t) = \frac{1}{t}F_1\left(\frac{x}{t}\right) + \frac{\lambda_D^2}{t^3}F_2\left(\frac{x}{t}\right) + O\left(\frac{1}{t^5}\right),$$

where

$$F_1\left(\frac{x}{t}\right) = \lim_{\alpha\to 0}\frac{1}{\pi}\,\mathrm{Im}\left(\frac{I[(x+i\alpha)/t]}{1-P[(x+i\alpha)/t]} - \frac{I(u_p)}{\{u_p-[(x+i\alpha)/t]\}P'(u_p)}\right),$$

and

$$F_2\left(\frac{x}{t}\right) = \lim_{\alpha\to 0}\frac{1}{\pi}\,\mathrm{Im}\left\{\frac{d^2}{d(x/t)^2}\left[\frac{I[(x+i\alpha)/t]}{\{1-P[(x+i\alpha)/t]\}^2} + \left(\frac{1}{P'^2(u_p)}\frac{d}{dv_p}\frac{I(\tau_p)}{\{\tau_p-[(x+i\alpha)/t]\}}\right)_{\tau_p=u_p}\right]\right\}.$$

In these equations u_p is defined by the solution to the equation $1-P(u_p)=0$.

It is seen that in the limit of long time ($t \gg \omega_{pi}^{-1}$), the first term in (14) is the predominant one. Since we shall only be interested in this limit, we write

$$n_{es}(x,t) = \frac{1}{t}\lim_{\alpha\to 0}\frac{1}{\pi}\,\mathrm{Im}\left(\frac{I[(x+i\alpha)/t]}{1-P[(x+i\alpha)/t]} - \frac{I(u_p)}{\{u_p-[(x+i\alpha)/t]\}P'(u_p)}\right). \tag{15}$$

This equation, which will be used for numerical calculations, is identical to what we would have obtained if we had assumed quasineutrality rather than introduced the Poisson equation, (2). We have thus shown that the quasineutrality assumption is good in the limit where $t \gg \omega_{pi}^{-1}$.

$n_{es}(x,t)$ as given by (15) takes a self-similar form as t^{-1} times some function of (x/t); this is a property which was found for stable distribution functions in Ref. 10. The first term in the large parentheses of (15) is equal to the expression obtained in Ref. 10. The last term is an extra contribution caused by the pole in the upper half of the τ_p plane. It could be argued that this contribution should rather be included in the unstable part of $n_e(x,t)$ [Eq. (9)]. We decided to keep it as part of $n_{es}(x,t)$ because of its self-similar form.

B. The unstable contribution

In order to calculate $n_{eu}(x,t)$ from (11) we need to find the spectrum of unstable waves, $\omega(k)$, from (8). The wavenumber, k_m, of the marginally stable wave is determined by

$$1 + (k_m\lambda_D)^2 - \frac{c_e^2}{n_0}\int_{-\infty}^{\infty}\frac{f_0'(v)}{v-[\omega(k_m)/k_m]}\,dv = 0. \tag{16}$$

We introduce $v_0 = \omega(k_m)/k_m$, which is the phase velocity of the marginally stable wave. As v_0 is a real number we have, directly from (16),

$$f_0'(v_0) = 0. \tag{17}$$

An appropriate formula for $\omega(k)$, k can be obtained by a Taylor expansion of (8) around v_0

$$\frac{\omega(k)}{k} = v_0 + z \tag{18}$$

$$1 + (k\lambda_D)^2 - \frac{c_e^2}{n_0}\int_{-\infty}^{\infty}\frac{f_0'(v)}{v-v_0}\,dv - z\frac{c_e^2}{n_0}\int_{-\infty}^{\infty}\frac{f_0''(v)}{v-v_0}\,dv = 0. \tag{19}$$

From (16), (18), and (19) we get

$$\omega(k) = k\left[v_0 + \frac{k_m^2-k^2}{\omega_{pi}^2}A(v_0)\right], \tag{20}$$

where ω_{pi} is the ion plasma frequency and where $A(v_0)$ is defined by

$$A(v_0)^{-1} \equiv -\lim_{\epsilon\to 0+} n_0^{-1}\int_{-\infty}^{\infty}\frac{f_0''(v)}{v-v_0-i\epsilon}\,dv. \tag{21}$$

Equations (11) and (20) constitute the basis for the numerical calculations of $n_{eu}(x,t)$ reported in the next section.

The instability under consideration is triggered at $(x,t) = (0,0)$. An observer moving through the plasma with a velocity within a certain interval, v_1 to v_2, will find that the instability grows at all times, i.e., that the instability is absolute. For velocities outside this interval the instability is convective. In finding v_1 and v_2 we roughly follow the procedure given by Baldwin and Rowlands.[7]

We insert (20) into (11) and get

$$n_{eu}(x,t) = \frac{1}{\pi}\,\mathrm{Re}\frac{I(\tau_c)}{I''(\tau_c)} \times \int_0^{k_m} \exp\left\{ikx - ikt\left[\tau_0 + \frac{k_m^2 - k^2}{\omega_{pi}^2}A(\tau_0)\right]\right\}dk. \quad (22)$$

Equation (22) is obtained by going to the limit $\alpha = 0$ and by assuming that the quantity in the bracket in (11) varies insignificantly with k in the interval 0 to k_m; this assumption certainly holds for weakly unstable plasmas where $k_m \ll \lambda_D^{-1}$. We want to calculate $n_{eu}(x,t)$ as felt by an observer moving through the plasma with the velocity, v, i.e., at the position $x(t) = vt$. Thus, we get

$$n_{eu}(x(t),t) = \mathrm{Re\ const}\int_0^{k_m} \exp\left\{ik\left[v - \tau_0 - \frac{k_m^2 - k^2}{\omega_{pi}^2}A(\tau_0)\right]t\right\}dk \equiv \mathrm{Re\ const}\int_0^{k_m} \exp[S(k)t]\,dk. \quad (23)$$

To determine for which velocities v the instability is absolute and for which it is convective we look for a curve in the complex k plane which connects $k = 0$ with $k = k_m$ and on which $\mathrm{Re}S(k) = 0$. If such a curve exists, we can change the integration contour into this curve; it is then clearly seen from Riemann's lemma that n_{eu} goes to zero for large t, i.e., that the instability is convective. If such a curve does not exist, the instability is absolute. For further discussion of this procedure, see Ref. 7.

In the appendix we describe a relatively simple procedure to determine for which v values we have absolute instability, and for which the instability is convective. We find that for v close to v_0 the instability is absolute, while v values very different from v_0 lead to convective instability. The limiting values, v_+ and v_-, are shown to be determined by the condition that $\mathrm{Re}S(k_s) = 0$. k_s are the k values for which $S(k)$ has saddle points.

III. NUMERICAL RESULTS AND DISCUSSION

Most authors who consider unstable waves are interested in growth rates and asymptotic expansions. Our Eq. (11) can also be used for this kind of analysis by leading to an expression for the density growth. Such an expansion, however, is of limited value because in an experiment a growing perturbation will soon reach a level where nonlinearities are important and an asymptotic expansion based on the results from the linear equations (1) to (3) becomes invalid. We study the initial linear growth of perturbations by performing numerical calculations of the stable as well as the unstable contribution discussed in the previous section.

We first consider the growing part of the solution, i.e., the expression in (11) which with the assumption $(k_m\lambda_D)^2 \ll 1$ can be reduced to (22). For simplicity, we shall assume that the ion velocity distribution functions $f_0(v)$ and $g(v)$ are symmetrical around $v = 0$ in some frame of reference. We shall solve the equations in this frame where from (17) we get $v_0 = 0$.

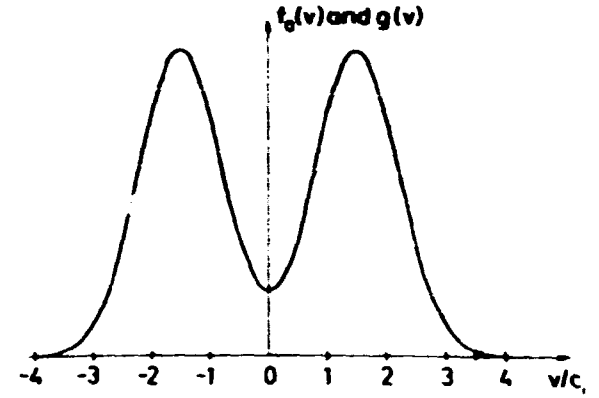

FIG. 1. The shape of the ion velocity distribution functions, $f_0(v)$ and $g(v)$, used in the numerical calculations.

$$f_0(v) \propto g(v) \propto \exp[-(v - v_d)^2/c_i^2] + \exp[-(v + v_d)^2/c_i^2]$$

is an example of such a distribution function; this function, which is shown in Fig. 1 for $v_d = 1.5c_i$ is used in the numerical calculations. From (21) we get that $A(0)$ is a purely imaginary quantity. From (22) we obtain the simplified integral

$$n_{eu}(x,t) = \frac{1}{\pi}\,\frac{I(0)}{I''(0)} \times \int_0^{k_m} \cos kx \exp\left[t\frac{\mathrm{Im}A(0)}{\omega_{pi}^2}k(k_m^2 - k^2)\right]dk. \quad (24)$$

Because the integrand has a maximum for $k = 3^{-\frac{1}{2}}k_m$, the wave with this wavenumber will have the largest growth rate, which can be found to be $3^{-\frac{1}{2}}2k_m^3\,\mathrm{Im}A(0)\omega_{pi}^{-2}$. This growth rate is in agreement with our numerical calculations of the expression (24) presented in Fig. 2. In the figure we show $n_{eu}(x)$ calculated for various values of the dimensionless time parameter, $\tau = \mathrm{Im}A(0)k_m^3\omega_{pi}^{-2}t$. For $t = 0$, we notice that $n_{eu}(x,t) \propto \sin k_m x / k_m x$ which is not the initial condition given by (4). This is, of course, because we have not included the term giving the stable contribution.

Using the procedure mentioned at the end of Sec. II on our simplified case we get, after straightforward algebra, $v_\pm = \pm\sqrt{3}k_m^2\,\mathrm{Im}A(0)\omega_{pi}^{-2}$. Also, this is in agreement with the numerical results shown in Fig. 2. From these results we get that an observer moving with a velocity in the interval between v_- and v_+ will see a growing perturbation, i.e., an absolute instability, while an observer with a velocity out-

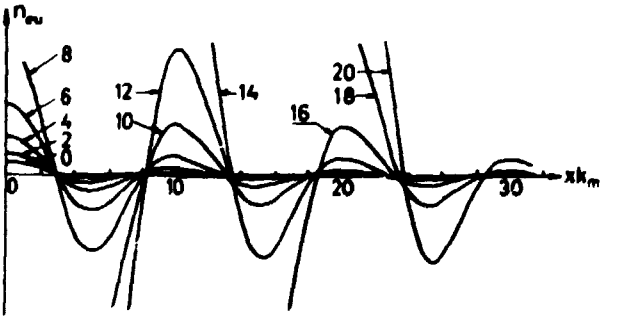

FIG. 2. Unstable contribution, $n_{eu}(x)$, at various times, versus distance xk_m. The dimensionless time τ written on the curves is given by $\tau = tk_m^3\,\mathrm{Im}A(0)\omega_{pi}^{-2}$.

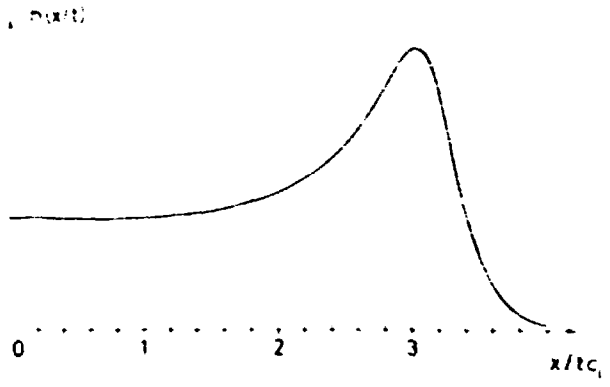

FIG. 3. The stable contribution, $n_{es}(x, t)$, for the case where $T_e/T_i = 4$ plotted as a function of $x/c_i t$.

side this interval will see a damped perturbation for sufficiently large t, i.e., a convective instability.

Let us now consider the stable part of the solution. This part is given by (15) and it can be written in the self-similar form $n_{es}(x, t) = t^{-1}h(x/t)$. We have calculated $h(x/t)$ numerically for a case where the ion velocity distribution functions, $f_0(v)$ and $g(v)$, again are the double-humped, symmetrical functions shown in Fig. 1. In order to insure that the plasma is unstable we have chosen $T_e/T_i = 4$.[15] In Fig. 3 we show the results as a function of $x/c_i t$, where $c_i^2 = 2\kappa T_i/m_i$.

We note that the stable contribution contains a positive pulse whose maximum moves through the plasma with a velocity about equal to $v_d + c_e$. Since in most cases this velocity is greater than v_c, which is the characteristic velocity of the front of the unstable contribution, it should be possible to experimentally observe the two contributions separately. Therefore, if the instability is observed at a fixed position in that frame of reference where $v_0 = 0$, the fast self-similar pulse from the stable contribution will arrive first and then the growing contribution from the unstable part will arrive and eventually dominate. The relative strength between $n_{eu}(x, t)$ and $n_{es}(x, t)$ depends on all the plasma parameters involved: $f_0(v), g(v), T_e/T_i$, and also on time and position of observation [see Eqs. (15) and (22)]. Since $n_{eu}(x, t)$ normally starts at a low level and $n_{es}(x, t)$ goes as t^{-1}, the latter term will in many cases be the predominant one at small times.

Baker[13] has examined the propagation of pulses excited by a grid in an unstable Q machine plasma with an ion velocity distribution function of the kind considered here. He actually sees two contributions: a fast damped pulse followed by a slower growing one. The main features of his observations are in agreement with our calculations. In order to claim that the Baker work constitutes an experimental verification of our theoretical results more detailed experimental work has to be performed. One feature that is likely to complicate such work is the fact that the propagation of the stable part of the pulse, $n_{es}(x, t)$, is independent of plasma density, while the unstable part, $n_{eu}(x, t)$, propagates in a way that depends on n_0 [n_0 enters into (22) through ω_{pi}^2]. Therefore, in a Q machine plasma where there is necessarily a radial density gradient, the propagation of the unstable part will depend on radius, while the stable part propagates independently of radius.

The solution to Eqs. (1) to (3) with another initial condition, e.g., a wave, can, in principle, be found from our results by performing a convolution of the Green's function with the given initial condition. Although this method may be unnecessarily complicated, it can give us some information about the propagation of waves from our knowledge of the Green's function. For stable plasmas, the Green's function only contains the self-similar part, and a wave is known to be damped.[2] We may therefore conclude that in cases where we consider unstable plasmas and find that the self-similar part of the Green's function predominates over the unstable part, a wave will decay. It has been discussed that for small times the self-similar part can predominate; in such cases a wave will start out as a decaying wave and only begin to grow when the unstable part of the Green's function becomes the predominant one. An effect of this kind, but for a boundary value problem, was observed experimentally by Christoffersen and Prahm.[3] Physically, the damping can be interpreted as a phase mixing of the particles in the initial density perturbation with the distribution function $g(v)$; only that part of $g(v)$ which corresponds to the distribution function in an unstable wave will grow.

To summarize, in this paper we have reported on a calculation of the development of a narrow perturbation in a plasma, unstable to an ion beam instability, i.e., we have found the Green's function for this problem. Our results are valid in a time period from a few times ω_{pi}^{-1} until the instability reaches a nonlinear level. We have determined in which frames of reference the instability is absolute and in which it is convective. In many cases a damped pulse will propagate faster than the region of instability, and this pulse can in the initial phase, depending on the excitation, have a considerable amplitude.

APPENDIX

We consider the complex function $S(k)$ of the complex variable, k [see Eq. (23)]

$$S(k) = i\left[k(v - v_0) - \frac{A(v_0)}{\omega_{pi}^2}k(k_m^2 - k^2)\right]$$

and want to discuss for which v values there exists a curve connecting $k = 0$ with $k = (\pm k_m, 0)$ on which $\mathrm{Re}S(k) = 0$.

We substitute

$$u = v - v_0$$

and

$$\beta = iA(v_0)/\omega_{pi}^2 \tag{A1}$$

and get

$$S(k) = k[\beta(k^2 - k_m^2) + iu]. \tag{A2}$$

The equation

$$\mathrm{Re}S(k) = \mathrm{Re}\{k[\beta(k^2 - k_m^2) + iu]\} = 0, \tag{A3}$$

being of third order in k, describes three curves in the complex $k = k_r + ik_i$ plane; these curves are obviously sym-

metrical around $k = 0$. In the general case where $\mathrm{Re}S(k_s) \neq 0$ [k_s being those k values for which (A2) has saddle points] the three curves cannot cut each other.

Before proceeding we note:

(a) k_m^2 is a real positive number depending only on the properties of the plasma under consideration.

(b) β is a complex number depending only on the plasma properties. From (21) and (A1) it follows that for unstable distribution functions where $f_0'(v_0) > 0$, the real part of β is negative, i.e., if we write $\beta = |\beta| \exp(i\theta_\beta)$, then

$$(\pi/2) + 2n\pi < \theta_\beta < (3\pi/2) + 2n\pi, \quad n = 0, 1, 2, \ldots.$$

(c) u is a real parameter to be varied from $-\infty$ to $+\infty$.

For $k \to \infty$ the curves described by (A3) asymptotically approach the straight lines through $k = 0$ which are determined by $\mathrm{Re}(\beta k_s^3) = 0$. In a polar system of coordinates this equation is written

$$|\beta| k_a^3 \cos(3\theta_a + \theta_\beta) = 0$$

and is satisfied for

$$\theta_a = (\pi/6) - (\theta_\beta/3) + p(\pi/3), \quad p = 0, 1, 2, \ldots. \tag{A4}$$

We note that for $p = n = 0$ we have $-\pi/3 \leq \theta_a \leq 0$, and we further note that θ_a only depends on the plasma properties and not on the chosen u value.

Because the left-hand side of (A3) is a third-order polynomial, any straight line in the k plane can only cut the curves defined by this equation in three points. From this it follows that the only point of intersection between the asymptotes and the curves is the origin of the k plane. Therefore, in the general case we can only have the three situations shown in Fig. 4. In situation (a) the three points, $k = (0, 0)$ and $k = (\pm k_m, 0)$ lie on three different curves, which corresponds to absolute instability. In situations (b) and (c) the three points lie on the same curve, which guarantees that the instability is convective. It is clear that a shift from one situation to another which can be obtained by varying u, will only occur for u values for which $\mathrm{Re}S(k_s) = 0$.

To determine which situation holds for an actual case we only have to determine the slope at $k = (0, 0)$ of the curve which passes through this point. If the slope is such that the curve falls within that 60° angle between the asymptotes in which the real k axis is situated, then we have situation (b) or (c). If it falls outside this angle, we have situation (a).

Around $k = 0$ (A3) can be approximated by

$$\mathrm{Re}(-\beta k_m^2 k + iuk) = 0.$$

From this we get that the slope at $k = 0$ is determined by

$$\frac{dk_i}{dk_r} = \frac{\beta_r k_m^2}{\beta_i k_m^2 - u},$$

which for $u = 0$ is written

$$\frac{dk_i}{dk_r} = \frac{\beta_r}{\beta_i}. \tag{A5}$$

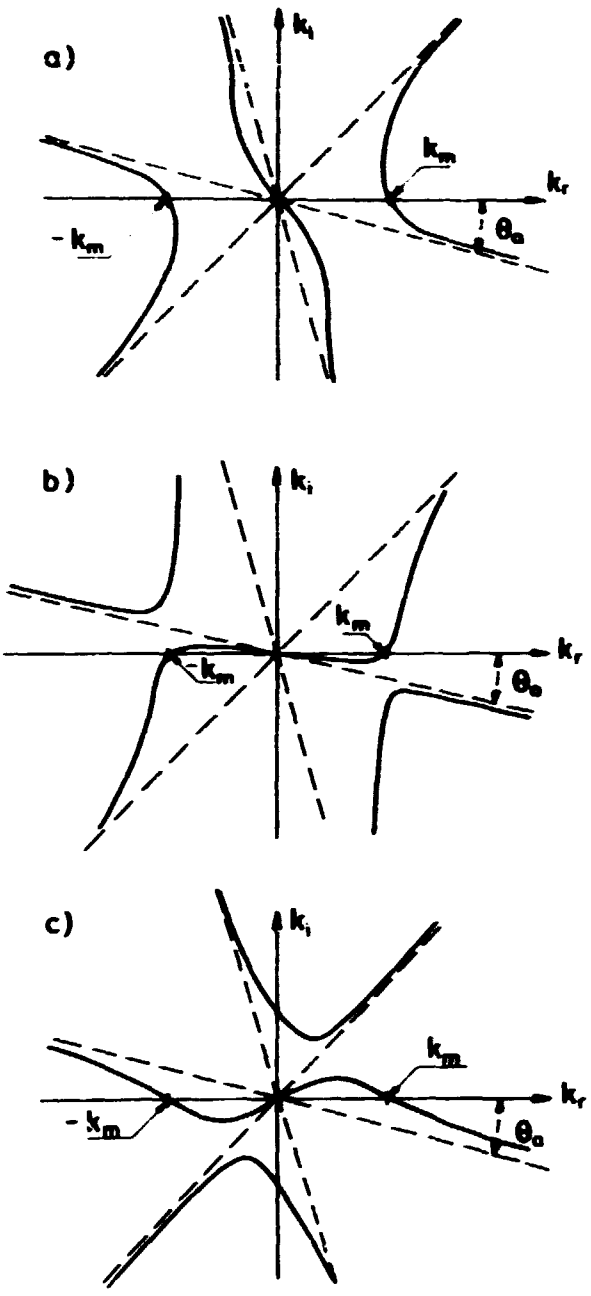

FIG. 4. The three drawings show the three possible general shapes of the curves which are described by $\mathrm{Re}S(k) = 0$. In situation (a) the three points $k = 0$ and $k = \pm k_m$ do not lie on the same curve; this corresponds to absolute instability. In situations (b) and (c) the three points lie on the same curve and, therefore, the instability is convective.

Simple analysis based on (A4) and (A5) shows that the line given by $k_r = k_i\beta_i/\beta_r$ falls outside that 60° angle between asymptotes in which the real k axis is situated. Therefore we have, as expected, an absolute instability for $u = 0$. To find the limiting value, u_+ and u_-, between absolute and convective instability we only have to find that u value for which $\mathrm{Re}S(k_s) = 0$. The saddle points are determined by

$$3\beta k_s^2 - \beta k_m^2 + iu = 0.$$

Inserting k_s determined by this equation into (A3) allows us to determine for which values of u $\mathrm{Re}S(k_s) = 0$.

* Present address: Plasma Physics Laboratory, Princeton University, Princeton, N.J. 08540.

[1] P. Sturrock, Phys. Rev. 112, 1488 (1958).
[2] P. Sturrock, *Plasma Physics*, edited by J. E. Drummond (McGraw-Hill, New York, 1961), Chap. 4.

M. Lee, Nucl. Fusion 27, 1141 (1987).

[8] K. V. Roberts, Phys. Fluids 9, 1499 (1966).

[9] E. S. Hall and J. W. Heckrotte, Phys. Rev. Lett. 20, 1370 (1968).

[10] D. V. Lee and K. V. Roberts, Phys. Fluids 13, 995 (1970).

[11] E. Ralchenko and Ya. Kolesnichenko, Phys. Fluids B 3, 2486 (1991).

[12] T. D. Rognlien and D. A. Swyler, J. Plasma Phys. 7, 131 (1972).

[13] V. Anderson, V. O. Jensen, P. Michelsen, and P. Nielsen, Phys. Fluids 14, 728 (1971).

[14] V. Anderson, G. B. Christiansen, V. O. Jensen, P. Michelsen, and P. Nielsen, Phys. Fluids 14, 980 (1971).

[15] G. B. Christiansen, V. O. Jensen, and P. Michelsen, Phys. Fluids 17, 1081 (1974).

[16] D. R. Baker, C. Barnes, and M. Ritter, in *Proceedings of the Third International Conference on Quiescent Plasmas* (Danish Atomic Energy Commission, Risø, Denmark, 1971), p. 111.

[17] D. R. Baker, Phys. Rev. Lett. 28, 1163 (1972) and Phys. Fluids 16, 1740 (1973).

[18] P. Michelsen and L. P. Pitaevskii, in *Proceedings of the Third International Conference on Quiescent Plasmas* (Danish Atomic Energy Commission, Risø, Denmark, 1971), p. 101.

[19] G. B. Christiansen and L. P. Pitaevskii, Phys. Fluids 16, 708 (1973).

Propagation properties of density pulses in an ion-beam plasma system

P. Michelsen, J. Juul Rasmussen, and N. Sato*

Association Euratom-Atomenergikommisionen, Danish Atomic Energy Commission Research Establishment Risø, DK-4 000 Roskilde, Denmark
(Received 8 December 1975)

Numerical calculations of the propagation properties of density pulses through an ion-beam plasma system are presented. Both stable and unstable situations are investigated. The calculations are based on the linearized Vlasov equation, which is solved as an initial value problem. Solutions are presented both for pure velocity modulation and for pure density modulation of the beam. The propagation properties are found to be strongly dependent on the modulation form. In the case of velocity modulation the perturbation grows even under stable conditions, while in the case of density modulation only an instability causes growth.

I. INTRODUCTION

The effects of an ion-beam traversing a plasma are of current importance in connection with plasma instability and heating, and have thus received increasing attention in recent years. Stability regions for the "ion–ion" instability were predicted by Harrison[1] and Stringer[2] in the case of two identically counter-streaming plasmas. Fried and Wong[3] considered the stability for various beam velocities, temperatures, and densities. Recently several investigators have reported experiments on this instability in Q machines[4,5] and in double-plasma (dp) machines.[6–9] Propagation of perturbations was investigated to confirm the instability. If the perturbation was observed to grow spatially in some region, the plasma was classified as unstable. Sato *et al.*[10] reported an experiment on the ion-beam plasma system, performed in a double-plasma-operated Q machine, where they found spatial growth of a perturbation even if the plasma was predicted to be stable according to the theories mentioned here. The growth was explained by linear wave theory for beam bunching. This beam bunching occurs in the case of velocity modulation, and the growth occurs for the ballistic contribution as well as for the collective modes.[10] Different methods for excitation were used in the experiments cited. Double-plasma-excitation,[6–10] i.e., modulating the beam velocity by superposing voltage variations on the bias of the driver plasma in a double-plasma-type plasma, always gives rise to velocity modulation without appreciable change of beam current. Grid excitation[4,5] also results in velocity modulation under some conditions.[11] Sato *et al.*[10] claim that their results of "beam bunching growth" could also be obtained using grid excitation.

In this paper we report numerical calculations of pulse propagation in an ion-beam plasma system, both under stable and unstable conditions. A convenient experimental method of classifying the plasma as stable or unstable is to observe the behavior of an excited pulse.[4,7,8] Therefore, we wish to emphasize the general features of pulse propagation, and the calculations are made for both pure velocity and pure density modulations of the beam. The calculations are based on the theory applied by Jensen *et al.*,[12] but deviate from this by using an initial pulse of finite width. This theory is summarized in Sec. II. Our results are obtained for an initial value problem, and therefore cannot be compared directly with experimental results. The details of the experiments should be described by a boundary value problem. However, our calculations describe the general behavior of pulse propagation.

In the case of velocity modulation a fast positive pulse and a slower negative pulse appear. Both grow initially, even under stable conditions, and reach a maximum amplitude. In the unstable situation, the slow pulse interacts with the plasma mode and forms the unstable mode, which continues the growth. The unstable mode consists of a negative and a somewhat slower and smaller positive contribution. In the case of density modulation, growth only appears in the unstable situation. The unstable mode is similar to that obtained for velocity modulation, but the polarity alters.

A survey of the cases treated is given in Table I.

II. THEORY

This section summarizes the theory used for the calculations. The ions are described by their linearized Vlasov equation, the electrons are modeled by a massless isothermal fluid, ions and electrons are coupled through the Poisson equation, and a one-dimensional situation is considered. Thus, the basic equations are

$$\frac{\partial f(x,v,t)}{\partial t} + v\frac{\partial f(x,v,t)}{\partial x} = \frac{c_e^2}{n_0}\frac{\partial n_e(x,t)}{\partial x}\frac{df_0(v)}{dv}, \tag{1}$$

$$\lambda_D^2\frac{\partial^2 n_e(x,t)}{\partial x^2} = n_e(x,t) - n_i(x,t), \tag{2}$$

and

$$n_i(x,t) = \int_{-\infty}^{\infty} f(x,v,t)\,dv, \tag{3}$$

where $c_e^2 = \kappa T_e/M$, $n_0 = \int_{-\infty}^{\infty} f_0(v)\,dv$ is the unperturbed uniform density for both ions and electrons, $\lambda_D = (\epsilon_0\kappa T_e/n_0e^2)^{1/2}$ is the electron Debye length, $n_{e,i}$ is the perturbed densities, $f_0(v)$ is the zero-order distribution function for the ions, and $f(x,v,t)$ is the perturbed distribution function. Equations (1)–(3) describe, for instance, motions along the magnetic field lines in a Q machine plasma.[13] To find the propagation of a pulse in the system, we consider the response to an initial perturbation with a velocity distribution

TABLE I. Parameters for the cases investigated. In all cases $T_e = T_i$.

Figure No.	Beam velocity v_b/c_i	Beam temperature T_b/T_i	Plasma-ion density n_i	Beam-ion density n_b	Pulse width α/λ_D	Modulation form	Stability
2	5	0.02	0	1	80	velocity	stable
3	5	0.02	0.5	0.5	80	velocity	stable
4	2	0.078	0	1	32	velocity	stable
5	2	0.078	0.5	0.5	32	velocity	unstable
6	2	0.078	0	1	32	density	stable
7	2	0.078	0.5	0.5	32	density	unstable

$$f(x, v, t=0) = g(v)\,\frac{1}{\pi}\,\frac{\alpha}{x^2+\alpha^2},$$

where α represents the width of the initial perturbation.

In Ref. 12 the equations are solved for a double-humped ion velocity distribution, the distribution function for a plasma traversed by an ion beam, in the limit $\alpha \to 0$, i.e., the Green's function for the system is found. These results are immediately generalized to the case of a finite α giving

$$n_e = n_{es} + n_{eu} = \frac{1}{t}\frac{1}{\pi}\,\mathrm{Im}\left(\frac{I\left(\frac{x+i\alpha}{t}\right)}{1-P\left(\frac{x+i\alpha}{t}\right)} - \frac{I(u_p)}{\left(u_p - \frac{x+i\alpha}{t}\right)P'(u_p)}\right)$$

$$+\frac{1}{\pi}\,\mathrm{Re}\,\frac{I(v_0)}{P'(v_0)}\int_0^{k_m}\exp\left\{ikx-\alpha k-ikt\times\left[v_0+\frac{k_m^2-k^2}{\omega_{pi}^2}A(v_0)\right]\right\}dk, \quad (4)$$

where

$$I\left(\frac{x+i\alpha}{t}\right) \equiv \int_{-\infty}^{\infty}\frac{g(v)}{\left(v-\frac{x+i\alpha}{t}\right)}\,dv$$

$$P\left(\frac{x+i\alpha}{t}\right) \equiv \frac{c_s^2}{n_0}\int_{-\infty}^{\infty}\frac{f_0'(v)}{\left(v-\frac{x+i\alpha}{t}\right)}\,dv,$$

where u_p is the solution to the equation $1 - P(u_p) = 0$ with $\mathrm{Im}\,u_p \geq 0$, v_0 is the velocity of the minimum in the zero-order distribution function, k_m is the maximum k value for which unstable oscillations occur,[12] $\omega_{pi}[= (e^2 n_0/\epsilon_0 M)^{1/2}]$ is the ion plasma frequency, and

$$A(v_0) \equiv \left(-\lim_{\epsilon\to 0^+}\frac{1}{n_0}\int_{-\infty}^{\infty}\frac{f_0''(v)}{v-(v_0+i\epsilon)}\,dv\right)^{-1}.$$

Equation (4) is the general solution for an unstable beam plasma system. In the case of a stable system, only the first term in the parentheses makes a contribution. The solution is valid for times that are long compared with a plasma period, i.e., $t\omega_{pi} \gg 1$, and for weakly unstable plasma, i.e., $k_m\lambda_D \ll 1$.

In Ref. 12 calculations of the density perturbation are only presented for distribution functions, $f_0(v)$ and $g(v)$, which are symmetric and consist of a sum of two Maxwellians. Generalizing, so that $f_0(v)$ may be a sum of two arbitrary Maxwellians and $g(v)$ may consist of any sum of Maxwellians, is straightforward. By substituting $z = k/k_m$ in the expression for n_{eu} in Eq. (4), we get

$$n_{eu} = k_m\frac{1}{\pi}\,\mathrm{Re}\,\frac{I(v_0)}{P'(v_0)} \times\int_0^1\left\{\cos[k_m z(x-tv_0)] + i\sin[k_m z(x-tv_0)]\right\} \times\exp[-i\beta_1(1-z^2)zt]\exp[(1-z^2)\beta_2 - k_m z\alpha]\,dz, \quad (5)$$

where

$$\beta = \beta_1 + i\beta_2 = (k_m^3/\omega_{pi}^2)[\mathrm{Re}\,A(v_0) + i\,\mathrm{Im}\,A(v_0)],$$

which is the expression used in the calculation described in the next section.

III. NUMERICAL RESULTS

Here, we study the propagation of a pulse through a beam plasma system by numerically calculating the density perturbation given in Eq. (4), using the expression for n_{eu} derived in Eq. (5). The zero-order distribution functions used consist of a sum of two Maxwellians:

$$f_0(v) = f_i(v) + f_b(v) = n_0\frac{1}{\sqrt{\pi}}\left(n_i\frac{1}{c_i}\exp\left[-\left(\frac{v}{c_i}\right)^2\right] + n_b\frac{1}{c_b}\exp\left\{-\left[\frac{(v-v_b)}{c_b}\right]^2\right\}\right),$$

where the indices i and b refer to plasma ions and beam ions, respectively, $n_{i,b}$ is the relative density ($n_i + n_b \equiv 1$), $c_{i,b} = (2\kappa T_{i,b}/M)^{1/2}$ is the thermal speed (beam and plasma ions are of the same kind), and v_b is the beam velocity. When an ion beam is accelerated to the velocity v_b, it is adiabatically cooled, and its temperature T_b is determined by[10]

$$T_b/T_i \simeq [1 - 3/2(v_b/c_i)^2]/2(v_b/c_i)^2.$$

$f_0(v)$ is shown in Fig. 1(a). In the calculations we only apply the initial perturbation to the beam. Velocity modulation of the beam is obtained by using an initial velocity distribution $g(v) = f_b(v+\tilde{v}) - f_b(v)$ i.e., $g(v)$ is the difference between two Maxwellians separated by $\tilde{v}$, the amplitude of the modulation. $g(v)$ for this case is shown in Fig. 1(b). Density modulation of the beam is realized by using a $g(v)$ proportional to $f_b(v)$. For the width of the initial pulse α, we use a characteristic width Δt of the temporal pulse from the cited experiments and multiply it by the beam velocity v_b. Δt is of the order of a few times ω_{pi}^{-1} giving the values for α/λ_D in Table I. $T_e = T_i$ in all the calculations.

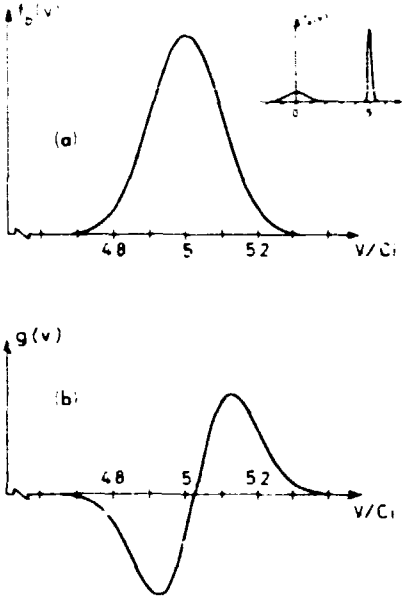

FIG. 1. (a) The zero-order distribution function. (b) The initial distribution function in the case of velocity modulation.

Figures 2–5 show the propagation properties of pulses in the case of velocity modulation, for $\bar{v}/v_b = 1$. As mentioned in Sec. II, the approximations are not valid for small values of $t\omega_{pi}$, which is indicated by dotting the curves. In Figs. 2 and 3 $v_b = 5c_i$ and $T_b = 0.02T_i$, giving $T_e/T_b = 50$, which means that the collective beam modes will dominate the free streaming contributions. The curves in Fig. 2 are calculated for the case where $f_0(v)$ only consists of a beam, $n_i = 0$, $n_b = 1$, and the situation is, of course, stable. Two pulses, a fast positive and a slow negative, are seen to grow initially until they reach a maximum amplitude at $x/\lambda_D \simeq 1500$. After this they propagate independently, with velocities approximately equal to those of the fast and of the slow beam mode, v_f and v_s, respectively. v_f and v_s are given by[10]

$$v_{f,s} = v_b \pm \epsilon^{1/2} c_e (1 + 3T_b/T_e)^{1/2} ,$$

where

$$\epsilon \equiv n_b/(n_b + n_i) .$$

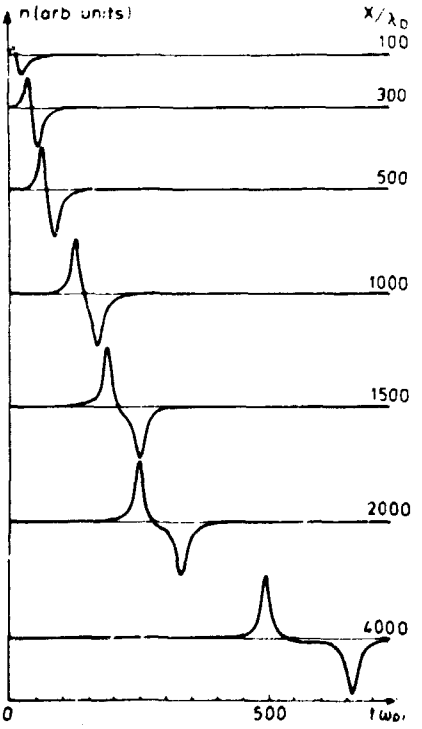

FIG. 2. Pulse propagation for velocity modulated beam in a stable system, $v_b = 5$, $n_i = 0$, $n_b = 1$.

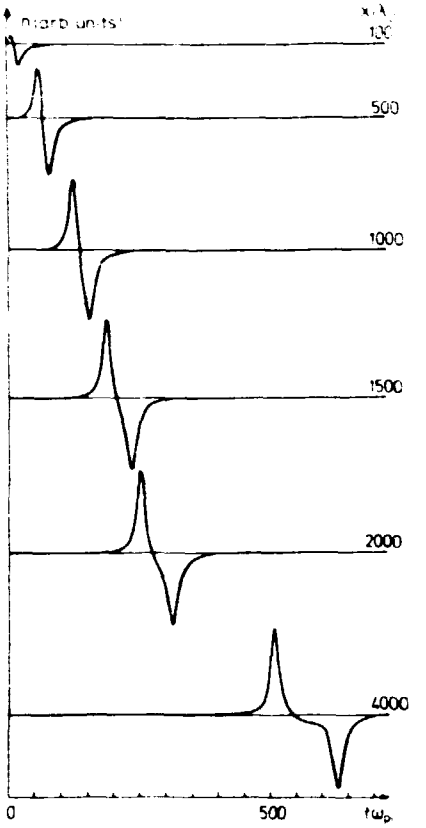

FIG. 3. Pulse propagation for velocity modulated beam in a stable system, $v_b = 5$, $n_i = 0.5$, $n_b = 0.5$.

The amplitudes of the pulses are nearly constant, but a small damping can be observed when going to larger x/λ_D values. The damping is expected to be small because of the high temperature ratio T_e/T_b and the high velocities. This propagation behavior was observed experimentally by Sato *et al.*[10] In Fig. 3 a plasma is added, and here $n_i = n_b = 0.5$; the situation is still stable.[3] The propagation properties are similar to those of Fig. 2 and no contribution appears from the plasma. However, the velocities of the fast and of the slow pulse, after reaching maximum amplitude, are changed according to the expression for v_f and v_s, in this case $\epsilon = 0.5$, and the maximum amplitudes have increased. By applying the theory of beam bunching the maximum amplitude is found to be proportional to $1/\epsilon^{1/2}$.[10] Figures 4 and 5 show calculations for a smaller beam velocity $v_b = 2c_i$ and $T_b \simeq 0.08T_i$, giving $T_e/T_b \simeq 13$ – the collective beam modes will still dominate. Figure 4 corresponds to Fig. 2, $n_i = 0$, $n_b = 1$, and also here the initial growth appears; but the maximum amplitudes are reached for a smaller x/λ_D value, $x/\lambda_D \simeq 200$, and

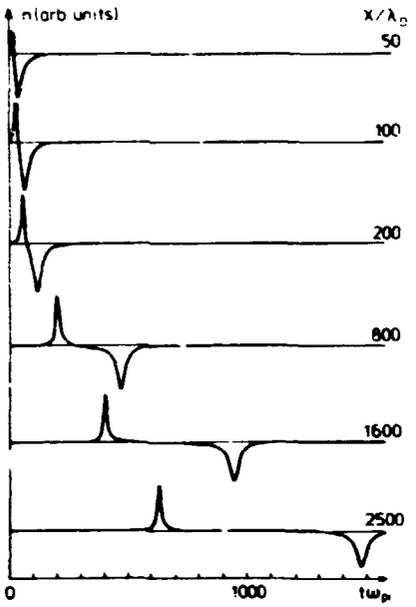

FIG. 4. Pulse propagation for velocity modulated beam in a stable system, $v_b = 2$, $n_i = 0$, $n_b = 1$.

the damping is more significant now, especially for the negative pulse, due to its small velocity. Figure 5, with $n_i = n_b = 0.5$, shows an unstable situation.[3] The initial behavior is similar to that in Fig. 4, but only the fast pulse reaches a maximum amplitude and then decays weakly, while the slow pulse, through interaction with the plasma mode, gives rise to the unstable mode that continues the growth. Both contributions to the unstable mode propagate with velocities smaller than v_b.

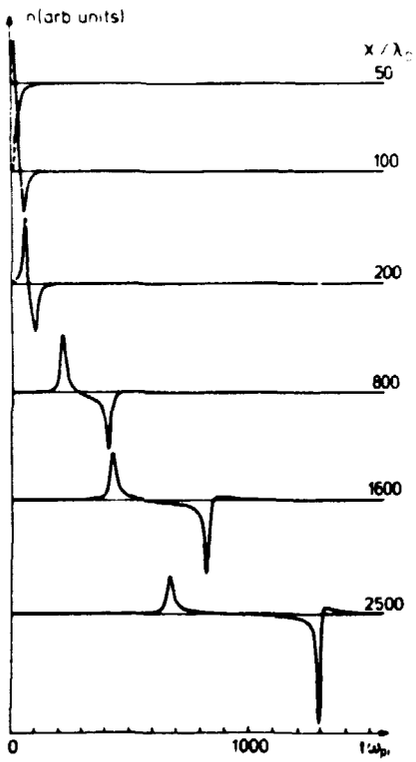

FIG. 5. Pulse propagation for velocity modulated beam in an unstable system, $v_b = 2$, $n_i = 0.5$, $n_b = 0.5$.

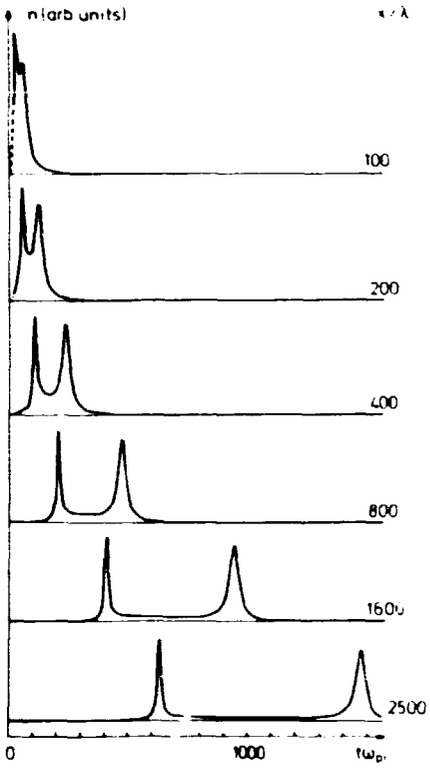

FIG. 6. Pulse propagation for density modulated beam in a stable system, $v_b = 2$, $n_i = 0$, $n_b = 1$.

Figures 6 and 7 show the properties for density modulation. We take $v_b = 2c_i$ and $T_b \simeq 0.08T_i$. The amplitude $\tilde{n}$ of the modulation will not affect the shape of the propagation but only change the amplitude, since the calculations are based on a linear theory. Figure 6 illustrates the stable case, $n_i = 0$, $n_b = 1$. The perturbation splits up into two positive pulses, which for large values of x/λ_D propagate with velocities approximately equal to v_f and v_s, and both decay. Figure 7 shows the propagation in the unstable situation: $n_i = n_b = 0.5$. We still have the splitting into two positive pulses, which initially decay, but the slow pulse now interacts with the plasma mode and gives the unstable mode which grows, while the fast pulse continues the decay, propagating with approximately the velocity v_f. The unstable mode shows the same behavior as in the case of velocity modulation, except that the polarity is altered.

IV. DISCUSSION AND CONCLUSION

In this paper we have presented numerical calculations of the propagation properties of pulses in an ion-beam plasma system. Although our results cannot directly describe experiments as mentioned in Sec. I, we believe they are very useful in giving the general behavior of the pulse propagation. By calculating the propagation properties for both pure velocity and pure density modulation, we have shown that the behavior is strongly dependent on the modulation form, i.e., the shape of the initial distribution. The same conclusion is found in Ref. 14, which also investigates the dependence of other parameters under stable conditions.

Owing to the "beam-bunching growth" in the case of

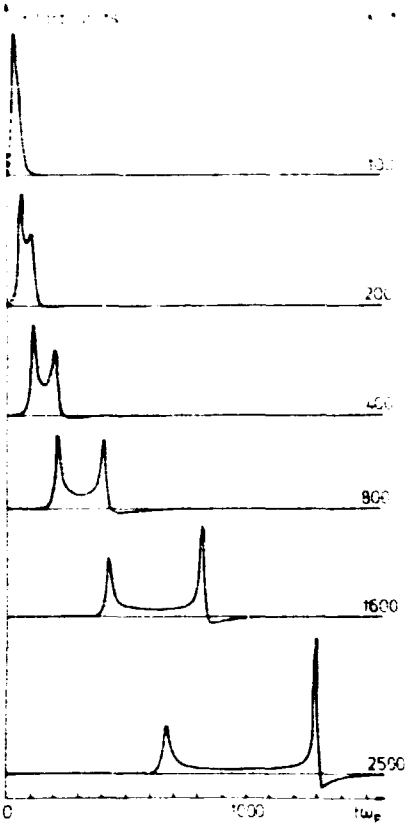

FIG. 7. Pulse propagation for density modulated beam in an unstable system, $v_b = 4$, $n_i = 0.5$, $n_b = 0.5$.

velocity modulation, much care should be taken when classifying the plasma as unstable if only based on the observation of a growing perturbation. Even if the plasma is unstable, it will be very difficult to determine the correct unstable growth rate, i.e., to distinguish the unstable growth from the "beam-bunching growth." In the case of pure density modulation, on the other hand, only an instability will cause growth. Experimental excitations often give initial distributions that are complicated functions.[11] However, in many cases these may be described as a combination of density and velocity modulation. Under such circumstances we expect results which also show some initial growth due to beam bunching, and therefore the same difficulties will arise as in the case of pure velocity modulation. One can argue that the "beam-bunching growth" will only be appreciable at small distances from the exciting point, while the unstable growth will continue for a longer distance until nonlinear effects make it saturate. Our results show, however, that "beam-bunching growth" can easily continue until $x \simeq 1500\ \lambda_D$, which corresponds to $x \simeq 15$–45 cm under characteristic experimental conditions ($\kappa T_e \simeq 0.2$ eV, $n_0 \simeq 10^8 - 10^9$).

We have only considered weakly unstable situations; naturally, the results for the unstable part are only valid until the instability reaches a nonlinear level. The unstable mode shows similar features in the two cases of modulation, except for the altered polarity, a large contribution originating from the slow beam mode and a somewhat slower and smaller contribution originating from the plasma mode. Both contributions have velocities below the beam velocity. The reason for the difference in amplitude of the two contributions is partly due to T_e/T_i, T_e/T_b, i.e., the beam mode is stronger than the plasma mode, and to the fact that the beam mode is more strongly excited than the plasma mode because the modulation is applied to the beam.

Our results can be applied to any kind of beam-plasma system, and also other instabilities, "electron–electron" and "electron–ion," must be treated carefully to avoid mixing of unstable growth with "beam-bunching growth."

ACKNOWLEDGMENTS

We thank V. O. Jensen and H. L. Pécseli for their interest and valuable discussions. One of the authors (N. S.) is very grateful to V. O. Jensen and Professor Y. Hatta for their encouragement.

*Present address: Department of Electronic Engineering, Tohoku University, Sendai, Japan.
[1]E. R. Harrison, Proc. Phys. Soc. **80**, 132 (1962).
[2]T. E. Stringer, J. Nucl. Energy C **6**, 267 (1964).
[3]B. D. Fried and A. Y. Wong, Phys. Fluids **9**, 1084 (1966).
[4]D. R. Baker, C. Bartoli, and M. Bitter, in *Proceedings of the Third International Conference on Quiescent Plasmas* (Danish Atomic Energy Commission, Risø, Denmark, 1971), p. 111; D. R. Baker, Phys. Rev. Lett. **28**, 1189 (1972); and Phys. Fluids **16**, 1730 (1973).
[5]G. B. Christoffersen and L. P. Prahm, Phys. Fluids **16**, 708 (1973).
[6]D. Grésillon and F. Doveil, Phys. Rev. Lett. **34**, 77 (1975).
[7]Y. Kiwamoto, J. Phys. Soc. Jpn. **37**, 166 (1974).
[8]R. J. Taylor and F. V. Coroniti, Phys. Rev. Lett. **29**, 34 (1972).
[9]T. Fujita, T. Ohnuma, and S. Adachi, Phys. Fluids **18**, 1216 (1975).
[10]N. Sato, H. Sugai, and R. Hatakeyama, Phys. Rev. Lett. **34**, 931 (1975).
[11]G. B. Christoffersen, in *Proceedings of the Third International Conference on Quiescent Plasmas* (Danish Atomic Energy Commission, Risø, Denmark, 1971), p. 55.
[12]V. O. Jensen, P. Michelsen, and H. C. S. Hsuan, Phys. Fluids **17**, 2208 (1974).
[13]S. A. Andersen, G. B. Christoffersen, V. O. Jensen, P. Michelsen, and P. Nielsen, Phys. Fluids **14**, 990 (1971) and G. B. Christoffersen, V. O. Jensen, and P. Michelsen, Phys. Fluids **17**, 390 (1974).
[14]V. O. Jensen and P. Michelsen, Risø Report No. 257 (1972).

Plasma Physics, Vol. 21, pp. 173 to 182
© Institute of Physics and Pergamon Press Ltd., 1979
Printed in Northern Ireland

0032-1028/79/0201-0173$02.00/0

WAVE PROPAGATION IN AN ION BEAM–PLASMA SYSTEM

T. D. JENSEN, P. MICHELSEN and J. JUUL RASMUSSEN
Association Euratom, Risø National Laboratory, DK-4000 Roskilde, Denmark

(*Received* 12 *April* 1978, *and in revised form* 17 *August* 1978)

Abstract – The spatial evolution of a velocity- or density-modulated ion beam is calculated for stable and unstable ion beam plasma systems, using the linearized Vlasov–Poisson equations. The propagation properties are found to be strongly dependent on the form of modulation. In the case of velocity modulation, the perturbation grows initially and then shows a periodic change of amplitude along the beam, while in the case of a density modulation only an instability causes growth. The findings are in agreement with experimental results obtained by SATO *et al.* (1977).

1. INTRODUCTION

THE PROPAGATION of waves in a plasma traversed by an ion beam has recently received much attention because of its importance in connection with plasma instabilities and heating. Regions of instability for the ion-beam instability have been calculated by several authors, e.g. HARRISON (1962), STRINGER (1964), FRIED and WONG (1966) and MICHELSEN and PRAHM (1971). Several investigators have reported experiments on this instability in Q-machines, BAKER (1972 and 1973) and CHRISTOFFERSEN and PRAHM (1973), and in double-plasma devices, GRÉSILLON and DOVEIL (1975), KIWAMOTO (1974), TAYLOR and CORONITI (1972) and FUJITA *et al.* (1975). The propagation of both short pulses and continuous waves has been studied in such systems, and the system has been classified as unstable in cases where the pulse or the wave amplitude increased away from the exciter. In an experiment performed in an ion-beam plasma system generated in a double-plasma-operated Q-machine, SATO *et al.* (1975) and (1977) found spatial growth although the plasma was predicted to be stable according to theory. This growth was explained by linear theory for beam bunching, which occurs in the case of velocity modulation, both for the ballistic contribution as well as for the collective modes. Ion waves in double-plasma devices are normally excited by velocity modulation of an ion beam, but also grid excitation of waves in other machines often gives rise to perturbations in the ion velocity distribution, which may be characterized as velocity modulation, or as a combination of velocity and density modulation, CHRISTOFFERSEN (1971) and GRÉSILLON (1971).

Recently, we performed calculations on pulse propagation in an ion beam plasma system (MICHELSEN *et al.*, 1976; RASMUSSEN, 1977). Here we report analytical and numerical calculations of wave propagation in stable and unstable ion beam plasma systems. The calculations, based on the Vlasov–Poisson equation, were motivated by the interesting measurements of SATO *et al.* (1977). Therefore, to obtain the best agreement with the experiment, the equations were solved as a boundary value problem. The theory is similar to that applied by CHRISTOFFERSEN *et al.* (1974), but it is extended to include unstable systems.

The theory is summarized in Section 2, the numerical calculations and results are given in Section 3, while Section 4 contains a discussion and conclusion.

2. THEORY

We describe the motion of the ions by their linearized Vlasov equation, and that of the electrons by a massless isothermal fluid. Ions and electrons are coupled through the assumption of quasi-neutrality, i.e. $(k\lambda_D)^2 \ll 1$ (λ_D is the Debye length). In one dimension our basic equations are

$$\frac{\partial f(x, v, t)}{\partial t} + v\frac{\partial f(x, v, t)}{\partial x} = \frac{e}{M}\frac{\partial \phi(x, t)}{\partial x}\frac{\partial f_0(v)}{\partial v} \tag{1}$$

$$T_e\frac{\partial n(x, t)}{\partial x} = n_0 e\frac{\partial \phi(x, t)}{\partial x} \tag{2}$$

and

$$n(x, t) = \int_{-\infty}^{\infty} f(x, v, t)\,dv, \tag{3}$$

where $f_0(v)$ is the zero-order distribution function, $f(x, v, t)$ is the perturbed distribution function, $\phi(x, t)$ is the perturbed electrical potential, n_0 is the zero-order density given by $n_0 = \int_{-\infty}^{\infty} f_0(v)\,dv$, and $n(x, t)$ is the perturbed density. These equations describe, e.g. ion acoustic waves in a Q-machine plasma (JENSEN, 1976).

The equations are solved with the following boundary values: $f(x = 0, v, t) = g(v)\exp(-i\omega_0 t)$,

$$n(x = 0, t) = \int_{-\infty}^{\infty} g(v)\exp(-i\omega_0 t)\,dv = \eta\exp(-i\omega_0 t) \tag{4}$$

Additionally, we assume that $f_0(v)$ and $g(v)$ is zero for $v \leq 0$, i.e. we need not specify the boundary values at $x \to \infty$. To solve equations (1)–(3) we can then use a Laplace transform in space, and a Fourier transform in time (NIELSEN, 1969; PÉCSELI, 1974; CHRISTOFFERSEN *et al.*, 1974). The analysis resembles the usual Landau-type of analysis used for the initial value problem (e.g. MONTGOMERY, 1971), and we find the following expression for the spatial variation of the perturbed density (see the Appendix):

$$\begin{aligned} n(x) = \frac{1}{\pi}\int_0^{\infty}\frac{1}{k}\,\mathrm{Im}\left\{M_b\left(\frac{\omega_0}{k}\right)\right\}\exp(ikx)\,dk \\ + \mathrm{Res}\left\{\frac{1}{k}M_a\left(\frac{\omega_0}{k}\right)\exp(ikx)\right\}\Big|_{k=k_p^*} \\ + \mathrm{Res}\left\{\frac{1}{k}M_b\left(\frac{\omega_0}{k}\right)\exp(ikx)\right\}\Big|_{k=k_p} \end{aligned} \tag{5}$$

where Im{ } and Res{ } stand for the imaginary part and the residue of the quantity in the braces, and $M_{a,b}$ is defined in the Appendix. For a stable case, only the first term makes a contribution. $n(x)$ in (5) is a complex quantity, where the modulus and the phase, respectively, give the amplitude and the phase of the perturbed density.

In the calculation of $n(x)$, use is made of a zero-order distribution function, which consists of a sum of two drifting Maxwellians:

$$f_0 = f_i + f_b = n_0 \frac{1}{\sqrt{\pi}} \left(n_i \frac{1}{c_i} \exp\left[-\left(\frac{v - v_i}{c_i} \right)^2 \right] + n_b \frac{1}{c_b} \exp\left[-\left(\frac{v - v_b}{c_b} \right)^2 \right] \right), \tag{6}$$

where the indices i and b refer to plasma ions and beam ions, respectively, $n_{i,b}$ is the relative density ($n_i + n_b = 1$), $c_{i,b} = (2T_{i,b}/M)^{1/2}$ is the thermal speed (beam and plasma ions are of the same kind), and $v_{i,b}$ is the drift velocity. Using an $f_0(v)$ just described and a $g(v)$, which also consists of Maxwellians, the plasma dispersion function can be used in our calculations. Only an approximate solution can be obtained with these distributions, since $f_0(v) \neq 0$ and $g(v) \neq 0$ for $v \leq 0$. However, the approximation is good for Maxwellians with drift velocities greater than $2c_i$. The ion distribution in a single-ended Q-machine is approximately described by a drifting Maxwellian, ANDERSEN *et al.* (1971).

3. NUMERICAL RESULTS

In this section the propagation properties of ion-acoustic waves in the beam plasma system are studied by numerical calculation of the density perturbation given in (5) using the distribution function in (6). Special attention is paid to the difference between the propagation of waves generated by a velocity modulation and a density modulation of the beam. Velocity modulation of the beam is obtained by using a velocity distribution $g(v) = f_b(v + \bar{v}) - f_b(v)$, i.e. $g(v)$ is the difference between two Maxwellians separated by $\bar{v}$, (MICHELSEN *et al.*, 1976). In all the calculations $\bar{v} = 0.05\, c_b$. Density modulation of the beam is realized by using a $g(v)$ that is proportional to $f_b(v)$. The drift velocity of the background plasma v_i is $2c_i$ to satisfy the assumption used in Section 2. The result of the calculations of the wave propagation is shown in Figs 1–3, where the perturbed density $n(x)$ (solid line) is plotted versus the normalized distance $x(\omega/c_i)$. The dashed line in the figures indicates the wave amplitude.

Figure 1 shows the propagation properties of waves in the case of density modulation for decreasing values of v_b. In Figs 1(a) and (b) the system is stable and the wave patterns show a periodical oscillation in the amplitude superimposed by a monotonic damping. The amplitude oscillation is interpreted as caused by the beating between the fast and the slow ion-beam mode (SATO *et al.*, 1977). The phase velocities of the fast and slow beam mode, v_f and v_s respectively, are approximately given by

$$v_{f,s} = v_b \pm n_b^{1/2} c_e (1 + 3T_b/T_e)^{1/2}. \tag{7}$$

In accordance with this expression, the pitch length in the interference pattern decreases with decreasing v_b. Since the slow mode is more strongly damped than the fast mode, the interference becomes weaker for increasing distance. This effect becomes more pronounced for decreasing v_b, because the difference in the damping of the fast and slow mode becomes larger. Close to the exciter, the waves have an 'average' phase velocity close to v_b, but far away the phase velocity approaches v_f. Note, however, that the phase of the wave shows abrupt changes

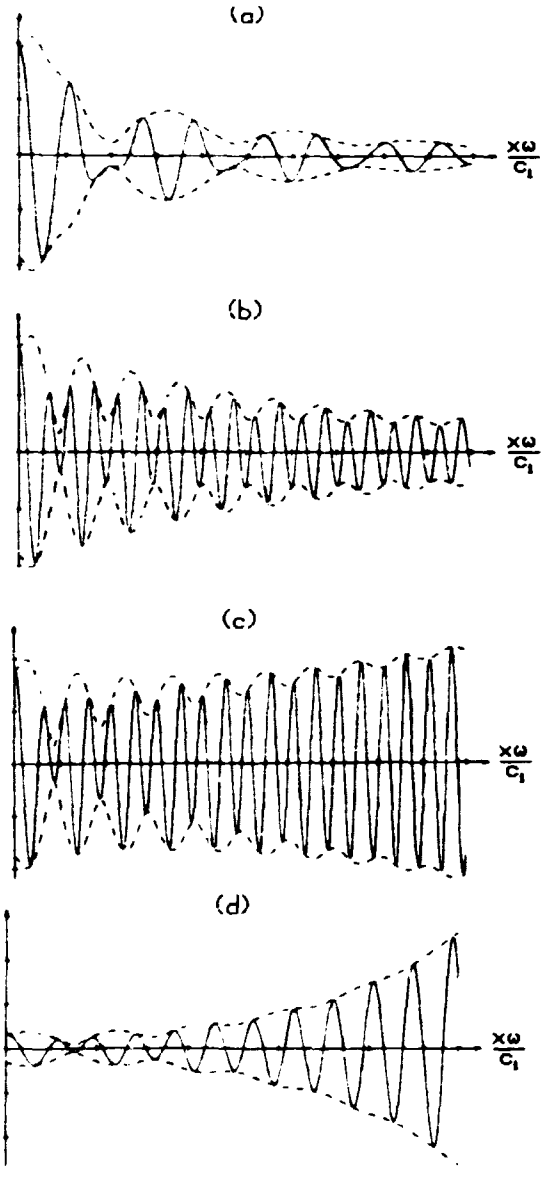

FIG. 1.—Wave propagation for density modulation. $T_h = T_i$, $T_e = 5T_i$; $n_i = n_b$; $v_i = 2c_i$; abscissa = $50x\omega/c_i$ per division. Stable cases: (a) $v_h = 9c_i$ and (b) $v_b = 6.1c_i$. Unstable cases: (c) $v_h = 6.0c$, and (d) $v_b = 5c_i$.

where the amplitude has minima. Figures 1(c) and (d) show unstable situations, MICHELSEN and PRAHM (1971). Again we have the amplitude oscillations, but after a few wavelengths the amplitude grows exponentially and here the phase velocity approaches the velocity of the unstable mode, i.e. the velocity of the minimum in $f_0(v)$ (JENSEN *et al.*, 1974).

Calculations with a velocity modulation of the beam showed that the main

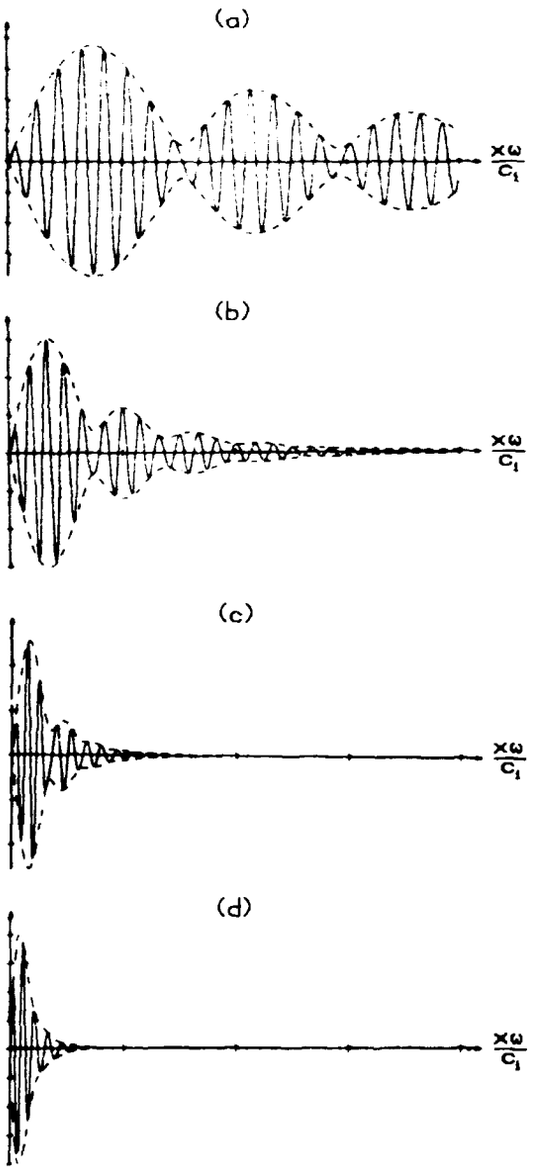

FIG. 2.—The wave propagation dependence of the drift velocity. Compare SATO *et al.* (1977) Fig. 4. $T_i = T_e$; $n_b/n_i = 0.47$; $v_i = 2c_i$; abscissa = 250 $x\omega/c_i$ per division. (a) $v_b = 8c_i$; $T_b = 0.09\ T_i$; (b) $v_b = 6c_i$; $T_b = 0.2\ T_i$; (c) $v_b = 4.5c_i$; $T_b = 0.4\ T_i$; and (d) $v_b = 3.5c_i$; $T_b = 0.8\ T_i$.

change from Fig. 1 is that waves excited by velocity modulation grow from zero at the exciting point. But after a few wavelengths no significant differences are observed.

Figures 2 and 3 show propagation properties of waves excited by velocity modulation. The parameters of the distribution functions are chosen similar to those in the experiments of SATO *et al.* (1977). In Fig. 2 we show the wave pattern

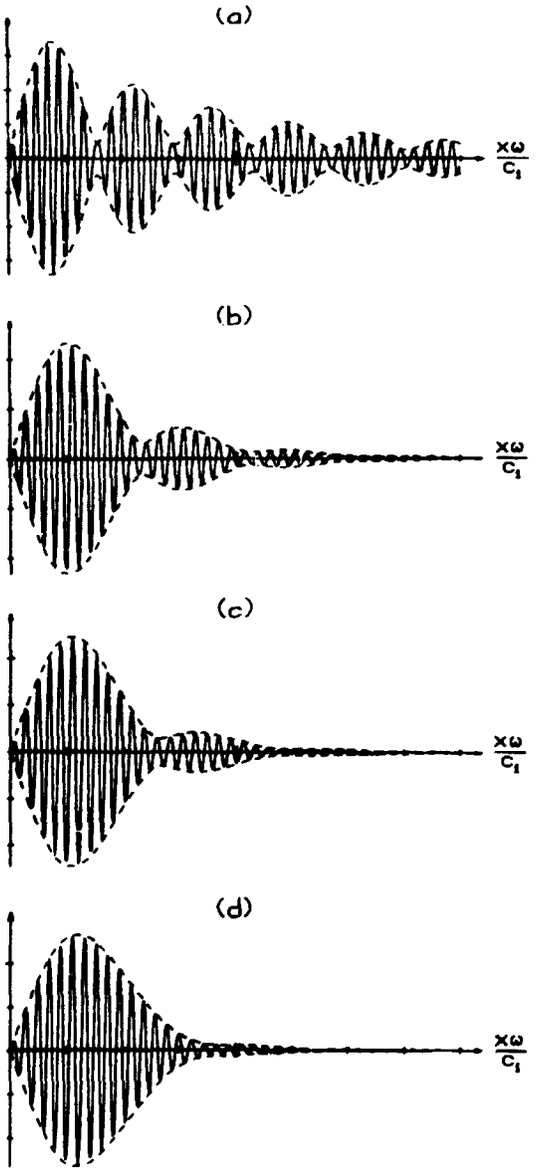

FIG. 3.—Time wave propagation dependence of the relative beam density. Compare SATO *et al.* (1977), Fig. 8. $T_b = 0.1\ T_i$; $T_e = T_i$; $v_b = 8.3\ c_i$; $v_i = 2c_i$; abscissa = 250 $x\omega/c_i$ per division (a) $n_b/n_i = 0.47$; (b) $n_b/n_i = 0.11$; (c) $n_b/n_i = 0.064$; and (d) $n_b/n_i = 0.015$.

for varying beam velocities, v_b. We note that the tendency for the perturbed density to split up into a perfect interference pattern is weakened when v_b decreases. For $v_b = 3.5\ c_i$, the amplitude damps away monotonically without any oscillations. The wavelength λ and the pitch length 1 of the periodic amplitude variation decrease as v_b decreases. In Fig. 3 the wave pattern is shown with n_b as a parameter. As n_b decreases, 1 increases (e.g. equation (7)) and the periodic change of the amplitude gradually disappears. For small values of n_b, the perturba-

tions grow initially and then they damp away monotonically after reaching maximum. The phase velocity is close to v_t when the wave is strongly damped. A comparison between the measurements by SATO *et al.* (1977) and our corresponding calculations shows an excellent agreement.

4. DISCUSSION AND CONCLUSION

We have presented calculations of the spatial evolution of density waves in an ion beam plasma system (stable or unstable), in the cases where the wave is excited either by a pure velocity or by a pure density modulation of the beam. In the case of the velocity modulation, initial growth and subsequent amplitude oscillation are found for the stable situation (Figs 2 and 3). This behaviour was also found in the experiment of SATO *et al.* (1977). By using the data from their experiment in our calculations, we found excellent agreement between our results (Figs 2 and 3) and their measurements.

It has been claimed (e.g. JENSEN, 1976) that the propagation of ion waves depends strongly on the distribution function in the perturbation at the boundary (i.e. $g(v)$) when $T_e/T_i \leqslant 3$, and the ballistic contribution dominates the collective modes.

We also see that the shape of $g(v)$ influences the wave propagation, even if $T_e/T_i \geqslant 5$, and the collective modes dominate after a few wavelengths. this result was demonstrated clearly by investigating the propagation of density pulses (MICHELSEN *et al.*, 1976). Also a purely ballistic theory (i.e. $T_e = 0$) will result in amplitude oscillations in the case of velocity modulation (SATO *et al.*, 1977). We also found these oscillations in the case $T_e = 0$. A density modulation only gives a monotonically decaying amplitude (e.g. JENSEN and MICHELSEN, 1972).

When the plasma is unstable with respect to the ion–ion instability (Figs 1(c) and (d)), we still find the amplitude oscillations caused by the interference between the slow and the fast beam mode close to the exciter, before the unstable mode begins to dominate. Thereafter the amplitude grows exponentially superimposed on a decaying oscillation, followed by a decrease in the phase velocity. Near the exciter, where the beating between slow and fast beam mode is dominant, the phase velocity is close to the beam velocity, while in the region where the growth is significant, the phase velocity approaches the velocity of the unstable mode which is less than the beam velocity. These properties of wave propagation in an unstable ion-beam plasma system, with parameters comparable to those used here, were observed experimentally by CHRISTOFFERSEN and PRAHM (1973). The shape of $g(v)$ was found to be unimportant for the unstable growth, which is also clear from (5). For pulse propagation, however, the shape of $g(v)$ can effect the form of the unstable pulse (MICHELSEN *et al.*, 1976). Even if $g(v)$ has no influence on the growth of the unstable mode, one can imagine that it will have some importance for the wavepattern in the unstable situation. Further, $g(v)$ could be chosen so that the one mode is preferentially excited, and this will dominate for several wavelengths. Actually, PÉCSELI (1975) has shown that, for a given development of the density perturbation, a $g(v)$ always can be prescribed (although this is not always physically possible).

We only considered weakly situations, and our results for the unstable mode are, of course, only valid until the instability reaches a nonlinear level. In

experiments on the ion-ion instability (e.g. Baker, 1972, 1973; Christoffersen and Prahm, 1973; Gresillon and Doveil, 1975; Fujita *et al.*, 1975), it has been found that the unstable wave grows initially, but is subsequently saturated due to nonlinear effects and damped: a behaviour very similar to that which can be found in the case of a velocity modulation of the beam, e.g. Figs 3(c) and (d). It should be emphasized that the difference can be seen from the phase velocity. In the stable case with beam-bunching, the phase velocity tends to increase and approaches the velocity of the fast beam mode, i.e. *larger* than the beam velocity. In the unstable case, on the other hand, the phase velocity decreases and approaches the velocity of the unstable mode, i.e. *smaller* than the beam velocity.

The amplitude oscillations caused by the beating between normal modes propagating in the same direction are found not only in beam plasma systems (DP-type plasmas), but also in single-ended Q-machines under the 'electron-rich condition'. Ion acoustic waves in such a plasma are usually excited by grids, which often give rise to complicated, perturbed, distribution functions (Christoffersen, 1971; Gresillon, 1971). If the ion beam temperature is much lower than the electron temperature, we should expect the excitation of both the fast and the slow beam mode, and therefore amplitude oscillations (Buzzi, 1974).

Finally, we should like to point out that amplitude oscillations of plasma waves have usually been interpreted as due to nonlinear effects, our calculations, on the other hand, show that the same behaviour may occur as a mere superposition of linear normal modes, in agreement with experimental observations (e.g. Sato *et al.*, 1975, 1977; Gresillon and Doveil, 1975).

REFERENCES

Andersen S. A., Jensen V. O., Michelsen P. and Nielsen P. (1971) *Physics Fluids* **14**, 728.
Baker D. R. (1972) *Phys. Rev. Lett.* **28**, 1189.
Baker D. R. (1973) *Physics Fluids* **16**, 1730.
Buzzi J. M. (1974) *Physics Fluids* **17**, 716.
Christoffersen G. B. (1971) Proc. 3rd intern. Conf. Quiescent Plasmas, Elsinore, Risø Rep. 250, 55.
Christoffersen G. B. and Prahm L. (1973) *Physics Fluids* **16**, 708.
Christoffersen G. B., Jensen V. O. and Michelsen P. (1974) *Physics Fluids* **17**, 390.
Fried B. D. and Wong A. Y. (1966) *Physics Fluids* **9**, 1084.
Fujita T., Ohsuma T. and Adachi S. (1975) *Physics Fluids* **18**, 1216.
Gresillon D. (1971) *J. Physique* **32**, 269.
Gresillon D. and Doveil F. (1975) *Phys. Rev. Lett.* **34**, 77.
Gould R. W. (1964) *Phys. Rev.* **A136**, 991.
Harrison E. R. (1962) *Proc. Phys. soc.* **80**, 432.
Jensen V. O. and Michelsen P. (1972) Risø Rep. 257.
Jensen V. O., Michelsen P. and Hsuan H. C. S. (1974) *Physics Fluids* **17**, 2208.
Jensen V. O. (1976) Risø Rep. 322.
Kiwamoto Y. (1974) *J. Phys. Soc. Japan* **37**, 466.
Michelsen P. and Prahm L. (1971) Proc. 3rd intern. conf. Quiescent plasmas, Elsinore, Risø Rep. 250, 103.
Michelsen P., Rasmussen J. Juul and Sato N. (1976) *Physics Fluids* **19**, 1021.
Montgomery, D. C. (1971) *Theory of Unmagnetized Plasma*. Gordon and Breach.
Nielsen P. (1969) Risø Rep. 190.
Pécseli H. L. (1974) *Physics Fluids* **17**, 378.
Pécseli H. L. (1975) *Physica scripta* **11**, 311.
Rasmussen J. Juul (1977) Risø M. Rep. 1950.
Sato N., Sugai H. and Hatakeyama R. (1975) *Phys. Rev. Lett.* **34**, 931.
Sato N., Sugai H. and Hatakeyama R. (1977) *Plasma Phys.* **19**, 187.
Stringer T. E. (1964) *J. Nucl. Energy* **c6**, 267.
Taylor R. J. and Coroniti F. V. (1972) *Phys. Rev. Lett.* **29**, 34.

APPENDIX

Here we summarize the analysis for solving (1)–(3) with the boundary conditions (4). By applying the Laplace transform in space and the Fourier transform in time, i.e.

$$f(k,\omega) = \int_{-\infty}^{\infty}\int_{0}^{\infty} e^{-i(\omega t - kx)} f(x,t)\,dx\,dt$$

we obtain

$$n(\omega,k) = \frac{1}{ik}2\pi\delta(\omega_n - \omega)\left[\frac{\dfrac{\omega_p^2}{k}\displaystyle\int_{-\infty}^{\infty}\frac{g(v)}{v-\omega/k}\,dv}{1-\dfrac{\omega_p^2}{n_0}\displaystyle\int_{-\infty}^{\infty}\frac{f_0(v)}{v-\omega/k}\,dv} + \eta\right]$$

$$= \frac{1}{ik}2\pi\delta(\omega_n - \omega)M\left(\frac{\omega}{k}\right) \tag{A1}$$

where $\omega_p = (n_0 e^2/M\varepsilon_0)^{1/2}$. The inverse transform is

$$n(x,t) = \frac{1}{4\pi^2}\int_{-\infty}^{\infty}\exp(-i\omega t)\int_{-\infty}^{\infty}\exp(ikx)n(k,\omega)\,dk\,d\omega$$

$$= \frac{1}{2\pi}\exp(-i\omega_n t)\int_{-\infty}^{\infty}\frac{1}{ik}M\left(\frac{\omega_n}{k}\right)\exp(ikx)\,dx$$

The integrands in the v-integrations in $M(\omega_n/k)$ have poles for $v = \omega_n/k$. We obtain an analytic continuation of $M(\omega_n/k)$ termed $M_+(\omega_n/k)$, by prescribing that the v-integration path shall run *below* the pole. For a stable situation, the function $M_+(\omega_n/k)$ has no poles in the complex k plane with $\operatorname{Im} k < 0$. For an unstable situation, $M_+(\omega_n/k)$ has one pole $k = k_p$ for $\operatorname{Im} k_p < 0$. We note that there are no singularities at the origin because we find from (A1) that $\lim_{k\to\infty}[(1/k)M(\omega_n/k)] = 0$. We then move the k-integration contour to the real axis and split up the integration into two contributions:

$$n_+(x,t) = \frac{1}{2\pi}\exp(-i\omega_n t)\left[\int_{-\infty}^{0}\frac{1}{ik}M_+\left(\frac{\omega_n}{k}\right)\exp(ikx)\,dk\right.$$

$$\left. - \int_{0}^{\infty}\frac{1}{ik}M_+\left(\frac{\omega_n}{k}\right)\exp(ikx)\,dk\right] \tag{A2}$$

If the plasma is unstable, we must add the residue contribution from the unstable pole. To carry out the integration in (A2) we change the contour of the k-integration into the complex k-plane (Gould,

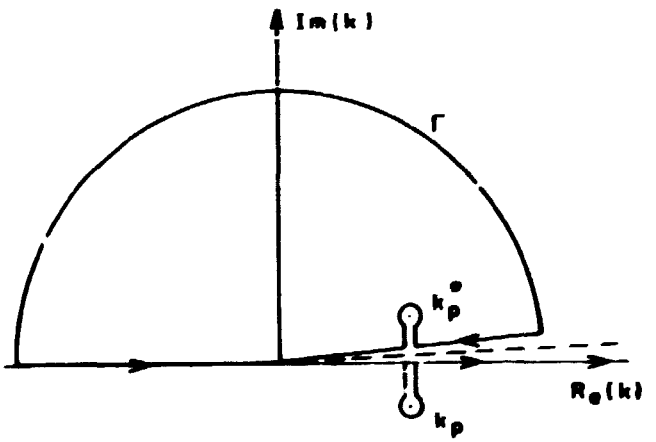

FIG. A1.—Integration contour. k_p is the unstable pole, and the dashed line is a branch cut.

1964). That is we define a new function $M_a(\omega_0/k)$ as the analytic continuation of $M(\omega_0/k)$, where, in contrast to $M_b(\omega_0/k)$, it is specified that the integration path in the v-integrations shall run *above* the poles. We thus have the following relation

$$M_a^*(\zeta^*) = M_b(\zeta),$$

where the asterisk denotes the complex conjugate.

As a consequence of the assumption that there are no ions with negative velocity, i.e. $f_0(v) \equiv g(v) \equiv 0$ for $v < 0$, we can replace M_b by M_a in the first integral in equation (A2), because M_b and M_a are equal on the real negative k-axis. As M_a is analytical for a stable case in the upper k half-plane, we can change the integration contour to run just above the positive real k-axis, as shown in Fig. A1. Because the integration along the half-circle Γ is zero, we can reduce equation (A2) to one integral running from 0 to ∞. If the plasma is unstable, we have to add the residue of the unstable pole in k_p, and the residue of the function $M_a(\zeta)$ in k_r^* (Fig. 1). We then find the total expression for the perturbed density, after having omitted the time dependence, as written in (5).

Stability limits of the ion beam excited electrostatic ion cyclotron instability

P. Michelsen

Association Euratom, Atomenergikommissionen, Danish Atomic Energy Commission Research Establishment Risø, Roskilde, Denmark

(Received 26 June 1975; final manuscript received 2 October 1975)

The dispersion relation for low-frequency electrostatic waves was analyzed numerically to find the region of instability for an ion beam plasma versus beam velocity v_b, and versus electron to ion temperature ratio. For $v_b > 1.6\,a$ the marginal unstable mode has a perpendicular wavenumber $k_\perp \neq 0$.

When electrons drift with respect to the ions in a homogeneous magnetized plasma either the ion acoustic or the electrostatic ion cyclotron instability may be excited. For a plasma with an electron to ion temperature ratio around one ($T_e/T_i \simeq 1$) the latter is known to be unstable at the lowest drift velocity.[1-4]

The case where an ion beam passes through a plasma has been less studied. Several authors have computed stability diagrams showing at which ion beam velocities and for which temperature ratios the plasma becomes unstable to an ion acoustic mode propagating in a nonmagnetic plasma or along the magnetic lines.[4,5] The stability criterion for ion cyclotron waves in a system of two identical counterstreaming ion beams has been studied by Weibel.[6] By using an iteration method he found that a mode propagating nearly perpendicular to the magnetic field becomes unstable at a beam velocity of around eight times the thermal velocity if the temperature ratio is equal to one. At lower beam velocities, at which the parallel mode is unstable at low temperature ratios ($\Theta = T_e/T_i > 3,5$), Weibel's iteration scheme is less suitable. However, this range is of interest in connection with recent experiments[7] and theories[8] on the ion beam instability. An experimental observation of electrostatic ion cyclotron waves excited by a high energetic ion beam was recently reported by Ishizuka *et al.*[9] This kind of instability may also be important for neutral heating of a plasma to thermonuclear temperatures, as recently discussed by Stix.[10]

We have studied a beam plasma system, similar to that in Ref. 6, that consists of two counterstreaming ion beams propagating through an electron fluid. We numerically calculated the limit of stability for various temperature ratios Θ and beam velocities v_b. The direction of wave propagation for the marginal stable wave was also computed. The main results of these calculations are shown in Figs. 1 and 2. From these figures it can be seen that for a beam velocity of $\gtrsim 1.6$ times the ion thermal velocity a, the wave which becomes unstable at the lowest temperature ratio is the one which propagates at a finite angle to the magnetic field. For increasing beam velocities, the necessary temperature ratio for instability decreases and the wave vector eventually becomes perpendicular to the magnetic field lines.

We consider a plasma consisting of two identical ion beams moving with the velocities $+v_b$ and $-v_b$, respectively, and an electron background which we assume can be described as an isothermal fluid. Most laboratory

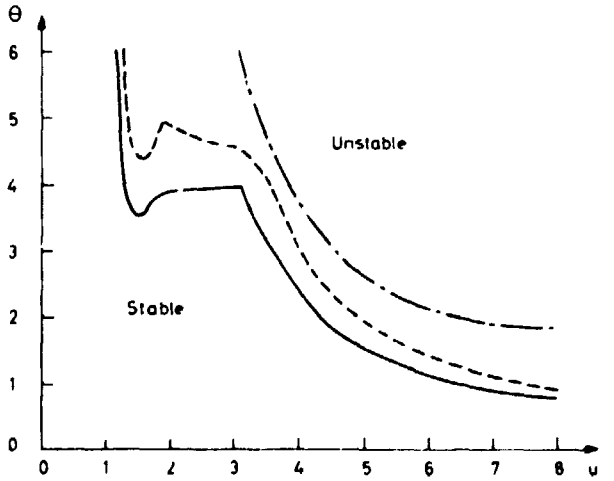

FIG. 1. Limits of stability versus normalized beam velocity $u = v_b/a$ and temperature ratio $\Theta = T_e/T_i$: (a) full line (——) $\omega_r = \omega_i = 0$, (b) dotted line (------) $\omega_r = 0$ and $\omega_i = 0.1 a k_z$, (c) dot and dashed line (– – –) $\omega_r \neq 0$ and $\omega_i = 0$.

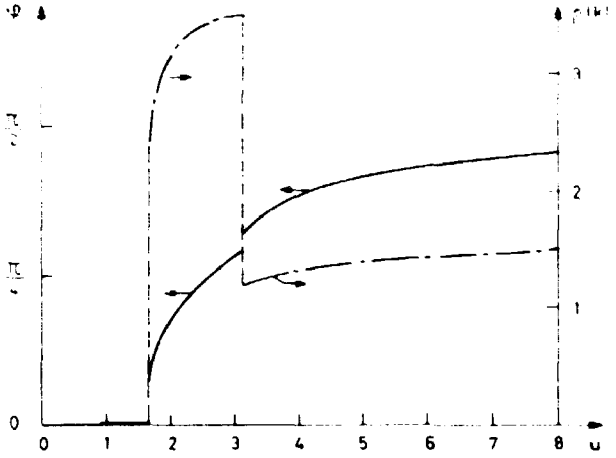

FIG. 2. Length and angle of wave vector k for marginal stable waves versus normalized velocity $u = v_b/a$: (a) full line (——) is the angle of propagating, and (b) the dot and dashed line (– – –) is the length of the wave vector.

plasmas have a cyclindrical shape and are therefore best described in a cylindrical geometry. On the other hand, when we assume no azimuthal variation of any quantities, the system may just as well be described in two-dimensional Cartesian coordinates. In this case where we assume the magnetic field to be in the z direction the dispersion relation is given by (see e.g., Stix[11])

$$k^2 + k_{de}^2 + \tfrac{1}{2} k_{di}^2 \sum_{v=kv_b} \sum_{n=-\infty}^{\infty} \exp(-\lambda) I_n(\lambda) \times \left[1 + \frac{\omega - rk_z}{ak_z} Z\left(\frac{\omega + n\Omega_i - rk_z}{ak_z}\right)\right] = 0 , \quad (1)$$

where $k^2 = k_x^2 + k_z^2$ is the wavenumber squared, k_{De} and k_{Di} are the wavenumbers corresponding to the Debye length ($k_D = 2\pi/d$) for the electrons and for the ions, respectively, Ω_i is the ion cyclotron frequency, λ is $\frac{1}{2}(ak_x/\Omega_i)^2$, I_n is the modified Bessel function of order n, and $Z = Z_R + iZ_I$ is the plasma dispersion function.[12]

We now divide the discussion into two parts. First, let us consider the case $\omega_r = 0$ ($\omega = \omega_r + i\omega_i$). Because of the symmetry of the ion distribution function, it is likely that the most unstable wave is the one with phase velocity, $\omega_r/k = 0$. This is also the result of Weibel's calculation[6] and a conclusion of our own examination of the case $\omega_r \neq 0$.

By letting $\omega_r = 0$, the imaginary part of the dispersion relation is automatically satisfied and the real part reduces to

$$1 + h^2 - \exp(-\lambda) I_0(\lambda) \tfrac{1}{2} \Theta Z_R'(u) + 2\Theta \exp(-\lambda) \times \sum_{n=1}^{\infty} I_n(\lambda)(1 + \tfrac{1}{2} u Z_R(u - n\Omega) + \tfrac{1}{2} u Z_R(u + n\Omega)) = 0 , \quad (2)$$

where we have introduced the normalized quantities $u = v_b/a$, $\Omega = \Omega_i/ak_z$, and $h = k/k_{De}$.

To further simplify this equation we shall first assume $\lambda \ll 1$, which reduces the dispersion relation to a quadratic equation in λ. Then, for a fixed u value it is possible to find a maximum of Θ by varying k_z. The result of this shows that for small drift velocities ($u \lesssim 2$) the most unstable mode (i.e., the one which is unstable for the smallest Θ) is the wave propagating parallel to the magnetic field lines ($k_x = 0$). At higher drift velocities the most unstable waves are found to have $k_x\rho \sim 1$ (ρ is the ion gyroradius), which means the approximation $\lambda \ll 1$ breaks down.

To proceed without the assumption $\lambda \ll 1$ we notice that Eq. (2) can be solved with respect to Θ, and we can calculate Θ versus $\mathbf{k}$, i.e., vs Ω and λ. By making a rough plot of $\Theta(\mathbf{k})$ we find the approximate minimum of Θ and then a numerical iteration procedure can give the exact value. Some results with $(\rho k_{De})^2 = 200$ are shown in Figs. 1(a) and 2. Figure 1 shows the minimum temperature ratio at which a mode is marginally unstable versus the beam velocity. Figure 2 shows the length and the angle of the wavevector for the marginal stable mode versus the beam velocity. In Fig. 2 we notice two discontinuities of $\mathbf{k}$ vs u. The first occurs at $u \approx 1.6$ when the marginally unstable mode changes from being parallel to propagating at an angle relative to the magnetic field lines. For $u > 3.1$, an approximate solution to Eq. (2) giving a minimum value of Θ can be found by noticing that $Z_R(u - n\Omega)$ has a minimum at $u - n\Omega \approx 0.9$. Using $n = 1$ determines Ω versus u and the dispersion relation reduces to an expression giving Θ as a function of λ. Because $ak_z = \Omega_i/\Omega$ in this case, we have $k_z = n\Omega_i/[a(u - 0.9)]$, which is a fairly good approximation to the curves in Fig. 2 for $u > 3.1$. In the interval $1.6 < u < 3.1$, several terms in Eq. (2) are of the same order of magnitude and no simple approximation seems useful. To obtain information on the growth rate of the unstable waves, Fig. 1(b) includes a curve giving the solution to Eq. (1) with $\omega_i/ak_z = 0.1$.

The case $\omega_r \neq 0$ is more difficult, especially because we also have to solve the imaginary part of the dispersion relation. However, since in this case the temperature ratio Θ can be expressed explicitly using the real part of Eq. (1), a numerical method of solution is still possible. The solution to the imaginary part of the dispersion relation is found by an iterative procedure determining a zero of a function. Since we are only interested in the threshold value for instability ($\omega_i = 0$), the imaginary part of the plasma dispersion function $Z_i(\xi)$ is simply $\exp(-\xi^2)/\sqrt{\pi}$. Furthermore, it appears that it is only necessary to keep a few terms in the sum because of the fast decrease of the $I_n(\lambda)$ function with increasing n. When a solution of the imaginary part of the equation is found, Θ is given from the real part of the dispersion relation, and the minimum value of Θ can be found by varying $\mathbf{k}$, as in the case $\omega_r = 0$. The result of this calculation is shown in Fig. 1(c), and we notice that for all u values the curve for marginal stability of the second band ($\omega_r \neq 0$) is above that of the first band ($\omega_r = 0$).

We specially notice the following among the results presented in Figs. 1 and 2. First, at a beam velocity higher than $1.6a$ the most unstable waves are some with $\omega_r = 0$ and a perpendicular wavenumber greater than zero ($k_x > 0$). At even higher beam velocities the plasma becomes unstable at lower temperature ratios simi-

lar to the case where ion cyclotron waves are unstable because an electron beam penetrates the plasma. With a beam velocity of around $7a$ the waves are unstable even for a temperature ratio $\Theta \simeq 1$, and the unstable modes propagate nearly perpendicular to the magnetic field.

[1]W. E. Drummond and M. N. Rosenbluth, Phys. Fluids **5**, 1507 (1962).
[2]R. W. Motley and N. D'Angelo, Phys. Fluids **6**, 296 (1963).
[3]J. M. Kindel and C. F. Kennel, J. Geophys. Res. **76**, 3055 (1971).
[4]T. E. Stringer, J. Nucl. Energy C **6**, 267 (1964).
[5]B. D. Fried and A. Wong, Phys. Fluids **9**, 1084 (1966).
[6]E. S. Weibel, Phys. Fluids **13**, 3003 (1970).
[7]D. R. Baker, Phys. Fluids **16**, 1730 (1973).
[8]V. O. Jensen and P. Michelsen, Phys. Fluids **17**, 2208 (1974).
[9]H. Ishizuka, H. Ono, and S. Kojima, J. Phys. Soc. Jpn. **36**, 1158 (1974).
[10]T. H. Stix, Phys. Fluids **16**, 1922 (1973).
[11]T. H. Stix, *The Theory of Plasma Waves*, (McGraw-Hill, New York, 1962), p. 225.
[12]B. D. Fried and S. D. Conte, *The Plasma Dispersion Function* (Academic, New York, 1961).

Unstable electrostatic ion cyclotron waves excited by an ion beam

P. Michelsen, H. L. Pécseli, J. Juul Rasmussen, and N. Sato*

Association Euratom-Risø/Forskningsafdelingen, Danish Atomic Energy Commission, Research Establishment Risø, Roskilde, Denmark
(Received 6 October 1975)

Electrostatic ion cyclotron waves were observed in a quiescent cesium plasma into which a low-energy beam of sodium ions was injected. The instability appeared when the beam velocity was above 12 times the ion thermal velocity. The waves propagated along the magnetic field with a velocity somewhat smaller than that of the beam. The dispersion relation was in good agreement with theory.

I. INTRODUCTION

Recently, the instabilities that can arise in a plasma with an ion beam were theoretically investigated by Stix.[1] Some of these instabilities may occur, for instance, in a fusion plasma heated by neutral beam injection. One of the instabilities of possible importance is the electrostatic ion cyclotron instability, which was first seen experimentally by D'Angelo and Motley[2] in a Q-machine plasma where the electrons had a slow drift. A condition for the onset of the instability was given by Drummond and Rosenbluth.[3] The condition for the instability in a plasma with a group of drifting ions was examined theoretically by Weibel[4] and Michelsen.[5] An experiment on the electrostatic ion cyclotron instability caused by an ion beam was recently reported by Ishizuka *et al.*[6] This experiment was performed in a pulsed helium plasma into which a high-energy ion beam of several keV was injected.

Here, we report an experiment performed in a cesium plasma into which a sodium beam was injected. The beam was produced using a simple ion emitter described previously by Sato *et al.*[7] The beam energy is very low (2–10 eV) compared with that in Ref. 6. Two unstable modes appeared when the beam energy was above a threshold value (≈5 eV). The frequencies of these modes were close to the ion cyclotron frequencies for Cs and Na (Ω_C, Ω_N), respectively. The measured dispersion relation for both modes showed good agreement with the theoretical prediction for ion cyclotron waves. The waves were found to propagate along the direction of the magnetic field in contrast with the experiment in Ref. 2 where no propagation was found. The phase velocity was comparable to but smaller than the beam velocity. The phase velocity was also investigated for waves excited by a sinusoidal modulation of the ion beam energy; in this case it was close to the beam velocity.

II. EXPERIMENTAL SET-UP

The experiment was performed in the Risø Q machine running in single-ended mode. A Cs plasma is produced by surface ionization on a hot tantalum plate (2200 °K) of 3 cm in diameter. A magnetic field with a strength up to 0.7 T confines the plasma in the radial direction. The plasma column is terminated by an electrostatic energy analyzer,[8] which is movable along the plasma column giving a maximum length for the plasma of 1.2 m.

The ion beam, consisting of Na ions, was produced by means of an ion emitter.[7] A nickel–chromium or platinum wire of about 0.5 mm in diameter was used to make one bifilar winding about 5 mm in diameter. The wire was then covered by a thin layer of sodium silicate (Na_2O, $2SiO_2$). The emitter was inserted into the plasma column. When it was heated to about 1100 °K by passing a dc current through the wire, it emitted Na ions; their energy was determined by the bias of the emitter.

Two different kinds of Langmuir probe were used for detection of the waves. Because of the rather low plasma density ($n \approx 10^8$–10^9 cm^{-3}), both probes were quite large. One probe used for measuring the dispersion relation was shaped like an asterisk and consisted of molybdenum wires, 25 mm in length and 0.5 mm in diameter. It could be moved along the plasma column to measure the parallel wavelength. The other probe was a small circular plate, 2 mm in diameter, perpendicular to the magnetic field and movable in the radial direction. This probe was used for measuring the radial wave propagation.

A diagram of the set-up is given in Fig. 1(a) showing the ion emitter, the probes and the energy analyser.

III. MEASUREMENTS

The ion velocity distribution function measured with the energy analyzer for various energies of the ion beam is shown in Fig. 1(b). Although most beam ions have velocities close to that corresponding to an acceleration through the potential of the ion emitter, some ions achieve velocities that lie between that of the beam and that of the background ions. During the wave measurements the velocity distribution was in all cases similar to those shown in Fig. 1.

The frequency spectrum shown in Fig. 2(a) is typical of the case where the bias of the ion emitter is above +5 V. When the emitter is positively biased, it is obvious that an electron current is drawn between the hot plate and the emitter. This, of course, could also give rise to the onset of the instability, as described in Ref. 2. We checked that this was not the case by switching off the heating current through the emitter without changing the bias. When the emitter became

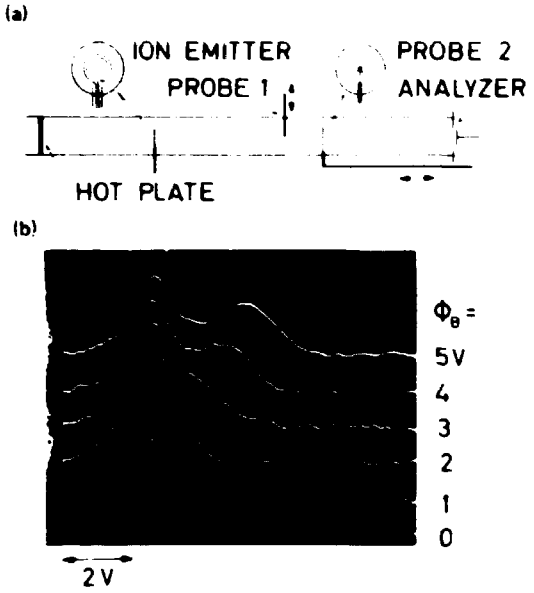

FIG. 1. (a) Experimental setup. (b) Ion velocity distribution functions for various beam energies Φ_B.

cold, the oscillations disappeared although the electron current was unchanged. The two peaks seen on the frequency spectrum varied with the magnetic field strength, as shown in Fig. 2(b). The solid lines show the cyclotron frequencies for Cs and Na, respectively, and it is seen that both instabilities follow a dispersion relation given by[2]

$$\omega^2 = \Omega^2 + c^2 k_\perp^2 \ ,$$

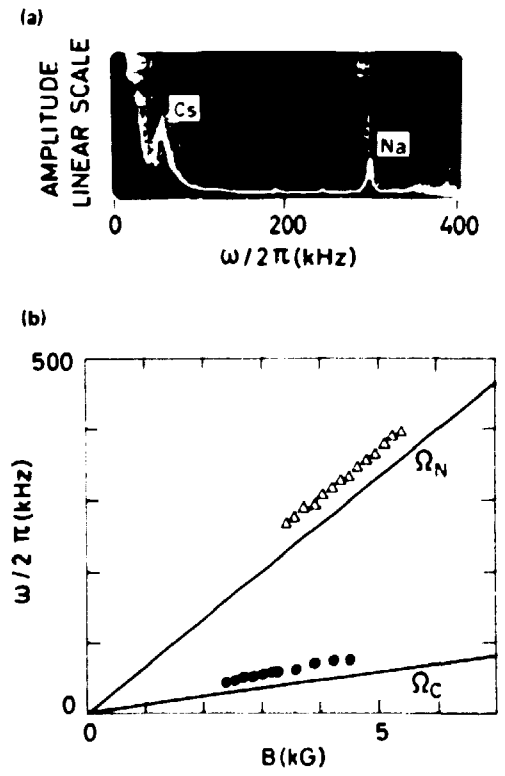

FIG. 2. (a) Frequency spectrum showing the two unstable modes. (b) Frequency of the unstable modes versus magnetic field strength. The two lines are the cyclotron frequencies for Cs(Ω_C) and for Na(Ω_N), respectively.

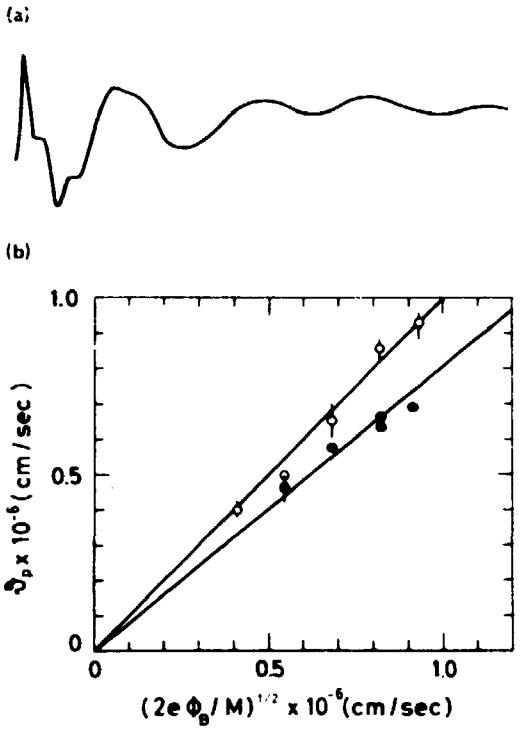

FIG. 3. (a) Output from lock-in amplifier versus distance for the unstable Cs mode. (b) Phase velocity of self-excited waves (•) and of external excited waves (○) versus beam velocity.

where Ω is the cyclotron frequency for the ion in question and c is the corresponding sound speed. A minor correction to this for our condition is given in Sec. IV.

In all cases the oscillation at the frequency near the Cs cyclotron frequency was stronger than that near the Na cyclotron frequency, and only for the former was it possible to measure the parallel wavelength. A typical wave pattern measured along the plasma column with the asterisk-shaped probe is shown in Fig. 3(a). The signal is measured using a lock-in amplifier where a reference signal is obtained from the ion emitter. As can be noticed from the figure, the oscillation is damped along the plasma column away from the emitter. It was also found that there was a change in the ion distribution function along the plasma column so that the region between the beam and the background ions gradually became filled up along the distance from the emitter. The wavelength was measured and the phase velocity calculated from wave patterns like that in Fig. 3(a). The result is shown in Fig. 3(b) where the measured phase velocities are plotted versus the beam velocity. This beam velocity is simply calculated using the assumption that the beam energy corresponds to an acceleration of the ions through a potential equal to that of the emitter.[7] A comparison with measurements of the ion distribution function shows that this is a fair approximation. It is seen from the figure that the phase velocities are comparable to but smaller than the beam velocity, which should, of course, be theoretically expected for a beam plasma instability.

To determine the beam velocity more accurately we

excited oscillations with frequencies above the unstable frequency by modulating the beam energy with a small sinusoidal signal applied to the ion emitter.[7-9] The phase velocities of the excited wave patterns are also shown in Fig. 3(b).

The radial propagation of the self-excited waves was measured with a radially movable probe. We observed that axisymmetric modes were excited. The results could be interpreted as a combination of a strong radial standing wave and a somewhat weaker radially propagating wave.

IV. DISPERSION RELATION AND DISCUSSION

The experimental results obtained were all in good qualitative agreement with the various theoretical descriptions of these waves.[2,4,5] To examine this agreement in greater detail we must consider the dispersion relation with the parameters that are relevant to this experiment. A general dispersion relation for electrostatic waves in a magnetized plasma can, for instance, be found in Ref. 10.

If we assume that the phase velocity is small compared with the electron thermal velocity, that the wavelength is long compared with the electron Debye length and the electron gyroradius, and that $T_\perp = T_\parallel$, we get the following simplified dispersion relation:

$$1 + \sum_j \sum_{n=-\infty}^{\infty} \frac{T_e}{T_j}\frac{n_j}{n_e} e^{-\lambda_j} I_n(\lambda_j) \left[1 + \frac{\omega - V_j k_\parallel}{a_j k_\parallel} Z\left(\frac{\omega + n\Omega_j - V_j k_\parallel}{a_j k_\parallel}\right)\right] = 0 ,$$

where the index j refers to the ion species, and the index e refers to the electrons. V_j is the drift velocity, Ω_j is the cyclotron frequency, a_j is the thermal speed $[= (2\kappa T_j/M_j)^{1/2}]$, I_n is the modified Bessel function of order n, $\lambda_j = \frac{1}{2}(k_\perp \rho_j)^2$, where ρ_j is the ion gyroradius and Z is the "plasma dispersion function."[11]

Now let us consider a plasma consisting of a beam of Na ions streaming with a mean velocity V through a background of Cs ions. Since $\lambda_j < 1$, we neglect terms with $|n| > 1$. The dispersion relation is then reduced to

$$\begin{aligned} 1 &+ \alpha_C \Gamma_{0C}\left[1 + \frac{\omega}{a_C k_\parallel} Z\left(\frac{\omega}{a_C k_\parallel}\right)\right] \\ &+ \alpha_N \Gamma_{0N}\left[1 + \frac{\omega - V k_\parallel}{a_N k_\parallel} Z\left(\frac{\omega - V k_\parallel}{a_N k_\parallel}\right)\right] \\ &+ \alpha_C \Gamma_{1C}\left[2 + \frac{\omega}{a_C k_\parallel} Z\left(\frac{\omega + \Omega_C}{a_C k_\parallel}\right) + \frac{\omega}{a_C k_\parallel} Z\left(\frac{\omega - \Omega_C}{a_C k_\parallel}\right)\right] \\ &+ \alpha_N \Gamma_{1N}\left[2 + \frac{\omega - V k_\parallel}{a_N k_\parallel} Z\left(\frac{\omega + \Omega_N - V k_\parallel}{a_N k_\parallel}\right)\right. \\ &\left. + \frac{\omega - V k_\parallel}{a_N k_\parallel} Z\left(\frac{\omega - \Omega_N - V k_\parallel}{a_N k_\parallel}\right)\right] = 0 , \end{aligned} \tag{1}$$

where indices C and N now refer to Cs and Na ions, and we have introduced

$$\alpha_j = \frac{T_e}{T_j}\frac{n_j}{n_e} \quad \text{and} \quad \Gamma_{nj} = e^{-\lambda_j} I_n(\lambda_j) .$$

To proceed we first assume that temperature effects are of minor importance, and, therefore, we can use the asymptotic approximation $Z(\xi) \simeq -\xi^{-1}$. If we introduce this into the equation, we obtain, after a simple calculation,

$$1 - \frac{n_C}{n_e} k_\perp^2 a_C^2 \frac{1}{\omega^2 - \Omega_C^2} - \frac{n_N}{n_e} k_\perp^2 a_N^2 \frac{1}{(\omega - k_\parallel V)^2 - \Omega_N^2} = 0 ,$$

which has the two solutions

$$\omega^2 \simeq \Omega_C^2 + a_C^2 k_\perp^2 \frac{n_C}{n_e} , \tag{2}$$

$$(\omega - V k_\parallel)^2 \simeq \Omega_N^2 + a_N^2 k_\perp^2 \frac{n_N}{n_e} . \tag{3}$$

Our measurements concerning the mode near the Cs cyclotron frequency are well described by Eq. (2). However, the mode near the Na cyclotron frequency cannot be described by Eq. (3). This will be further discussed at the end of the section.

To get information on the stability criterion, we must consider the plasma dispersion function without making an asymptotic approximation. Let us assume we have a solution where $\omega \gtrsim \Omega_C$, and that the parallel wavenumber is determined from $\omega/k_\parallel \lesssim V$. From inspection of the real part of Eq. (1), we then find that a solution where the electron temperature is minimized, and where the imaginary part of the equation is also satisfied, requires

$$\frac{\omega - \Omega_C}{a_C k_\parallel} \simeq \frac{\omega - V k_\parallel}{a_N k_\parallel} \simeq \text{const} ,$$

where the constant is between 0.9 and 1.5, and typically can be put equal to 1.3. Introducing this into the dispersion relation and neglecting all small terms, we obtain

$$\frac{T_e}{T_C} = \left[c_1 + c_2 (V/a_C)\right]^{-1} ,$$

where

$$c_1 = \frac{n_N}{2n_e}\frac{T_C}{T_N}\Gamma_{0N} Z_R'\left(\frac{\omega - V k_\parallel}{a_N k_\parallel}\right)$$

and

$$c_2 = -\frac{n_C}{n_e}\Gamma_{1C} Z_R\left(\frac{\omega - \Omega_C}{a_C k_\parallel}\right) .$$

Here, we introduce some numbers relevant to our experiment, $n_N = n_C$ and $T_C = T_N$. We note that Γ_{1C} has a very broad maximum $\simeq 0.22$ for $\frac{1}{2}k_\perp^2 \rho^2 \simeq 1.5$, which corresponds to about one wavelength across the plasma column. For the oscillations given by Eq. (2), the stability limits we obtain are then

$$\frac{T_e}{T_C} \simeq [0.13 + 0.11 (V/a_C)]^{-1} ,$$

which for $T_e \simeq T_C$ gives $V/a_C \simeq 8$. This is in agreement with our measurements for the signal near Ω_C, where we only observed the instability when the acceleration voltage was above 5 V corresponding to $V/a_C \simeq 12$.

As mentioned in Sec. IV, the other solution to the dispersion relation, Eq. (3), does not describe the

other unstable mode, marked Na on Fig. 2. In fact, the mode given by Eq. (3) should be stable. The most obvious explanation for the appearance of this mode seems to be that there exists a background of nearly stationary Na ions. This is, indeed, not surprising because the ion emitter produces a beam in both directions along the magnetic field. The beam ions moving toward the hot plate will probably be reflected from this with an energy corresponding to that which they can obtain from acceleration through the plasma sheath; therefore, they receive a mean energy along the magnetic field equal to that of the Cs ions and are not noticed on the energy analyzer. For the beam moving through this Na background, a theory similar to that in Sec. IV can be applied. This means we obtain a dispersion relation for the "Na mode" that is identical to (1), except for the index C that must be interchanged with an N, and in agreement with the measurements in Fig. 2. The threshold beam energy for this mode to become unstable depends on the ratio between beam density and background density which is not known precisely. If we assume this density ratio to be about one, we can use the calculated stability threshold in Refs. 4 and 5 directly. The result for the necessary beam energy in this case is nearly the same as that found in Sec. IV, in agreement with our observation that in most cases the two modes appeared simultaneously.

ACKNOWLEDGMENTS

We thank N. D'Angelo for his interest and for valuable discussions, and M. Nielsen and B. Reher for their skilled technical assistance. One of the authors (N.S.) is very grateful to Dr. V. O. Jensen and Professor Y. Hatta for their encouragement.

*Present address: Department of Electronic Engineering, Tohoku University, Sendai, Japan.

[1] T. H. Stix, Phys. Fluids **16**, 1922 (1973).
[2] R. W. Motley and N. D'Angelo, Phys. Fluids **6**, 296 (1963).
[3] W. E. Drummond and M. N. Rosenbluth, Phys. Fluids **5**, 1507 (1962).
[4] E. S. Weibel, Phys. Fluids **13**, 3003 (1970).
[5] P. Michelsen, Phys. Fluids **19**, 337 (1976).
[6] H. Ishizuka, H. Ono, and S. Kojima, J. Phys. Soc. Jpn. **36**, 1135 (1974).
[7] N. Sato, Y. Hatta, R. Hatakeyama, and H. Sugai, Appl. Phys. Lett. **24**, 300 (1974).
[8] S. A. Andersen, V. O. Jensen, P. Michelsen, and P. Nielsen, Phys. Fluids **14**, 728 (1971).
[9] N. Sato, H. Sugai, and R. Hatakeyama, Phys. Rev. Lett. **34**, 931 (1975).
[10] T. H. Stix, *The Theory of Plasma Waves* (McGraw-Hill, New York, 1962), p. 225.
[11] P. D. Edelstand S. D. Conte, *The Plasma Dispersion Function* (Academic, New York, 1965).

Ion-beam-excited, electrostatic, ion cyclotron instability

P. Michelsen, H. L. Pécseli, and J. Juul Rasmussen

Association Euratom-Research Establishment Risø, 4000-Roskilde, Denmark
(Received 26 October 1976; final manuscript received 21 January 1977)

The stability limits of the ion-beam-excited, electrostatic, ion cyclotron instability were investigated in a Q-machine plasma where the electrons could be heated by microwaves. In agreement with theory, the beam energy necessary for excitation decreased with increasing electron temperature.

The ion-beam-excited, electrostatic, ion cyclotron instability is one of the microscopic instabilities that may accompany neutral beam injection in toroidal devices.[1] Partly for this reason, considerable efforts have been made in order to investigate this instability, both experimentally and theoretically.[2–7] Ion cyclotron oscillations excited by drifting electrons were investigated several years ago by D'Angelo and Motley.[8] In connection with this experiment some controversy arose when the criterion for instability[9] (critical electron drift) was investigated for varying electron temperature. An experiment by Levine and Kuckes[10] showed that the critical drift *increased* with increasing electron temperature in contradiction to the theoretical predictions of Drummond and Rosenbluth.[9] We, therefore, felt it worthwhile to investigate the instability criterion for the ion-beam-excited counterpart of this instability for varying electron temperatures and to compare it with existing theories.

The experiment was conducted in the Risø Q machine running in single-ended mode. The setup was similar to that used in the experiment described in Ref. 3. An Na or Cs plasma is produced by surface ionization on a hot tantalum plate (2200 K) 3 cm diam. The plasma is confined radially by a homogeneous magnetic field of strength up to 0.7 T. The plasma column is terminated by an electrostatic energy analyzer. An Na ion beam is produced by means of an ion emitter. The beam energy is determined by the emitter bias.

The electrons could be heated in a microwave resonator surrounding the plasma and operating at a frequency around the electron cyclotron frequency.[11] The microwave power could be varied from 0–500 mW, resulting in an electron temperature increase up to approximately 1.5 eV. This temperature is determined by investigations of the phase velocity of ion acoustic waves and also verified by Langmuir probe characteristics.

In Figs. 1(a) and (b) the ion velocity distributions are shown as measured on the energy analyzer. The peak on the left shows the ions in the bulk plasma and the peak on the right shows the ion beam. In Fig. 1(a) the parameter is the potential applied to the ion emitter. From the figure it can be seen that the beam energy is very close to the energy expected from this potential. The temperature of the plasma ions is 0.1–0.2 eV, while that of the beam ions is approximately 0.1 eV. In Fig. 1(b) the beam energy is kept constant equal to 6 eV, and the ion velocity distributions are shown for varying microwave power giving an electron temperature of 0.2–1.5 eV. For this beam energy and in this temperature range, the plasma is unstable with respect to the electrostatic ion cyclotron instability. This is seen to give a change in the distribution function in agreement with quasi-linear theory (i.e., a flattening of the distribution) that is most noticeable at high electron temperature. Similar observations were made by Baker[12] in investigations of ion beam instabilities.

The investigations of the instability criterion gave the result shown in Fig. 2. For fixed microwave power, i.e., a constant electron temperature, the beam energy was increased until the ion cyclotron instability was recognized on a spectrum analyzer. A dispersion relation for these waves has been presented in Ref. 3. The triangles in Fig. 2 represent the case discussed hitherto, a sodium ion beam in a sodium plasma, and they are measured simultaneously with the distribution functions in Fig. 1. The circles in Fig. 2 represent the case investigated in Ref. 3, i.e., a sodium beam in a cesium plasma. In both cases, the beam energy necessary for the excitation of the instability was found to decrease with increasing electron temperature. This result has also recently been found theoretically.[5,6] The

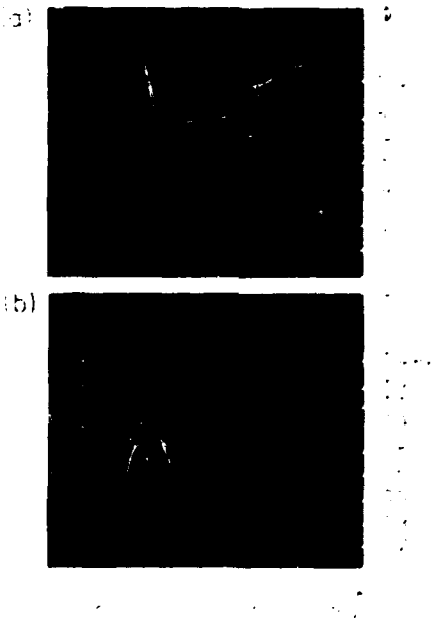

FIG. 1. The ion velocity distribution function as a function of ion energy. The numbers on the curves are (a) the ion emitter bias in volts, (b) the electron temperature.

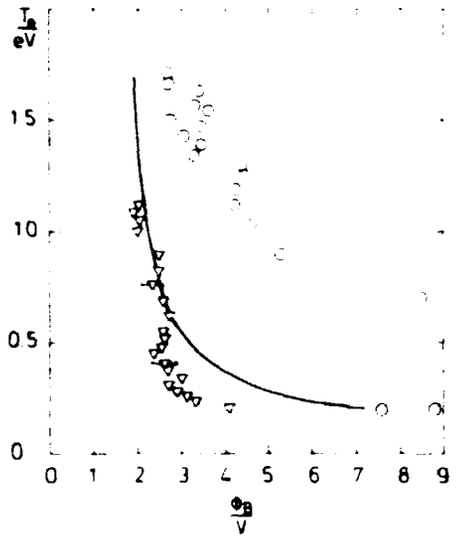

FIG. 2. The electron temperature versus beam energy giving marginal stability. The triangles represent an Na beam in an Na plasma and the circles represent an Na beam in a Cs plasma. The solid line is the theoretical curve for the case where the parameters of the beam are equal to those of the bulk plasma. The horizontal lines indicate error bars.

theoretical curve (solid line), taken from Ref. 6, shown in Fig. 2 gives the stability limit for the case where the density and temperature of the beam are equal to those of the background plasma. This is close to our experimental situation in the case of an Na beam in an Na plasma, see Fig. 1(a). Figure 2 shows very good agreement for this case, both with respect to the shape and to the absolute values. For the other case considered, an Na beam in a Cs background, the shape of the measured curve shows the same dependence between beam velocity and electron temperature.

In conclusion, it was experimentally determined that the beam velocity necessary for the excitation of electrostatic ion cyclotron waves decreases with increasing electron temperature. This is in agreement with theoretical predictions based on the general electrostatic dispersion relation.[13]

We thank M. Nielsen and B. Reher for skillful technical assistance.

[1]T. H. Stix, Phys. Fluids **16**, 1922 (1973).
[2]H. W. Hendel, M. Yamada, S. W. Seiler, and H. Ikezi, Phys. Rev. Lett. **36**, 319 (1976).
[3]P. Michelsen, H. L. Pécseli, J. J. Rasmussen, and N. Sato, Phys. Fluids **19**, 453 (1976).
[4]P. Michelsen, H. L. Pécseli, J. J. Rasmussen, and N. Sato, Phys. Lett. A **55**, 345 (1976).
[5]E. S. Weibel, Phys. Fluids **13**, 3003 (1970).
[6]P. Michelsen, Phys. Fluids **19**, 337 (1976).
[7]F. W. Perkins, Phys. Fluids **19**, 1012 (1976).
[8]R. W. Motley and N. D'Angelo, Phys. Fluids **6**, 296 (1963).
[9]W. E. Drummond and M. N. Rosenbluth, Phys. Fluids **5**, 1507 (1962).
[10]A. M. Levine and A. F. Kuckes, Phys. Fluids **9**, 2263 (1966).
[11]H. L. Pécseli and P. I. Petersen, Risø Report No. 290 (1973).
[12]D. R. Baker, Phys. Fluids **16**, 1730 (1973).
[13]T. H. Stix, *The Theory of Plasma Waves* (McGraw-Hill, New York, 1962), p. 225.

Errata

Appendix II

p. 223, 1. column, line 4: ϕ_{fl} should read ϕ_t.

" " , " 11: Ref. 2 should read Ref. 7.

p. 225, 1. column, " 10: 3 should read 8.

" " " 19: Ref. 2 should read Ref. 7.

Appendix III

p. 390, Eq. 5: $\varepsilon(k,\omega)$ should read $(k\lambda_0)^2\varepsilon(k,\omega)$.

" , 2. column, line 12: $\exp[i(\omega' t - k' x)]$ should read $\exp[-i(\omega' t - k' x)]$.

" , 2. column, " 20: (4) should read (5).

p. 395, Fig. 3 in the figure caption: $T_e/T_i = 2$ should read $T_e/T_i = 1$.

p. 397: The drawings in Figs. 6 and 7 should be interchanged.

p. 398, Eq. (38): $\cos[\omega(\frac{x_a}{v_a} - \frac{x}{v})]$ should read $\cos[\omega(\frac{x_a}{v_a} - \frac{x_a}{v})]$.

Sales distributors:
Jul. Gjellerup, Sølvgade 87,
DK-1307 Copenhagen K, Denmark

Available on exchange from:
Risø Library, Risø National Laboratory,
P. O. Box 49, DK-4000 Roskilde, Denmark

ISBN 87-550-0678-7
ISSN 0106-2840